INVESTIGATION OF COMBINED BIOLOGICAL ROLES OF NEURAMINIDASE 1 AND N-ACETYLGALACTOSAMINYLTRANSFERASE ENZYMES IN GLYCOLIPID METABOLISM

A Thesis Submitted to
The Graduate School of
İzmir Institute of Technology
in Partial Fulfillment of the Requirements for the Degree of

MASTER OF SCIENCE

in Molecular Biology and Genetics

by
Tuğçe ŞENGÜL

July 2020
İZMİR

ACKNOWLEDGEMENTS

As my best regards, I would like to express my deepest appreciation and thanks to my supervisor Prof. Dr. Volkan SEYRANTEPE for his patience, understanding, belief and support during my undergraduate and graduate period.

I would like to thanks to to Prof. Dr. Yiğit UYANIKGİL for analysis of histologic results.

I would like to thank to The Scientific and Technological Research Council of Turkey (TÜBİTAK) (117Z259) for financial support of the project and providing scholarship during my master years.

I would like to express my appreciation to my co-workers and best friends, Melike CAN, Hatice Hande BASIRLI and Deniz AK for their endless support and help during the thesis project. I am also grateful to every member of Seyrantepe Laboratory and Molecular Biology and Genetics Department for their help.

At last, I would like to thank my family, my father Mustafa Şengül, my mother Fatma Şengül and my brother Alp Buğra Şengül for their sincere love, endless patience, encouragement and support during my life.

ABSTRACT

INVESTIGATION OF COMBINED BIOLOGICAL ROLES OF NEURAMINIDASE 1 AND N-ACETYLGALACTOSAMINYLTRANSFERASE ENZYMES IN GLYCOLIPID METABOLISM

Gangliosides, sialic acid-containing glycosphingolipids, are responsible for neurogenesis and synaptogenesis which are essential for vertebrate nervous system. N-Acetylgalactosaminyltransferase (Galgt) is glycosyltransferase that plays essential role during complex gangliosides biosynthesis. Expression of Galgt increases at the late stage of development which can be evidence for complex gangliosides role in nervous system development and differentiation.Sialidases are responsible enzymes for sialic acid removal from glycoproteins, glycolipids or oligosaccharides. Neu1 is one of the mammalian sialidase which catabolizes sialoglycoconjugates in lysosomes. Neu1 gene mutations in human result in lysosomal storage disease called sialidosis. Created Neu1 knockout mice model have demonstrated similar symptoms with sialidosis type II. In sialidosis patients, increased ganglioside levels are detected in visceral organs but not in brain. In vitro studies have demonstrated that GM3 is a substrate of Neu1. Until this research, role of Neu1 enzyme on glycosphingolipid metabolism in the absence of complex gangliosides has not been investigated. Therefore this study have been provided comparision of 2-and 4-month-old Neu1-/-, Galgt-/- and Neu1-/-Galgt-/- mice to WT mice and each other by molecular biological, biochemical, histological, immunohistochemical and behavioral analysis in cortex, cerebellum and thalamus regions. In the concept of this thesis, we found effect of single and double deficienct of Neu1 and Galgt enzymes on the distinct cellular events (apoptosis, ER stress, oxidative stress), altered glycolipid and oligosaccharide metabolism, nerve cell death,oligodendrocyte intensity decrease, impairment in locomotor activity, motor coordination, memory capability as age dependent and region specific manner.

ÖZET

NÖROMİNİDAZ 1 ve N-ASETİLGALAKTOSAMINİLTRANSFERAZ ENZİMLERİNİN GLİKOLİPİT METABOLİZMASINDAKİ BİRLEŞİK BİYOLOJİK ROLÜNÜN ARAŞTIRILMASI

Gangliositler (sialik asit içeren glikosfingolipitler), omurgalı sinir sisteminin nöron ve sinaps gelişim sürecinden sorumlu olan temel bileşiklerdendir. . N-Asetilgalaktozaminiltransferaz (Galgt), karmaşık gangliosit biyosentezi boyunca önemli rol oynayan bir glikoziltransferaz enzimidir. Galgt ifade düzeyi, gelişimin son evrelerinde artış gösterir, bu durum karmaşık gangliositlerin sinir sisteminin gelişmesi ve farklılaşmasındaki rolünün bir kanıtı olabilir. Sialidazlar, glikoproteinlerden, glikolipitlerden veya oligosakkaritlerden sialik asit uzaklaştırılmasından sorumlu enzimlerdir. Neu11 memeli sialidazlarından biri olup, lizozomlarda sialoglikokonjugatları katabolize eder. İnsanda Neu1 genindekı mutasyonlar lizozomal depo hastalığı olan sialidoza sebep olur. Yaratılan Neu1 gen eksikliğine sahip fareler, sialidoz tip II ile benzer semptomlar göstermiştir. Sialidoz hastalarının iç organlarında gangliosit artışı görülürken, aynı artış beyinde görülmemiştir. *In vitro* çalışmalar GM3'ün bir Neu1 substratı olduğunu göstermiştir. Bu araştırmaya kadar, kompleks gangliositlerin yokluğu durumda Neu1 enziminin glikosfingolipid metabolizması üzerindeki rolü araştırılmamıştır. Bu nedenle, bu çalışma 2 ve 4 aylık Neu1 - / -, Galgt - / - ve Neu1 - / - Galgt - / - farelerinin WT fareleri ve birbirleriyle korteks, beyincik ve talamus bölge bazlı, moleküler biyolojik, biyokimyasal, histolojik, immünohistokimyasal ve davranışsal olarak karşılaştırılması sağlanmıştır. Bu tez kapsamında, Neu1 ve Galgt enzimlerinin tek ve çift eksikliğinin farklı hücresel olaylarda (apoptoz, ER stresi, oksidatif stres), değişen glikolipit ve oligosakkarit metabolizmasında, sinir hücresi ölümünde, oligodendrosit yoğunluğunun azalmasında, lokomotor aktivite,motor koordinasyon ve hafıza kapasitesi üzerindeki etkisi yaşa ve beyin bölgelerine bağlı olarak bulunmuştur.

Dedicated to my precious family….

TABLE OF CONTENTS

LIST OF FIGURES

Figure **Page**

Figure **Page**

Figure **Page**

Figure **Page**

Figure **Page**

Figure **Page**

Figure **Page**

Figure **Page**

LIST OF TABLES

CHAPTER 1

INTRODUCTION

Sphingolipids are subgroup of glycolipids and they includes sphingosine at their main structre that have 18-carbon amino alcohol and unsaturated hydrocarbon chain .This structure is found at the outer surface of cell membrane and provides attachment of carbohydrates to cell membrane (Kolter et al.1999).

1.1. Glycosphingolipids

Sphingolipids that have ceramide in their backbone with saccharide (glucose, galactose) are called as glycosphingolipids (GSL). Mammalian central nervous system are enriched for glycosphingolipids when compared the other tissues (Coet et al.1998). During neurotogenesis, synaptogenesis and maintenance of nervous system GSLs play essential role (Olsen et al.2017). GSLs can be separated from each other as neutral or acidic and this separation is done either having sialic acid residue or not (Xu et al.2010).

1.2 Gangliosides

Gangliosides are sialylated glycosphingolipids. They have sialic acid on their carbohydrate group including glucose,galactose and N-acetylgalactosamine. Ganglioside can be found in whole body but especially gray matter and neurons are enourmously rich for ganglioside (Olsen et al.2017). Because of that plasma membrane of nerve cells is enriched for gangliosides and gangliosides have role in development and maintenance, cell–cell recognition, signal transduction, growth, and motility (Xu et al.2010).Additionally 10-20% of total lipids are formed by gangliosides in eukaryotic cells (Xu et al.2010).

1.1.1. Ganglioside Biosynthesis

Gangliosides are started to synthesize in endoplasmic reticulum and synthesis is completed at Golgi apparatus. Ceramide backbone of ganglioside is found in endoplasmic reticulum and it is transferred to Golgi apparatus for stepwise addition of glucose,galactose, N-acetylgalactosamine and sialic acid residue by glycosyltransferases (Schengrund et al.2015). Lactosylceramide formation is the first step for many gangliosides except G_{M4}, it is derived from galactosylceramide. For the first step, galactose is added to glucosylceramide by Lactosylceramide synthase (B4Galt6). 0-series gangliosides(G_{A2}, G_{A1},G_{M1b} and G_{D1c}) are derived from Lactosylceramide. When one sialic acid residue is added to lactosylceramide by G_{M3} synthase, G_{M3} ganglioside is synthesized. Addition of one sialic acid residue to G_{M3} forms G_{D3} and one sialic acid residue addition to G_{D3} forms G_{T3} by the G_{D3} synthase ($G_{D3}S$) and Sialyltransferase III (STIII) enzymes respectively. Complex gangliosides are derived from G_{M3},G_{D3} and G_{T3} gangliosides and each simple ganglioside is precursor of a-,b- and c- series of gangliosides respectively. To synthesize more complex gangliosides first step is addition of N-acetylgalactoseamine residues to simple gangliosides by β1–4Nacetylgalactosaminyltransferase enzyme (Galgt1, G_{A2}/G_{M2}/G_{D2}/G_{T2} synthase) that forms G_{A2}, G_{M2}, G_{D2}, G_{T2} gangliosides. Addition of galactose residues to G_{A2}, G_{M2}, G_{D2}, G_{T2} gangliosides by Galactosyltransferase (B3Galgt4,G_{A1}/G_{M1}/G_{D1b}/G_{T1c} synthase) form G_{A1}, GM1, GD1b, and GT1c. Addition of one sialic acid residue to these gangliosides by Sialyltransferase IV (STIV) results in G_{M1b}, G_{D1a}, G_{T1b}, and G_{Q1c} gangliosides synthesis. Sialyltransferase V (STV) catalyzes one sialic acid addition to these gangliosides and the most complex gangliosides, GD1c,GT1a, GQ1b, and GP1c, are synthesized (Schengrund et al.2015;Robert et al.2011) (Figure 1.1).

1.1.2. Degradation of Gangliosides

Degredation og gangliosides is carried out by enzymes, activator proteins(sphingolipids activator proteins –SAPs) and negatively charged lipids that are found in lysosome (Kolter et al.1999). During degredation process, stepwise removal of carbohdrate and sialic acid residues is catalyzed by lysosomal exohydrolases and protein

cofactors (Xu et al.2010). In addition to that sialidase enzymes play role to remove sialic acid residues from gangliosides. Previous studies has showed that sialidase *Neu4* shows its activity on G_{D1a} (Seyrantepe et al.2008) and G_{M2} (Seyrantepe et al.2010) , whereas sialidase *Neu1* shows its activity on GT1b, GD1b, GD2, GD3 and GM3 gangliosides (Timur et al.2015) and sialidase *Neu3* shows its activity on GM2 and GM3 gangliosides (Seyrantepe et al.2018) (Figure 1.2).

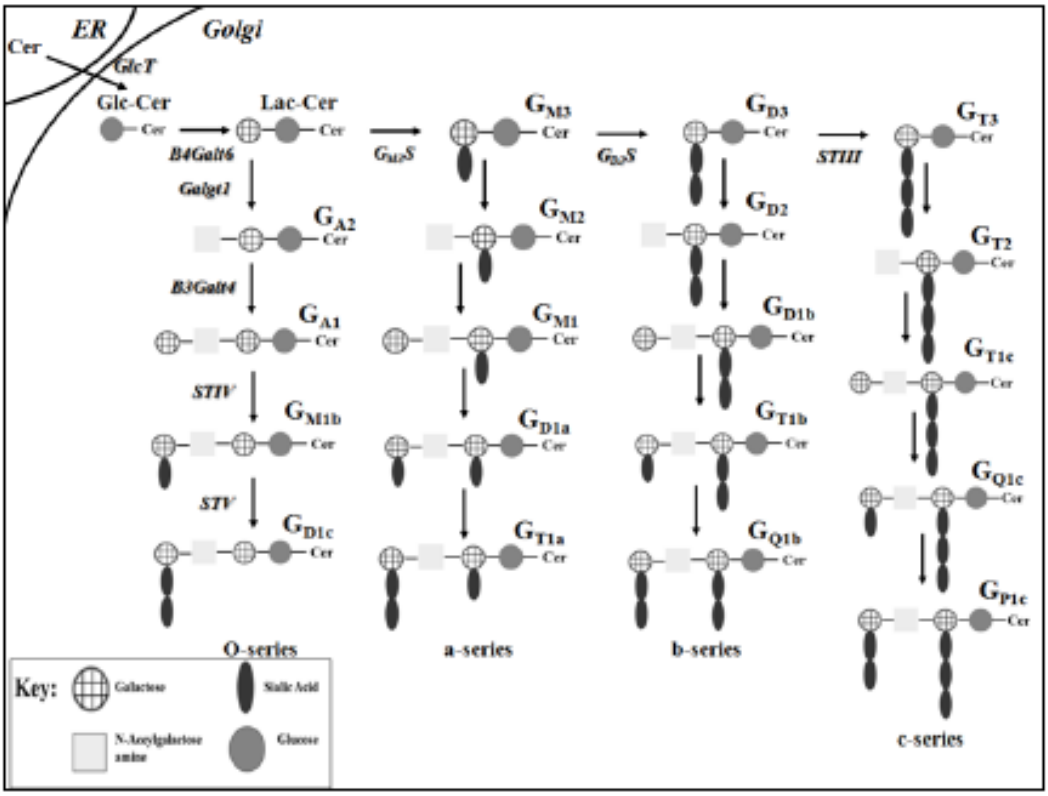

Figure 1.1. Ganglioside biosynthesis pathway in human by courtesy of Xu et al. 2010. Synthesis of gangliosides are carried out as stepwise addition of monosaccharides to ceramide by glycosyltransferases in the ER and Golgi apparatus. It is started with addition of glucose residue to ceramide by by β-glucosyltransferase (GlcCer synthase). Then sialic acid residues are added to corresponding gangliosides by specific sialyltransferases. Precursors of 0-, a-, b- and c- series gangliosides are synthesized, LacCer, GM3, GD3, and GT3 respectively. By adding of monosaccharides and sialic acid residues to these precursors, complex gangliosides are synthesized.

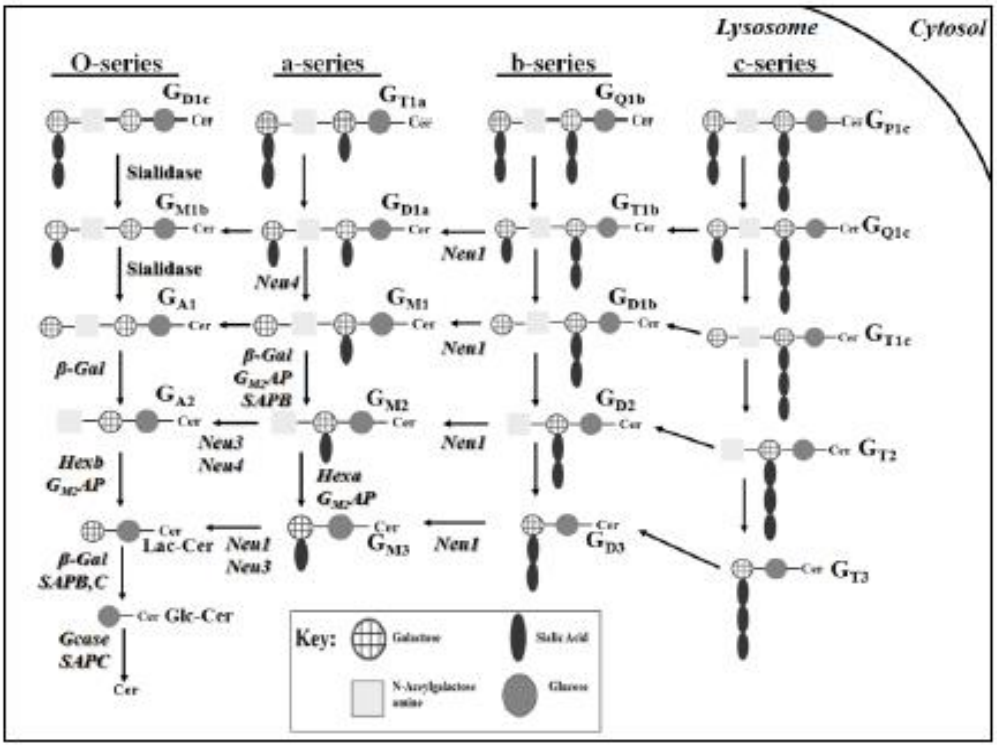

Figure 1.2. Ganglioside degredation pathway in human . Degradation of gangliosides takes plave in lysosomes as sequantialy. Sialidases are responsible enzymes for catalzying removal of sialic acid resdiues from gangliosides by courtesy of Xu et al. 2010.

1.2. B4GALNT1-/- (Galgt-/-) Mice Model

B4GALNT1**(**β-1,4-N-acetylgalactosaminyltransferase; GM2/GD2 synthase) is the key enzyme that plays role in biosynthesis of almost all complex gangliosides. It is called with many different names and in this thesis study it is named as Galgt enzyme. It transfers a N-acetylgalactosamine (GalNAc) to GM3 or GD3 so helps –a and –b series complex gangliosides synthesis completion (Takamiya et al.1996) (Figure 1.3 A).

In firstly generated β-1,4-N-acetylgalactosaminyltransferase (GM2/GD2 synthase; EC 2.4.1.92) gene disrupted mice model, any defects in their nervous system, behaviors and gross appearance were not detected (Takamiya et al. 1996) except being sterile of male mice. Only decreased nerve conduction velocity was seen.In this experiment 10 weeks-old mice were used for both histologic and behavior analysis so no differences between WT and mutant mice were found. On the other hand, TLC results

showed GM3 and GD3 ganglioside expression was much higher in mutant mice brain than WT and it was concluded that increased expression of simple gangliosides can compensate the complex ganglioside absent (Takamiya et al. 1996) (Figure 1.3 B).

Wallerian degeneration (after axonal injury nerve fiber is cut or crush away from the injured site results in degeneration) evidences were demonstrated in B4GALNT1-/- mices' peripheral and central nerves (Sheikh et al. 1999). This result indicated that complex gangliosides are needed for axon integrity maintenance. Therefore accumulated GM3 and GD3 in that mice causes axonal degeneration.

GM2/GD2 synthase enzyme deficient mice were subjected to behavioral tests and progressive neuropathies such as reflexes, strength, motor coordination and balance deficits were detected mutant mice. Additionally hindpaw clasping and impaired extension were seen in mutant mice. Age-dependent neurodegenerative phenotypes such as tremor and catalepsy were also detected in 12 months-old mutant mice (Chiavegatto et al.2000).

In another study, electron microscopy analysis revealed that central and peripheral axonal degeneration, myelin volume reduction and axo-glial junction integrity loss takes place in 12 months-old mutant mice (Yao et al.2014).

β-1,4-N-acetylgalactosaminyltransferase (GM2/GD2 synthase; EC 2.4.1.92) gene deficient mice is used as a model for different diseases. Recent studies showed that this mice model exhibits similar phenotypes with Hereditary Spastic Paraplegia (HSP) patients (Bhuiyan et al. 2019). More than 80 genetic types of this diseases and related gene variants were identified and β-1,4-N-acetylgalactosaminyltransferase gene is one of them which is inherited as autosomal recessive. In the β-1,4-N-acetylgalactosaminyltransferase gene deficient patients have complicated type of HSP in which neurological and lower-extremity problems are seen in juvenile onset. Amyotrophy, dysarthria, ataxia, devolepmental delay and dystonia are clinical features of disease caused by β-1,4-N-acetylgalactosaminyltransferase gene deficiency (Boukhris et al.2013, Harlalka et al. 2013)

As neurodegenerative disorder, Parkinson's disease (PD) is the second most common cause of death which affects almost 1% total population of people over 65 age. Characterized symptoms of PD contains resting tremor, postural rigidity, bradykinesia, autonomic instability, cognitive and emotional disorders. In recent studies, it has been revealed that abnormal brain ganglioside pattern, especially GM1 ganglioside lacking, is

seen in Parkinson's disease (Wu et al.2011). *B4GALNT1-/-* mice model showed PD like symptoms including progressive motor impairments, strial dopamine depletion, strial dopamine neurons death at substantia nigra pars compacta and alpha synuclein accumulation. In this mice LIGA-20, blood brain barrier permable GM1 analog, administration was applied and significant improvements were detected in PD symptoms (Wu et al.2011). In recent study, it has been showed that *B4GALNT +/-* mice developed sporadic Parkinson's diease and physical symptoms were rescued by GM1 oligosaccharide treatment (Chiricozzi et al.2019)

1.4. Sialidases

Sialidases,neurominidases, are responsible enzymes for sialic acid removal from sialoglycoconjugates,glycoproteins,glycolipids or oligosaccharides (Saito et al.2002). In mammals there are four different sialidases and they are controlled by four different genes that are *Neu1, Neu2,Neu3* and *Neu4*. Sialidase *Neu1, Neu2,Neu3* and *Neu4* shows their activity in different subcellular localization; lysosomal (Seyrantepe et al.2004), cytosolic (Miyagi et al. 1985) plasma-membrane associated (Miyagi et al. 1990) and mitochondrial (Yamaguchi et al.2005) respectively.

1.4.1. Sialidase Neu1

Neu1 is the responsible gene for encoding lysosomal sialidase Neu1 enzyme in which deficiency results in sialidosis that is neurosomatic, lysosomal storage disease. NEU1 gene is located on the chromosome 6 in human (Oohira et al. 1985; Harada et al.1987) and this gene is expressed in pancreas most abundantly while less expression is seen in brain (Bonten et al.1996).

Neu1 catalyzes the cleavage of sialic acid residues on glycoproteins, glycolipids (with the help of detergents or sphingolipid activator Sap B), and oligo- or poly-saccharides (Frisch and Neufeld, 1979)

Neu1 is found in the protein complex together with glycosidase β-galactosidase and the carboxypeptidase protective protein/cathepsin A (PPCA) (Verheijen et al.1982;

Pshezhetsky et al.2001). PPCA can be called as chaperone molecule for lysosomal glycosidases because it stabilizes these enzyme in the lysosome and controls their activity. Mutation in the PPCA results in deficient of glycosidase activity and galactosialidosis (D'Azzo et al.1982).

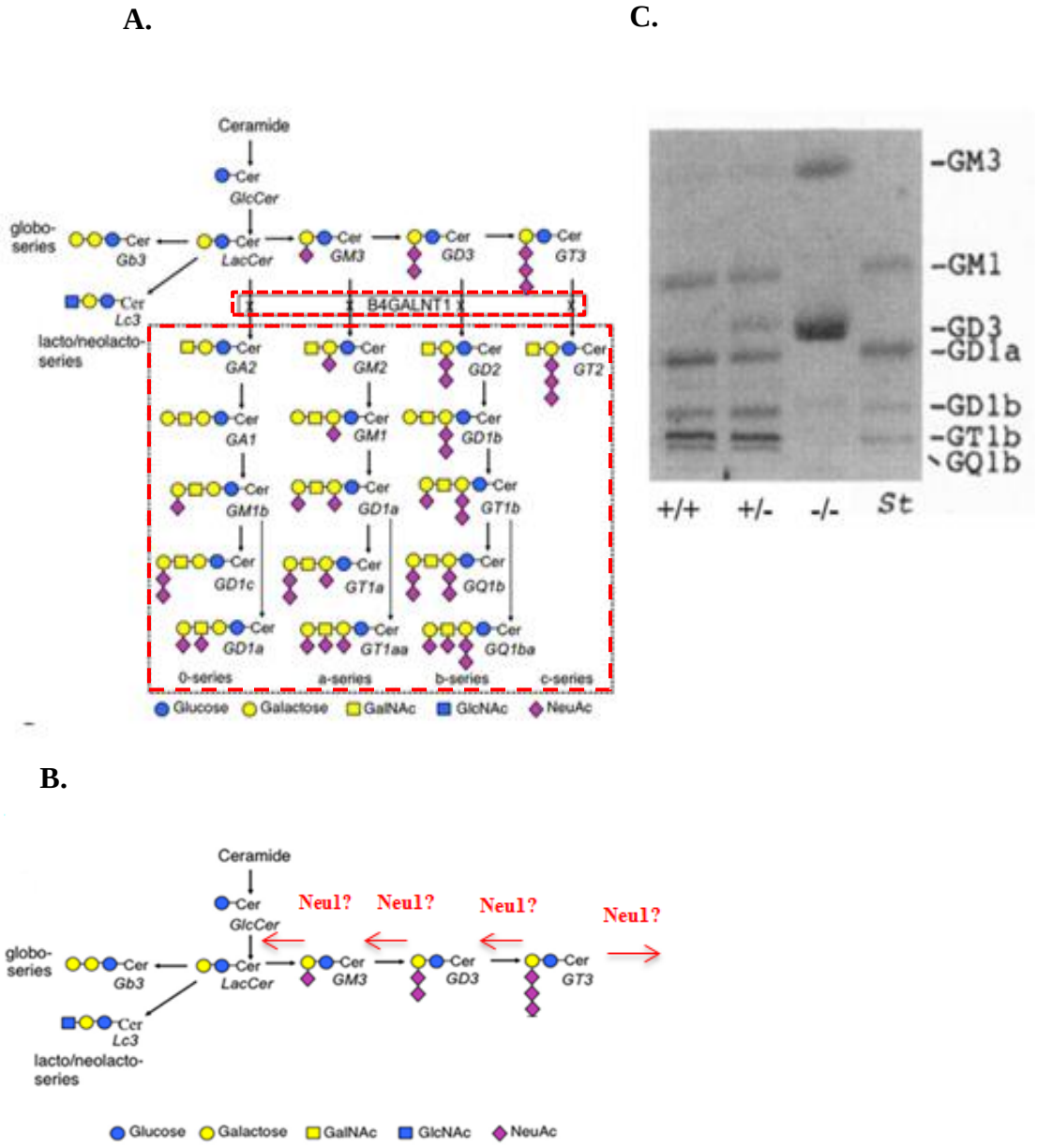

Figure 1.3. Synthesis pathway of gangliosides .Line dash square indicates 0-, a-, b- and c-series gangliosides whose biosynthesis are catalyzed by B4GALNT1 enzyme by courtesy of Yao et al.2014 (A). Potential involment of Neu1 sialidase for sialic removal from simple gangliosides, GM3, GD3 and GT3, in the B4GALNT1 enzyme deficient mice (B). Brain TLC of acidic glycosphingolipids of 12 weeks old normal, heterozygous, and homozygous mutant mice by courtesy of Takamiya et al.1996 (C).

Besides the catabolic role of Neu1 in lysosome, it has role in cellular immune response. For example, activated $CD4^+$ and $CD8^+$ T cells need Neu1 sialidase activity for IFN-γ production. In addition to that Neu1 sialidase activity is needed for IL-4 production (Chen et al.1997;Wang et al.2004). In another study revealed that Neu1 forms a cell surface complex with PPCA and elastinbinding protein (EBP) that is β-GAL spliced variant. This complex provided tropoelastin release and attachment to the elastic fibers on the cell surface by sialidase activity of Neu1 (Hinek et al.1995;Hinek et al.2006). In recent study, complex formation with Neu1, Toll like receptors 2,3, and 4 was demonstrated in the pathogen-induced Toll like receptor activation (Amith et al.2009). In addition to that, altered sialylation in cancer cell is related with the metastasis and invasions (Dennis 1999 ;Hakomori 2002). Because of that sialidase Neu1 activity is important for cancer cells. Inverse correlation between Neu1 expression and metastasis capacity of rat 3Y1 transformants (Miyagi et al.1994) and murine colon adenocarcinoma (Colon 26) cells (Sawada et al.2002),B16 melanomacells (Kato et al.2001) and in human colon cancer HT-29 cells.

Neu1 is located on chromosome 17 in mice (Womack et al.1981) .Neu1 is expressed mostly in kidney and epididymis,moderatelylevels in brain and spinal cord, and lowest in adrenal gland, heart, liver, lung, and spleen (Igdoura et al.1998).

Sialidase Neu2 shows its activity in cytoplasm against oligosaccharides,glycopeptides and gangliosides,especially GM3 ganglioside (Miyagi et al.2012) .Additionally role of Neu2 in cellular differentiation, tumor malignancy, cell growth and apoptosis in some cancer cell lines (Stamatos et al. 2010), neuronal differentiation are demonstrated (Taeko Miyagi and Yamaguchi 2012).

Sialidase Neu3 is membrane associated sialidase and has catalytic activity on GM1, GD1a,GM2 and GM3 gangliosides (Seyrantepe et al.2018). In addition to that it regulates oligosaccharide pattern of ganglioside which affects insulin signaling, cell-cell recognation, differentiation and apoptosis (Miyagi et al. 2012). Also important contribution of Neu3 over apoptosis (Valaperta et al. 2006), immune response, monocyte differentiation (Stamatos et al. 2010) and cancer cells (Takahashi et al. 2015).

Sialidase Neu4 shows its activity on glycoproteins, oligosaccharides, sialylated glycolipids and gangliosides,especially GD1a, GM3 and GM2. It localizes both in lysosomal lumen (Seyrantepe et al.2004) and mitochondria membranes (Yamaguchi et

al.2005) .Additionally, Neu4-/- mice showed increaed ganglioside, ceramide, fatty acidsand cholesterol in brain,lung and spleen (Seyrantepe et al. 2008).

1.5. Lysosomal Storage Diseases

Alteration in the synthesis or degradation of glycosphingolipids, glycoproteins, and oligosaccharides causes appearance of lysosomal storage disease (LSD) pathophysiology. These alterations are generally caused by impairment/deficiency of lysosomal enzyme activity, cofactor protein or lysosomal protein transportation (Neufeld et al.1991). Cellular homeostasis change results in accumulation of specific substrate in the lysosome (Neufeld et al.1991). Lysosomal storage diseases are rare genetic disorders and more than 40 different lyosomal storage diseases are present. In most diseases progressive accumulation of substrate is seen which causes symptoms severity increment over time (Wraith 2004). Also severity of diseases is associated with residual enzyme activity. Additionally onset of these diseases can be divided into three according to remained enzyme activity: early onset (infantile), juvenile onset, late onset (adult). In lysosomal storage diseases, besides substrate accumulation due to lysosomal hydrolase deficiency, secondary metabolite (free oligocytes, glycoaminoacids, gangliosides) accumulation takes place in the cell and urine. Blockage of a degradation pathway in lysosome because of enzyme deficiency causes alteration of secondary metabolites and these alterations are important for diagnosis of LSDs (Breiden and Sandhoff 2020).

1.5.1. Sialidosis

Mutations including splice-site, insertions, deletions, nonsense and missense in NEU1 gene causes sialidosis (Seyrantepe et al.2003).

In sialidosis patients, oligosaccharides and glycopeptides accumulation in tissues and excretion of these compounds in urine and body fluids are observed. According to severity and ages of onset, sialidosis can be divided into two clinical variants which are Type I and Type II (Seyrantepe et al.2003). Type I can be called as mild form of disease in which cherry-red spot-myoclonus syndrome is charachterized. Myoclonus, ataxia and seziures are late onset symptoms and seen in Type I patients at 20-30 age. Type II can be clasified as early onset form of disease with progressive neurologic

deterioration,visceromegaly, dysostosis multiplex and mental retardation symptoms that are seen at birth or early infancy.

1.5.2 Mouse Models with NEU1 Deficiency

Neu1-/- mice show similar symptoms with Type II form of sialidosis including neurodegenerative and systemic impairments and premature death (de Geest 2002). Knockout mice have disease symptoms at birth and progressive accumulation of oligosaccharide in urea, lysosomal expansion in the nervous system, systemic organs and also in muscle and cartilage are seen. In addition to these symptoms, retardation in growth, hepatosplenomegaly, edema at limbs and eyelids, humpback, degeneration in nervous system are noticeable characteristics of this mouse. Their life span is between 6-7 months and at the end of this period, knockout mice have dyspnea, weight loss, edema diffusion, abnormal gait and tremor (de Geest 2002).

Neu1-/- mice and sialidosis patients have many symptoms in common including enlargement of spleen,muscle atrophy and hypotonia, lysosomal vacuolization in kidney that results in progression and diffusion of edema. Besides systemic organs, microglia and macrophages of mice show impairments in nervous system that result in microgliosis (de Geest 2002; Zanoteli et al.2010)

There are many studies to enlight pathogenesis mechanism of Neu1-/- mouse model. In one of this studies, it was established that NEU1 is negative regulator of cellular exocytosis in which it regulates levels of Lysosomal Associated Membrane Protein 1 (LAMP1) (Yogalingam et al.2008).In that mechanism LAMP1 plays essential role including association of lysosome to plasma membrane. However in NEU1 deficient condition, LAMP1 becomes oversialyated and increases docked lysosome number to the plasma membrane which results in excessive exocytosis. This situation is one of the reasons of sialidosis pathology that are splenomegaly, muscle atrophy, hearing loss, neurodegeneration and Alzheimer's disease like phenotype (Figure 1.4 G) (de Geest 2002). As Alzheimer's disease phenotype, oversialylated APP was seen in the absence of Neu1 and accumulated APP was noted in hippocampal neurons of Neu1-/-. Also Neu1−/− mice's cerebrospinal fluid had elevated Aβ42 level (Annunziata et al.2013). In another study, importance of Neu1 activity in phagocytosis of macrophages was shown

(Dridi et al.2013; Seyrantepe et al.2010). Moreover effect of NEU1 in insulin signaling was also demonstrated (Dridi et al.2013).

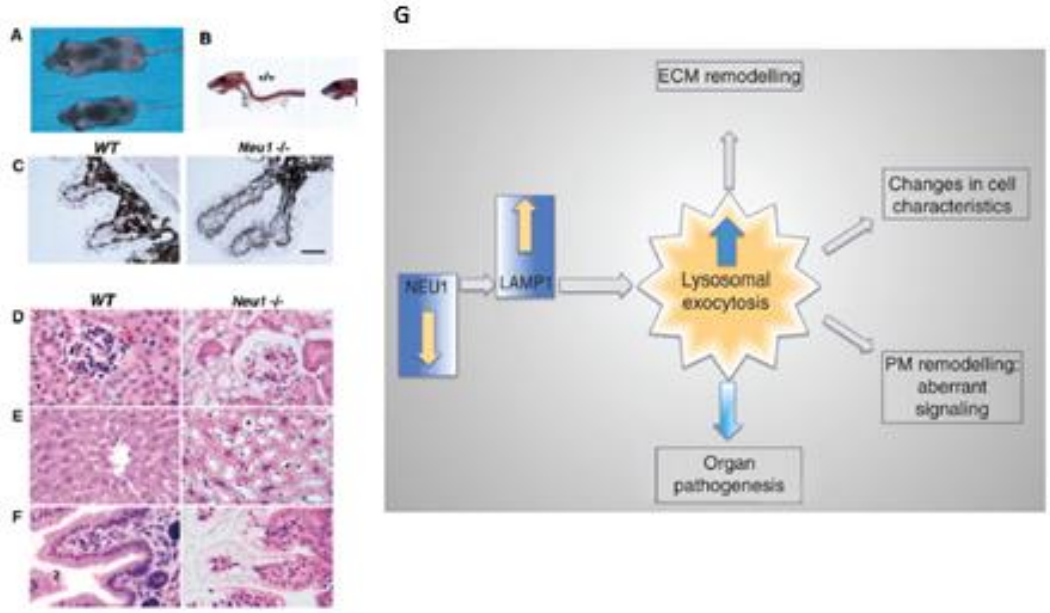

Figure 1.4. Phenotypic findings of Neu1-/- mice. Gross appearance comparision of 1-month-old WT and Neu1-/- mice (A). Skelatal staining of 5-month-old Neu1-/- mice showed cervical spine curvature. Histopathological findigs of 5-month-old Neu1-/- mice by H&E staining (C-F). Ballooned epithelial cells were observed in the eyes of Neu1-/- mice (C). Vacuolation in the kidney was seen (D). Ballooning of Kupffer cells and vacuolation in the hepatocytes (E). Excessively vacuolated apical epithelial cells of Neu1-/- mice' intestinal villi (F) by courtesy of de Geest 2002. Schematic representations of cellular events that takes place in the deficiency of Neu1 and excessive lysosomal exocytosis(G) by courtesy of d'Azzo et al. 2015 .

1.6. Aim of the Study

Sialidase Neu1 is known as lysosomal sialidase. It is involvement in removal of sialic acid residues on glycoproteins, glycolipids and oligo-or polysaccharides was shown *in vivo* studies. Although its ganglioside substrates (GT1b, GD1b, GD2, GD3 and GM3) are known, detailed analysis between Neu1 sialidase and complex gangliosides on the glycolipid metabolism was not performed before. Additionally, GM1 gangliosidosis and Galgt enzyme relation was studied in the β-gal-/-Galgt-/- mice previously (Tessitore et al.2004). However Sialidosis and Galgt enzyme relation or absence of complex

gangliosides' effect on Sialidosis have not been studied. Regarding the possible contribution of Neu1 enzyme on glycolipid metabolism, we aimed to understand altered cellular event in the absence of both Neu1 enzyme and complex gangliosides by generating Neu1-/-Galgt-/- mice. By the comparative analysis with newly generated Neu1-/-Galgt-/- models, existing Neu1-/- and Galgt-/- mice and control group, it was aimed to investigate biological roles of Neu1 and Galgt enzymes on glycolipid metabolism.

CHAPTER 2

MATERIALS and METHODS

2.1. Animals

There were two important mouse strain that were used in this research: Neu1-/- and Galgt-/- mouse strains. Neu1-/- mice was kindly donated by Prof. Alessandra d'Azzo (St. Jude Children's Research Hospital Genetic Department, Tennesse,USA). The Neu1+/- female and male mice were brought from USA to Turkey for placement in accredited animal facility of Izmir Institute of Technology Animal Research Center . Galgt-/- mouse strain was available in Izmir Institute of Technology Animal Research Center and this strain was gifted by Prof. Roger Sandhoff (Technical University of Applied Science in Mannheim, Germany) for the project "Intensified Cooperation (IntenC): Promotion of German-Turkish Higher Education Research" (Project number: 113T025). Heterozygous mice were bred (brothers and sisters were crossed) and animals were placed as each cage include five mice. For maintanence of mice, constant temperature, humidity and 12-h light:dark cycle were provided. Mice were fed as ad libitum. For all animal experiments, Turkish Institute of Animal Health guide for the care and use of laboratory animals was followed. Also ethical permissions were approved by the Institutional Animal Care and Use Committee of the Izmir Institute of Technology. To obtain four desired genotypes (WT, Neu1-/-, Galgt-/-, Neu1-/-Galgt-/-), firstly two female Neu1+/- and one male Galgt+/- mice were bred. Inbreeding was carried out among F2 generations and their offsprings (eight heterozygous female Neu1+/-Galgt+/- with four heterozygous male Neu1+/-Galgt+/-) in order to have control group, single knockouts (Neu1-/- and Galgt-/-) and double knockout (Neu1-/-Galgt-/-) mice (Figure 2.1). Owing to Neu1-/- male and female mice were sterile, Neu1+/- male and female mice were used for breeding. In addition to that Galgt-/- male mice were sterile but Galgt-/- female were not so Galgt+/- male mice were used for crossing with Galgt-/- female mice. Although Neu1-/- mice could live 6-7 month and Galgt-/- mice could live more than 12 month, sudden deaths at the age of 4 month were observed in double knockout mice

group, after that point end point of each genotype was determined as 4-month-old. Significant change in weight loss among mice groups was detected.

In order to understand if changed ganglioside pattern and Neu1 sialidase deficiency impact mice as age-dependent manner, experiment groups were designed as two-and four-month-old mice. Therefore phenotypic, biochemical, behavioral analyses of these mice were compared as two different age groups. When the experiment group reached to two-and four-month-old age, euthanasia was performed by cervical dislocation, mice brains were removed and separated as cortex, cerebellum and thalamus for the biochemical analysis (RT-PCR, Western Blot, DNA Fragmentation assay, TLC) . These brains were snap-freezed in liquid nitrogen and kept at -80°C until usage. Three different mice brains were used for each biochemical analysis. For histologic analysis, mice were anesthetized,brains were fixed by cardiac perfusion method and embedded in OCT filled cryomolds for cryosectioning as 10 µm. Sectioned brains were kept at -80°C until experiment day. During the lifetime of mice, control group, single and double knockout mice groups were weighted every two weeks.

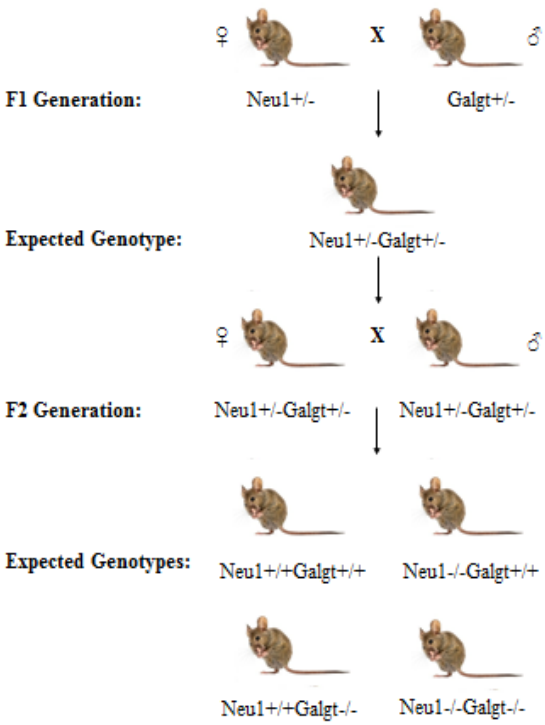

Figure 2.1. Representative breeding scheme for Neu1 and Galgt mice

2.2. Genotyping of Mice

2.2.1. Genomic DNA Isolation

Offsprings were weaned from their parents when they reach to 1-month-old age. Each mouse was labelled from its ear and tail was cut for genomic DNA isolation. Tails were put into Eppendorf tubes and 250µl of lysis buffer (including 10% 1M Tris pH 7.6,2.5% 0.2M EDTA, 20% SDS, 4% 5M NaCl) and 6 µl of Proteinase K (from 25µg/µl solution) were added. Overnight incubation in the shaking incubator for 90 rpm at 55˚C was performed. Next day, centrifugation was applied at 14.000rpm for 10 minutes. After that supernatant was taken to new tubes that included 250µl of 100% isoproponal. Tubes were shaken until DNA become visible and DNAs were taken by a tip and put into new tube including 250µl of 70% ethanol. For removing of impurities, 1 minute centrifugation at 14.000 rpm was done and supernatant was removed. DNA was waited for complete ethanol evaporation for 10 minutes. Then 100 µl of distilled water were added to DNAs and DNAs were incubated at 55˚C for 1 hour. After 1 hour either PCR reactions were performed or DNAs were kept at-20^{0}C until PCR reaction.

2.2.2. PCR Reaction for Neu1 and Galgt alleles

In order to detect wild type and mutant allele of Neu1 and Galgt, PCR reactions were carried out by isolated genomic DNAs. Wild type and mutant allele of Neu1 could be analyzed at the same PCR conditions while seperate PCR conditions were applied to detect Galgt wild type and Galgt knockout alleles. Both Neu1 and Galgt PCRs included approximately 100 ng of genomic DNA in the 50 µl of reaction mix. Neu1 PCR reaction mix contained 0.4 µM of each forward and reverse primer (Table 2.2), 400 µM of dNTP mix, 1.25 unit of Taq polymerase (GenDireX), 10X PCR buffer containing 2 mM of $MgCl_2$. Neu1 PCR conditions were: 1 cycle of 3 minutes at 94^{0}C; 30 cycles of 30 seconds at 94^{0}C, 30 seconds at 58.1^{0}C, 2 minutes at 72^{0}C; and 1 cycle of 10 minutes at 72^{0}C. PCR recation mix for Galgt wild type allele included 0.4 µM of each forward and reverse primer (Table 2.2), 500 µM of dNTP mix, 2,5 unit of Taq polymerase (GenDireX), 10X PCR without MgCl2, 3 mM $MgCl_2$. PCR conditions for Galgt wild type allele were 1

cycle of 3 minutes at 94^0C; 34 cycles of 45 seconds at 94^0C, 30 seconds at 65^0C, 3 minutes at 72^0C; and 1 cycle of 10 minutes at 72^0C. PCR reaction mix for Galgt knock out allele contained 0.4 μM of each forward and reverse primer (Table 2.2), 400 μM of dNTP mix, 1.25 unit of Taq polymerase (GenDireX), PCR buffer containing 2 mM of $MgCl_2$PCR conditions for that allele were 1 cycle of 3 minutes at 94^0C; 34 cycles of 40 seconds at 94^0C, 30 seconds at 61^0C, 3 minutes at 72^0C; and 1 cycle of 10 minutes at 72^0C.

Table 2.1 Primers for Neu1 and Galgt allele determination

Gene	Primer Name	Primer Sequence	Product Size
Neu1	MNTG-1	GACAGGGATCGCCGGGAGCTATGG	WT allele;180 bp
	MNTG-2	CACCAGGCTGAAGTCATCCTCTGC	KO allele;400bp
	lacZ	GATAGGTTACGTTGGTGTAGATGGGCG	
Galgt	Galgt WT-F	CGTGGAGCACTACTTCATGC	WT allele;608 bp
	Galgt WT-R	CTCTCCTCCCCTACCAGGTC	KO allele;1600bp
	Galgt KO-F	TCGTCCTGCAGTTCATTCAG	
	Galgt KO-R	ATATGGCTCCATCGGGCCTC	

2.3. Body Weight Measurement

Body weight of WT,Neu1-/-,Galgt-/- and Neu1-/-Galgt-/- mice was recorded every two weeks from their 6th week to 16th week.

2.4. Thin-Layer Chromatography Analysis

2.4.1. Lipid Isolation

In TLC method acidic and neutral lipids are analyzed separately. For this analysis cortex and cerebellum brain sections of 2 and 4-month-old WT, Neu1-/-, Galgt-/- and Neu1-/-Galgt-/- mice were collected with liquid nitrogen and stored at -80^{0}C until usage.

For experiment 50 mg cortex and cerebellum regions were weighted for each genotype and put into borosilicate tubes. 2 ml of distilled water was added to brain tissues and homogenized by using with Ultra Turrax Homogenizer (IKA, Germany). After homogenization, sonication was applied for 6 (4 x 1.5 min) minutes by Sonicator (Bandelin, Germany). Water was evaporated by nitrogen stream and for extraction 3 ml of 100% acetone was added to samples and centrifugation was done for 5 minutes at 2000 rpm. After centrifugation, upper phase that contains phospholipids and other small membrane lipids were removed. This step was repeated one more time. Then 1.5 ml of chloroform/methanol/distilled water (10:10:1) was added and centrifugation was done for 5 minutes at 2000 rpm. Upper phase was taken a new neutral glass tube , this process was repeated one more time and upper phase was collected to the same neutral glass tube. 2 ml of chloroform/methanol/distilled water (30:60:8) was added to residual time. pellet and centrifugation was done for 5 minutes at 2000 rpm. Upper phase was taken and added to tube containing previous upper phase. This step was repeated one more Then acidic and neutral glycosphingolipids were collected in the neutral tube.

To separate neutral and acidis glycosphingolipids from each other DEAE Sephadex A-25 resin and glass columns were prepared. This ion exchange column should be prepared freshly before the experiment. For this aim 10 ml of chloroform: methanol:0.8M sodium acetate (30:60:8) solution was added into 1gr of DEAE Sephadex A-25 resin (GE Health Care, Little Chalfont, United Kingdom). Solution and resin were incubated for 5 minutes at room temperature and after incubation centrifugation was done for 1 minute at 2000 rpm. Liquid phase was removed and resin was washed with chloroform: methanol:0.8M sodium acetate (30:60:8) solution three times. Then resin was incubated into the same solution for overnight. On the experiment day, liquid phase was removed and resin was washed with the same solution three times for usage.

For glass columns, glasswool was placed into the columns and 2 cm below the glasswool was labeled for resin amount. About 1000 ul resin (fulls 2 cm height) was added above glasswool and columns were washed 8 times with 1000 ul of chloroform/methanol/distilled water (30:60:8). Then new neutral glass tubes were placed below the columns and samples were started to load. After total ganglioside samples loading, 4 ml of methanol was added to glass columns. Obtained liquid in the neutral

glass tube was called as neutral gangliosides. Neutral gangliosides were evaporated with nitrogen stream in the Reacti-Therm Heating module (Thermo, Massachusetts, USA) in 55°C of water. After this process, evaporated samples can be kept at $+4^0$C for one or two days. For acidic ganglioside separation, new neutral glass tubes were placed under the glass columns. 50 mM potassium acetate (2.45g potassium acetate in 50 ml of methanol) was prepared freshly and 5 ml of potassium acetate was added to each column. After that process collected liquid contains acidic gangliosides. Then desalting process was applied to acidic gangliosides by Supelclean LC-18 column (Supelco, Sigma,Darmstadt, Germany). Chromabond Vacuum manifold (Macherey-Nagel, Düren, Germany) was adjusted to 5Hg and Supelclean LC-18 columns were placed on it. Column equilibration was provided by addition of 2 ml methanol, 2 ml potassium acetate, acidic gangliosides and 10 ml of distilled water respectively. Collected liquids under the columns were removed and new neutral glass tubes were put under the Supelclean LC-18 column. Acidic ganglioside elution was done by addition 4 ml of methanol and 4 ml of methanol/chloroform (1:1) solution to columns. Collected acidic gangliosides were evaporated with nitrogen stream in the Reacti-Therm Heating module (Thermo, Massachusetts, USA) in 55°C of water. After this lyophlization process, samples can be kept $+4^0$C for one or two days for analysis (Sandhoff et al.2002).

2.4.1.1. Thin Layer Chromatography

Thin Layer Chromatography method was used to separate ganglioside according to their polarities, structures and weights. Neutral and acidic samples were loaded separately onto 20cm x 20cm silica TLC plates (Merck, New Jersey, USA). Before the experiment silica plate was placed to 100^0C over for 30 minutes to remove humudity on the plate. Before the experiment TLC tank (Camag, Muttenz, Switzerland) was washed with distilled water and 100% methanol respectively and let it dry. For running solution, chloroform/methanol/$CaCl_2$ (60:35:8) was prepared and placed into the TLC tank. Tank was incubated with this solution during 2 hour 15 minutes to provide evaportaion of running solution in the TLC tank equally. Sample loading was performed by Linomat 5 (Camag, Muttenz,Switzerland) machine as automatically. For acidic gangliosides; lyophilized samples were dissolved in 100 ul of chloroform/methanl/distilled water

(10:10:1) solution and 45 ul of this solution was loaded. For neutral gangliosides; lyophilized samples were dissolved in the same amount solution but 20 ul of solution was loaded. Plates containing neutral and acidic gangliosides were placed into the TLC tank and ran for 10 cm.

2.4.1.2. Orcinol Staining

To visualize gangliosides, 0.06 g orcinol was disolved in 3,75 ml of 100% sulfuric acid and 11,25 ml of distilled water in TLC sprayer (Sigma,Darmstadt, Germany). Orcinol solution was waited to cool to prevent burning of plate during staining. This solution was sprayed onto TLC plate and plate was placed on the 120^0 C TLC plate heater (Camag, Muttenz, Switzerland) . When the bands became visible, plate was taken from heater and scanned with the HP scanner system. Ganglioside comparision between genotypes and age groups was done by brain ganglioside standards (Avanti Polar Lipids,Alabaster, Alabama, USA). Each band was analyzed by the ImageJ program.

2.4.2. Urine TLC

To collect urine samples mice were placed to metabolic cages (Techniplast). Cages included enough water and food for 16 hour and mice were stayed at these cages for overnight. Urines of mice were collected after 16 hour and kept at -20^0C until experiment day. To normalize urine amount for each sample, creatine was used as normalization agent and creatine assay kit (cat no ab204537, Abcam, Cambridge, UK) was used for this purpose. Firstly urine samples were centrifuged at 13.000 rpm for 10 minutes and supernatant was taken to new tube. Each urine sample was diluted as 1:50 with distilled water. 50 ul of each sample was loaded to 96-well plate as 2 replicates. 50 ul of distilled water was used as blank and loaded to plate. For creatine measurement, standarts were prepared. 50 ul of stock standard solution and 200 ul of distilled water were mixed and 1:1 serial dilution with distilled water was done from this stock. At the end 6 standards for creatine were prepared. 50 ul of each standard was loaded to plate as two replicates. 50 ul of creatinine detection reagent was added to each well. Plate was

mixed gently by tapping the sides of plate. Incubation for 30 minutes at dark was done and after incubation spectrometric measurement was performed at 490 nm by spectrophotometer (iMark microplate absorbance reader ,Biorad Laboratories, California,USA).

According to creatine amount, required urine amount (500 ng) for each sample was detected. Samples and sugar standards were loaded on 20 cm x 20 cm silica TLC plates (Merck, New Jersey, USA). 0.5 mg/ml of sugar standards (D+ Lactose Monohydrate, D+ Mannose,D+ Glucose,D+Galactose Sucrose, D+ Xylose and D+ Raffinose Pentahidrat (Sigma-Aldrich,Darmstadt, Germany)were prepared and 2 ul of each standard was loaded to TLC plate by glass pipette tips (Blaubrand, Merck, NewJersey, USA). 500 ng of urine samples with 15 ul volume was prepared and loaded to TLC plate after standard loading. For sample running, running solution butanol:acetic acid: water (2:1:1) was prepared and TLC tank was incubated with this solution for 2 hour 15 minutes. TLC plate was pre-heated for 30 minutes at 100^0C oven. Samples were run about 5 hours and then visualization was done by orcinol staining. For orcinol staining 0.05 g orcinol, 10 ml of 100% acetone and 0,5 ml of sulfuric acid were mixed and waited for cooling. This solution was sprayed to the plate and plate was incubated on the 120^0C heater until bands became visible. Then plate scanning with the HP scanner system was done and intensity of each band was analyzed by ImageJ program.

2.5. DNA Fragmentation Assay

In DNA fragmentation method, cortex, cerebellum and thalamus regions of brain were used for 4 genotype and two age groups. Before experiment day, tissues were incubated with 500 ul lysis buffer (10 mM Tris–HCl, pH 8.0, 100 mM NaCl, 25 mM EDTA, 0.5%SDS) and 12 ul of proteinase K solution at 40^0C for overnight .For DNA isolation, phenol-chloroform extraction method was used. After overnight incubation, one volume of phenol:chloroform:isoamyl alcohol (25:24:1) solution was added to samples and shaken for 20 seconds. Centrifugation was done at room temperature for 10 minutes at 13.000 rpm. After centrifugation upper phase was taken and transferred to new tube. These steps were done for thrice. After third repeat, one volume of chloroform was added to tube containing upper phases and centrifugation was done at room temperature for 10 minutes at 13.000 rpm. Then upper phase was transferred to new tube and these steps

were repeated one more time. Following reagents were added to remained upper phase: 3M of NaOAc (0.1 volume x volume of sample) and %100 ethanol (2.5 x volume of (sample+NaOAc). Then tube was shaken and DNA became visible. Tube was placed to -80^{0}C at least one hour. After -80^{0}C incubation, centrifugation at 4^{0}C for 30 minutes at 13.000 rpm was done and supernatant was removed. 150 ul of 70% ethanol was added to pellet and centrifugation at 4^{0}C for 10 minutes at 13.000 rpm was done. Supernatant was removed and ethanol washing step was repeated one more time. After washing DNA pellet was dried at room temperature for 10 minutes. 100 ul of TE buffer was added to DNA pellet and DNA concentration was measured by nanodrop (ND-1000). After nanodrop measurement, 2000 ng DNA samples were calculated and DNA, TE buffer, loading dye mixture was prepared. To visualize fragmented DNA, 2% agarose gel including 0.4μg/ml ethidium bromide was used. Samples were loaded to agarose gel and ran at 50 V constant voltages for 3 hours (Huang et al.1997).

2.6. RT-PCR Analysis

Gene expression analyses were carried out for three different groups of genes: oxidative stress genes (SOD2, catalase ve TTase1), ER stress genes (ATF6, Calnexin ve XBP1) and apaptotic genes (Bax, Bak, Bcl-XL ve Bcl-2). For this analysis 2 and 4-month-old WT,Neu1-/-, Galgt-/- and Neu1-/-Galgt-/- mice brains were dissected as cortex, thalamus and cerebellum, then snap-freezed in liquid nitrogen and kept at -80^{0}C until experiment day.

2.6.1. RNA Isolation

50 mg of brain section was weighted and placed to eppendorf tube containing RNase free beads, then 500 ul of Genezol reagent (Geneaid) was added to tissue. Homogenization (Retsch MM100) was performed for 30 seconds at 25 frequency (1/s). Samples were transferred to new tubes and waited for 5 minutes at room temperature. Then phase separation process was started by addition of 100 ul of chloroform and centrifugation at 15.000xg for 15 minutes at +4^{0}C. Aqueous upper phase was transferred to new tube for RNA precipitation. One volume of 100%isopropanol was added and

samples were incubated for 10 minutes at room temperature. Then samples were centrifuged at 15000xg for 10 minutes at $+4^0$C to form a RNA pellet. Supernatant was removed and continued with RNA pellet. RNA washing was done by adding 1 ml of 70% ethanol to pellet and centrifugation at 16000xg for 5 minutes at $+4^0$C. Supernatant was removed and RNA pellet was air-dried until pellet became invisible at the bottom of tube. RNA was resuspended with 30 ul of RNase-free water and incubated at 55^0C for 10-15 minutes to dissolve RNA pellet. RNA concentration of each sample was measured by NanoDrop Spectrophotometer (ND-1000).

2.6.1.2. cDNA Synthesis

20 ul of reaction mix was prepared including 1X RT buffer,4 mM dNTP mix, 1X RT Random primers, 50 units MultiScribe Reverse Transcriptase, water and RNA respect to each sample's concentration. Reaction was adjusted for 50 ng/ul of cDNA synthesis. c DNA conversion was performed by PCR that had 1 cycle 10 minutes at 25˚C; 1 cycles 120 minutes at 37˚C, 1 cycle 5 minutes at 85˚C conditions. After conversion, to confirm proper cDNA synthesis from each sample's RNA, GAPDH (housekeeping gene) PCR was performed. 25 ul of reaction mixture containing 0.8 mM of GAPDH gene primers, 10 mM of each dNTPs, 1X reaction buffer with MgCl2 and 1.75 units DNA polymerase (GeneAll) and 50 ng concentrated cDNA for each sample was prepared and run into these conditions: 1 cycle 2 minutes at 95˚C; 30 cycles 20 seconds at 95˚C, 15 seconds at 65˚C, 22 seconds at 72˚C; and 1 cycle 3 minutes at 72˚C. To visualize cDNAs, samples were loaded to 1% agarose gel and run at constant 90 volt for 30 minutes.

2.6.1.3. RT-PCR

After cDNA synthesis validation, 20 ul of reaction mixture containing 50ng cDNA, 0.4 uM each primer (Table 2.3) and 1X Roche LightCycler 480 SYBR Green I Master Mix was prepared and samples were subjected to RT-PCR (Roche LightCycler® 96 System) with these conditions: 1 cycle 10 minutes at 95˚C; 45 cycles 20 seconds at 95˚C, 15 seconds at 60˚C, 22 seconds at 72˚C. Reference gene was selected as GAPDH

and normalization of each expression level was done by GAPDH expression level. For each gene 3 replicates were loaded to plate and experiment was repeated as thrice for each genotype and age group. For statistical analysis, average of three mice belongs to each genotype was used in two-way ANOVA on GraphPad Prism software.

Table 2.2 Primers that are used in RT-PCR

Gene	Primer Sequences	PCR Product (bp)
ATF6	F:5'- TGGAAGTGGGAAGATCGGGA-3', R: 5'-AGGACAGAGAAACAAGCTCGG-3'	354
Calnexin	F:5'- ATTGCCAACCCCAAGTGTGA-3', R: 5'-TCCAGCATCTGCAGCACTAC-3'	362
XBP1	F:5'- TCCGCAGCACTCAGACTATG-3', R:5'-GACTCTCTGTCTCAGAGGGGA-3'	360
SOD2	F:5'- GTGTCTGTGGGAGTCCAAGG-3', R: 5'-CCCCAGTCATAGTGCTGCAA-3'	339
Catalase	F:5'- TTCGTCCCGAGTCTCTCCAT-3', R: 5'-GAGGCCAAACCTTGGTCAGA-3'	351
TTase1	F:5'- CTGCAAGATCCAGTCTGGGAA-3', R: 5'-CTCTGCCTGCCACCCCTTTTAT-3'	322
Bcl-2	F:5'- CGCAGAGATGTCCAGTCAGC-3', R: 5'-TATGCACCCAGAGTGATGCAG-3'	369
Bcl-XL	F:5'- TCAGCCACCATTGCTACCAG-3', R: 5'-GTCTGAGGCCACACACATCA-3'	356
Bax	F:5'- AGGATGCGTCCACCAAGAAG-3', R: 5'-CTTGGATCCAGACAAGCAGC-3'	306
GAPDH	F:5'- CCCCTTCATTGACCTCAACTAC-3', R:5'-ATGCATTGCTGACAATCTTGAG-3'	347

2.7. Western Blot Analysis

In order to homogenize brain samples, 500µl, 250µl and 100µl of protein lysis buffer (containing (1% TritonX100, 50mMHepes, 150mM NaCl, 10%Glycerol, 50mM Tris-Base, 1%PMSF, 1% protease inhibitor) was added to cortex,cerebellum and thalamus region respectively. Brain samples inside the lysis buffer were homogenized by mini homogenizator. After that process, the samples were incubated on ice for 1 hour and during 1 hour samples were vortexed every 10 minutes. After 1 hour incubation,

centrifugation was done for 15 minutes at 0^0C 14000rpm. Then supernatant including protein was transferred to new Eppendorf tube. To determine protein concentration of each sample, Bradford assay was performed. For this purpose, 1:80 (2ul of protein+158ul of distilled water) dilution was done for protein samples. To create a standard curve, BSA solution was used as standard and stock BSA solution was serially diluted to 100 µg/ ml, 80 µg/ ml,40 µg/ ml,20 µg/ ml BSA solutions. Samples and standards were put into 96 well plate as 50ul of diluted proteins and BSA solutions, 200 ul of Bradford Reagent (SERVA Electrophoresis Gmbh,Heidelberg,Germany). Samples and Bradford Reagent were incubated for 10 minutes at dark. Then absorbance of each samples were measured at 595 nm by microplate reader (iMark microplate absorbance reader ,Biorad Laboratories, California,USA). According to the BSA solutions absorbance, a standard curve graph was created and absorbance-concentration equation of this graph was used to calculate samples' concentration. By using these concentration required volume for 20ug protein was dtermined for each samples.

After determination of required volume for equal amount of protein in each sample, protein, water and loading buffer (including 40% Glycerol, 240mM Tris-HCl pH 6.8,8%SDS, 0.04%Bromophenol Blue, 5% β-mercaptoethanol) were mixed and these samples were boiled at 95^0C for 10 minutes. Before the sample preparation, 10% resolving gel (3 ml of Lower buffer, 4 ml of Acrylamide, 5 ml of water, 60 ul of SDS, 60 ul of APS, 6 ul of TEMED) and 5% stacking gel (1.5 ml of Upper buffer, 1ml of acrylamide, 3.5 ml of water, 60 ul of SDS, 60 ul OF aps, 6 ul of TEMED) were poured and waited for polymerization. Then sampled were loaded to that gel and proteins were separated depending on their molecular weights at 80V constant voltage for 2 hours in running buffer (0.25M Tris-Base, 1.92M Glycine, 1%SDS). After running, proteins were transferred to nitrocellulose membrane (BioRad) and let the proteins transfer in transfer sandwich with the help of transfer buffer (48mM Tris-Base, 39mM Glycine, 20%Methanol, pH 9.2) at 0.25A constant amper for 1hour and 15 minutes. After this process, blocking was done with 5% non-fat dried milk in PBS-T for 1 hour at room temperature on the shaker. After 1 hour, three times PBS-T washing was done for 5 minutes each. Primary antibodies were diluted in red solution (5% BSA, 0,02 NaAzide, phenol red in PBS-T, pH 7,5). Overnight incubation was done with corresponding primary antibodies Fas-Ligand(1:1000, Cell Signaling Technology), Caspase-9 (1:1000, Cell Signaling Technology), Caspase-3(1:1000, Cell Signaling Technology), BiP (1:1000, Cell Signaling Technology), at 4^0C on the shaker. β-actin (1:1000, Cell Signaling

Technology)was used as internal control and each blot was incubated with β-actin as 1hour at room temperature. On the following day, three times PBS-T washing was done for 5 minutes each and incubated with HRP-conjugated secondary antibody (1:10000 in blocking buffer) (Jackson ImmunoResearch Lab) during 1 hour at room temperature. As final washing, three times PBS-T washing was done for 5 minutes each. For protein visualization, LuminataTM Forte Western HRP Substrate (Millipore) was poured onto the blot and images were taken by Fusion SL, Vilber imaging system. For protein band intensity evaluation, Image J software was used and each band was normalized to its corresponding β-actin band intensity. Then GraphPad Prism software was used for statictical analysis.

2.8. Histologic Analysis

For histologic analysis 2 and 4-month-old WT,Neu1-/-, Galgt-/- and Neu1-/-Galgt-/- mice were anesthetized with intraperitonal injection of (ketamine/xylazine) and transcardiac perfusion method was performed with 0.9% NaCl followed by 4% paraformaldehyde in PBS (freshly prepared,ice-cold). For post-fixation, brains were incubated in 4% paraformaldehyde solution for overnight at 4^0C. Next day sucrose gradient was done and brains were incubated in 10% and 20% sucrose solution for two hours at $+4^0$C. Then soaked in 30% sucrose solution until tissue sinking at $+4^0$C. Brain tissues were embedded in OCT (Sigma-Aldrich, USA) filled mould and kept at -80^0C prior to cryostat sectioning. Coronol brain sections were collected with Cryostat (LeicaBiosystems, United States, CM1850-UV) as 10 um thickness.

2.8.1. Hematoxylin-Eosin Staining

Cortex, thalamus, hippocampus and cerebellum regions of each brain was stained with Hematoxylin-Eosin to understand morphological changes in genotype and age dependent manner. Taken slides from -80^0C were subjected to gradiual thawing on ice and at 55^0C incubator for 15 minutes to keep brain sections on the slide. Slides were washed with 1XPBS for 5 minutes and then rinsed with distilled water for 2 minutes. After elimination of water on the slides, Gill's hematoxylin (Merck, Germany) dye was

put onto each brain and waited for 3 minutes. Slides were washed with distilled water and running tap water for 1.5 and 2.5 minutes respectively. Differentiation step was applied with 70% ethanol:1N HCl (99:1, v/v) for 30 seconds and followed with tap water and distiiled water washing for 3 and 2 minutes respectively. Counterstaining was done with eosin Y solution 0.5% alcoholic (Merck, Germany) for 20 seconds. Dehydration was provided by 95% and 100% ethonal washing for 2 times as 2 minutes. After complete dehydration on the slides, slides were mounted with mounting medium (Richard-Allan scientific^{TM} cytoseal XYL,Thermofisher,UK). Then cortex,thalamus,hippocampus and cerebellum regions of brains were photographed on light microscopy (Olympus BX53) as 10x and 20x magnification.

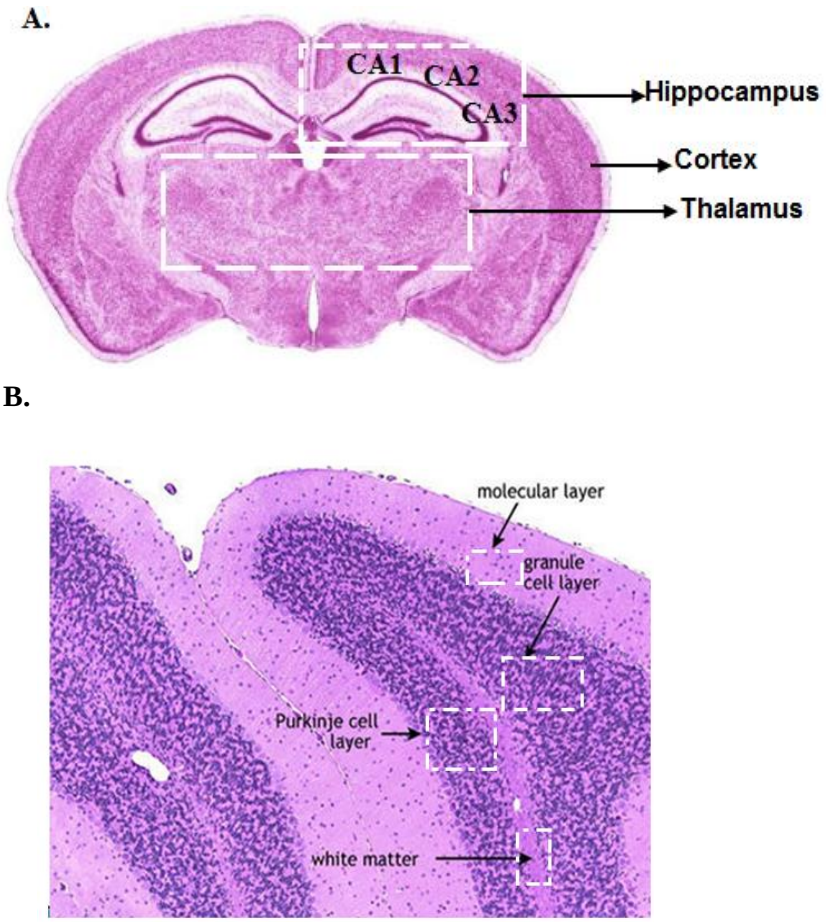

Figure 2.2. Coronal section of mouse brain representing hippocampus, cortex and thalamus regions (A) cerebellum including molecular layer, granule cell layer, Purkinje cell layer, and white matter (B) by courtesy of Woods et al 2013.

2.8.2. Cresyl Echt Violet Staining

To visualize neuron structure differences among different genotypes and age group, Cresyl Echt Violet staining was performed.

Gradual thawing of slides were performed as mentioned previous staining method. Slides were washed with 1XPBS for 5 minutes and let them dry. 20 ul of Cresyl violet dye (ScyTek Laboratories, Utah, USA) was dropped on each brain and incubated for 5 minutes. Then slides were immersed into distilled water for 5 seconds and into 100% ethanol for 10 seconds twice. Then slides were waited to dry and mounted with mounting medium(Richard-Allan scientific^{TM} cytoseal XYL,Thermofisher,UK). Images of cortex,thalamus,hippocampus and cerebellum regions of brains recorded with light microscopy (Olympus BX53) as 10x and 20x magnification.

2.8.3. Periodic acid-Schiff Staining (PAS)

In this staining technique, glycosphingolipid accumulation was detected in mouse brains.

Gradual thawing process was done and slides were washed with 1XPBS for 5 minutes and then rinsed. Slides were incubated with Carnoy's Solution (ethanol:chloroform: acetic acid / 6:3:1) for 10 minutes. After that slides were washed with distilled water for 2 minutes and rinsed.30 ul of 0,5% Periodic Acid solution (Merck,Germany) was dropped on the each brain and incubated for 5minutes. Then tap water and distilled water washing was done for 3 and 2 minutes respectively. After elimination of excess water on the brains, 30 ul of Schiff's reagent (Merck,Germany) was dropped on the each brain and 12 minutes incubation was done. Slides were washed with tap water and distilled water for 5 and 2 minutes respectively. After rinsing, slides were stained with Gill's hematoxylin (Merck, Germany) for 1.5 minutes. Then slides were washed under running tap water for 5 minutes. Dehydration was done with gradual ethanol washing. Slides were immersed into 70% ,96% and 100% ethanol for 1 minutes two times. After complete dehydration slides were mounted with mounting medium(Richard-Allan scientific^{TM} cytoseal XYL,Thermofisher,UK) and image of brain

regions were photographed with light microscopy (Olympus BX53) as 10x and 20x magnification

2.8.4. Luxol-Fast Blue Staining

To detect demyelination of axons, brains were dyed with Luxol-Fast Blue.

After gradual thawing and 5 minutes 1XPBS washing, slides were incubated with cold 100% acetone for 10 minutes. Then slides were washed with 1XPBS for 5 minutes and waited for drying. After that brains were dyed with Luxol-Fast Blue (ScyTek Laboratories, Utah, USA) and incubated at 60^0C incubator (ScyTek Laboratories, Utah, USA) during 2 hours. After incubation, slides were washed with distilled water and immersed into 0.05% lithiumcarbonate solution for 10 seconds as two times. Then slides were washed with distilled water two times for 5 seconds. Excess water was eliminated on the brains and brains were incubated with %0.1lik Cresyl Echt Violet (ScyTek Laboratories, Utah, USA) for 3 minutes. After incubation, slides were washed with distilled water and 100% ethanol 3 times for 5 seconds. Excess water was removed on the slides and mounting medium(Richard-Allan scientific^{TM} cytoseal XYL,Thermofisher,UK) was dropped on the slides. Then microscope image of brains were recorded with light microscopy (Olympus BX53)

2.9. Immunohistochemical Staining

2.9.1. Anti-NeuN Staining

To detect neuron number decrease or increase in mouse brain anti-NeuN staining was done for cortex,thalamus,hippocampus and cerebellum regions of 4 month-old WT,Neu1-/-,Galgt-/-,Neu1-/-Galgt-/- mice brain.

As mentioned histlogical analysis, gradual thawing was applied to slides. Then slides were washed with 1X PBS for 10 minutes. Then incubated in col acetone for 15 minutes. Slides were washed two times with 1X PBS for 5 minutes. After drying of slides, slides were placed into humidified chamber and blocked with blocking buffer (5% goat

serum and 0.3% Triton X-100 in PBS) for 1 hour at room temperature. After blocking, anti-NeuN primary anybody (Cell Signaling Technology, The Netherlands) was diluted as 1:50 in blocking buffer and slides into humidified chamber were incubated with this antibody for overnight at $+4^0$C. Next day, slides were washed three times with 1X PBS for 5 minutes. Goat anti-rabbit Alexa Fluor 568 secondary antibody was diluted in blocking buffer as 1:500 and slied into humidified chamber were incubated with secondary antibody for 1 hour at room temperature and dark. Then 1X PBS wash was done for 5 minutes as three times. Slides were mounted with mounted with Fluoroshield mounting medium including DAPI (Abcam, Cambridge, UK) and fluoresence images of cortex,thalamus, hippocampus and cerebellum region were taken by fluorescent Microscopy (BX53, Olympus, Germany) at the same light intensity for each genotype. To make sure about specific staining negative control(incubated with just secondary antibody) was used and signal was not detected from this control at the same light intensity. Neuron intensity for each genotype and each region was measured by Image J software.

2.9.2. Anti-CNPase Staining

To detect oligodendrocyte intensity of 4 month-old WT,Neu1-/-,Galgt-/-,Neu1-/-Galgt-/- mice brains, anti-CNPase staining was performed.

After gradual thawing of slides, slides were incubated with 4% PFA in 1X PBS for 15 minutes. Then slides were washed three times with 1X PBS for 5 minutes. After that slides were immersed into 100% cold methanol. Slides were washed with 1X PBS for 5 minutes. Slides were put into humidified chamber and blocked with blocking buffer (5% goat serum and 0.3% Triton X-100 in PBS) for 1 hour at room temperature. Anti-CNPase primary antibody (Cell Signaling Technology,The Netherlands) was diluted in blocking buffer as 1:100 and slides into humidified chamber were incubated with primary antibody for overnight at $+4^0$C. Next day slides were washed three times with 1X PBS for 5 minutes. Goat anti-rabbit Alexa Fluor 488 secondary antibody was diluted in blocking buffer as 1:500 and slides were incubated with secondary antibody for 1 hour at room temperature and humidified chamber. Then slides were washed three times with 1X PBS for 5 minutes each. Mounting was done with Fluoroshield mounting medium

including DAPI (Abcam, Cambridge, UK). Fluorescence images of cortex region were recorded with fluorescent Microscopy (BX53, Olympus, Germany) at the same light intensity for each genotype. As previously describied, negative control was used. Oligodendrocyte intensity of each brain was determined by Image J software.

2.9.3. TUNEL assay

In order to detect apoptosis in tissue, 4 month-old WT,Neu1-/-,Galgt-/-,Neu1-/-Galgt-/- mice brains were subjected to TUNEL assay (PROMEGA-DeadEnd^{TM}, Madison, USA)

Firstly gradual thawing of slides were provided and slides were washed in 1X PBS for 5 minutes. For apoptosis detection, slides were fixed by immersing in 4%PFA in PBS for 15 minutes firstly. Then slides were washed two times in PBS for 5 minutes each. For permeabilization, 20 µl of 20µg/ml of Proteinase K (stock proteinase K as 10 mg/ml and diluted as 1:500 in 1X PBS solution) solution was dropped to each brain on the slide and incubation was done for 20 minutes in room temperature. After slides were washed in 1X PBS for 5minutes.Slides were fixed again in 4% PFA in PBS for 5minutes.Slides were washed in 1X PBS for 5minutes. After this step, additional steps were performed for positive control. Slide that was selected as positive control was incubated with DNase I buffer for 5 minutes at room temperature in which 100 µl of DNase I buffer was dropped to each brain on the slide. Then 10µl of DNase I buffer containing DNase I was added to each brain and incubated for 10 minutes at room temperature. Then positive control slide was washed three times with distilled water for 2 minutes each. After this step, both experiment and positive control slides were equilibrated by adding 20 µl of equilibration buffer to each brain and incubating at room temperature for 5 minutes. Then 50µl of TdT reaction mix (containing 45µl of equilibration buffer, 5µl of nucleotide mix and 1 µl of rTdT enzyme) was added to brains and incubated for 60 minutes at 37^0C in a humidified chamber in dark. For negative control, selected brain was incubated with TdT reaction mix including deionized water instead of rTdT enzyme. Reaction was stopped by adding 20 µl of 2X SSC to each brain and incubating for 15 minutes. Slides were immersed three times into 1X PBS, 5 minutes each. Then PI staining was performed by incubation of slides with freshly diluted propidium iodide solution ,1µg/ml in 1X PBS, (stock PI is

1mg/ml) for 15 minutes at room temperature in the dark. After PI staining slides were washed three times with distilled water for 5 minutes each. Then slides were mounted with mounting medium. Apoptotic cells were detected by fluorescent Microscopy (BX53, Olympus, Germany) at the same light intensity for each genotype. Prepared negative and positive controls were used. Positive control was treated wşth DNase I to form DNA break and to detect apoptosis by reacting with TdT that gave green fluorescent light. Negative control was not treated with rTdT enzyme so no green light detection was accepted. PI dyed nuclei as red so apoptotic cells were recognized as yellow color. Image J software was used for determination of colocolized green and red fluorescent light intensity for each genotype.

2.10. Behavioral Tests

Four different behavioral tests were performed to understand effect of altered glycosphingolipid pattern on brain regions and functions.

2.10.1. Rotarod Test

In this test, mice's spending time on the accelerating rod (Pan-Lab Harvard Aparatus, Barcelona, Spain) was recorded to analyze motor coordination and activity impairment of mice as genotype and age dependent manner. Before the experiment, mice were put onto rod moving at constant speed and tried to learn balance and walk on this rod. Then each mouse put on the accelerating rod for three times in the experiment day .During walking of mouse on the rod, rod's speed was increased from 4 rpm to 40 rpm in 5 minutes (Miklyaeva et al. 2004). Time on the rod and speed of rod when the mouse felt down were recorded for each mouse. For this test, 6 mice per each genotype and age group were used. Statistical analysis of records was done by using GraphPad Prism software.

2.10.2. Passive Avoidance Test

In this test, effect of altered ganglioside pattern on short-term memory and hippocampus region of brain was detected. Test setup included two separated box as dark and light. Light box was illuminated with a lamp and this box was greater than dark box. These dark and light boxes were separated from each other with moving door. Experiment lasted during three days that were habituation, training, test days.

At the first day, mouse was put into light box as faced to closed door and waited for a minute. After a minute door opened and let mouse discover both light and dark boxes. When mouse entered to dark boxes, door automatically closed. After 10 seconds in the dark box, mouse was taken from box and put into its cage.

At the second day, the first day procedure was repeated but when mouse entered to dark box, mouse was subjected to 0.2 mA electrical shock for 2 seconds. After electrical shock, mouse was put into its cage.

At the third day, mouse was put into light box and door was opened to let mouse enter the dark box. Latency time to enter the dark box was recorded with ShutAvoidv1.8 (Harvard Apparatus). If mouse did not enter the dark box at the end of 300 seconds, door closed automatically and experiment was finished (Yamanaka et al. 1994) (Liu et al. 1997). 6 mice were tested for each genotype and age group. Records belongs to third day was statistically analyzed by GraphPad Prism software.

2.10.3. Limb Grip Strength Measurement Test

In this test, relation between altered ganglioside pattern and nerve-muscle function,muscle strength was conducted. Before the experiment,Grip Strength Meter (IITC LifeScience, USA). was reset and adjusted as gram. Tested mouse was held from its tail and subject to hold the T-shaped bar with its forepaws. When the mouse grabs the bar with its forepaws, mouse was moved as horizontally. During test, the mouse had to hold bar symmetrically with its two forepaws. The mouse was pulled as constant speed and force until it stopped to hold the bar. At that point grip strength was recorded. If mouse hold the bar with its only one forepaw or used its hindpaws, this record was eliminated. To reach the best performance, test was repeated as thrice (De Luca et al.2008). 6 mice were tested from each genotype and two age groups. Grip strength recors were analyzed by GraphPad Prism software.

2.10.4. Open Field Test

In this test anxiety like behavior, locomotors activities and sedation of mice were analyzed. For this test, 45cm x 45 cm square box surrounded with 40 cm height wall was used. This box had two different floor colors that were white and black. For detection of mice from camera, black floor was used for white mice and white floor was used for black mice. Before 30 minutes from experiment, mice were put into experiment room for habituation (Seibenhener et al. 2015). After habituation, mouse was hold from its tail and put into the corner of box. During 5 minutes, movement of mouse inside the box was recorded with camera and analyzed by SMART Video software (Panlab/Harvard Apparatus). Software detected border and center of square box and recorded the time that mouse spend both border and center of the box. Additionally total walking distance of mouse was recorded by the software. After 5 minutes, mouse was put into its cage. 6 mice per group were tested. Statistical analysis was done with Graphpad Prism software.

2.11. Statistical Analysis

Statistical analysis was done by using GraphPad QuickCalcs (GraphPad Software, La Jolla, CA, USA) statistical software. All data were represented as the mean ± SEM. In order to detect differences, two-way-ANOVA test was used for Westen Blot, RT-PCR, TLC,and behavioral, one-way-ANOVA was used for and immunohistochemical analysis. If a p value less than 0.05, it was accepted as statistically significant.

CHAPTER 3

RESULTS

3.1. Genotyping of Mice for *Neu1* and *Galgt* alleles

In order to detect wild type and mutant allele of Neu1 and Galgt genes, PCRs were performed by using Neu1 and Galgt allele-specific primers respectively. Alleles of genes (+/+,+/-,-/-) were evaluated according to visiualized amplified bands on the agarose gel (Figure 3.1 A-C).

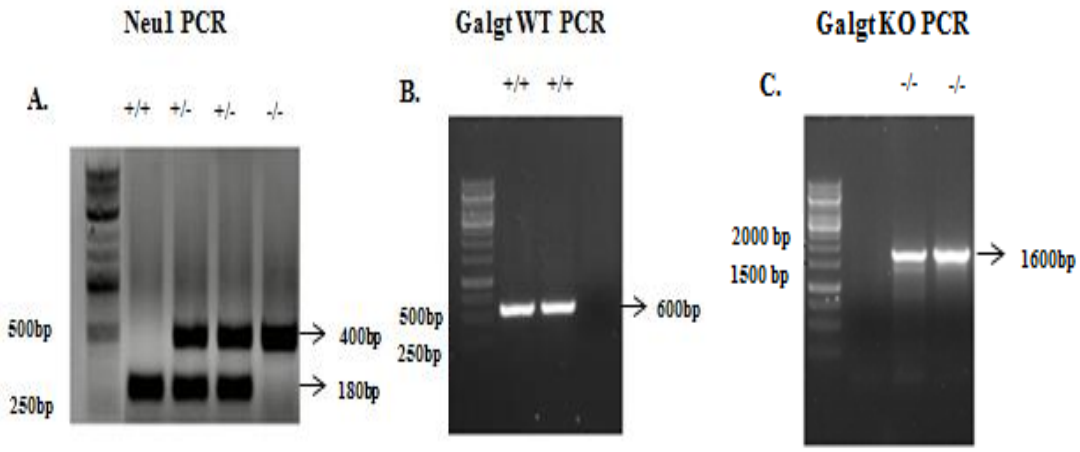

Figure 3.1. Genotyping of Neu1 wild type and knockout (A) Galgt wild type (B) Galgt knockout allele (C) Neu1 allele-specific PCR result for a 180 bp fragment in wild type mice (+/+), 400 and 180 bp fragments in heterozygous (+/-) mice, and 400bp fragment in homozygous (-/-) Neu1 deficient mice(A). Galgt wild type allele-specific PCR result for amplifying 600bp fragment (B).Galgt knock out allele-specific PCR result for amplifying 1600bp fragment (C).

3.2. Body Weight Measurement and Gross Appearance

WT,Neu1-/-,Galgt-/- and Neu1-/-Galgt-/- male and female mice' weight were recorded in every two weeks from their 6th week to 16th week. It was clearly seen that female and male mice's weight ordered from the highest to the lowest as WT, Galgt-/- ,Neu1-/- and Neu1-/-Galgt-/- along 16 weeks. WT and Galgt-/- mice continued to gain weight during 16 weeks while weight of Neu1-/- and Neu1-/-Galgt-/- mice remained stable.

When looked at the relative weight of male mice's compared to WT at their 16th week, significant decrease was observed in Neu1-/- (35%), Galgt-/- (13%) and Neu1-/-

Galgt-/- (52%) mice compared to WT (Figure 3.2 B). Also Neu1-/- (16,7 ± 1,2 g) and Neu1-/-Galgt-/- (12,5 ± 1,1 g) mice had lower weight than Galgt-/- mice (22,8 ± 1g). The lowest weight was detected in Neu1-/-Galgt-/- mice (Figure 3.2 B).

In relative weight of female's mice, decrement in Neu1-/- (12%) and Neu1-/-Galgt-/- (45%) mice' weight was obviously seen compared to WT (Figure 3.2 D). Galgt-/- mice (22±1g) had similar weight with WT (21,25 ± 0,75 g). Neu1-/-Galgt-/- mice had the lowest weight (11,75 ± 1g) at the end of 16 weeks (Figure 3.2 D).

Physical differences could be seen among 4-month-old WT,Neu1-/-,Galgt-/- and Neu1-/-Galgt-/- mice (Figure 3.2 E). Neu1-/- and Neu1-/-Galgt-/- mice were smaller than WT and Galgt-/- mice. Additionally, spinal curvature was detected in both Neu1-/- and Neu1-/-Galgt-/- mice. Moreover Neu1-/- and Neu1-/-Galgt-/- mice had swollen body compared to age-matched littermates.

3.3. Thin Layer Chromatography Analysis

In order to understand if Neu1 enzyme plays a role in the ganglioside metabolism of brain, TLC analysis was carried on for both neutral and acidic gangliosides. 2- and 4-month-old WT, Neu1-/-,Galgt-/- and Neu1-/-Galgt-/- mice brain's cortex and cerebellum regions were analyzed. To detect changed ganglioside pattern, GM1, GD1a, GD1b, GT1b, GD3, GM3 and o-acetyl GD3 band intensities were measured by ImageJ program and two-way ANOVA statistical analysis was done by GraphPad software.

In cortex region, 2- and 4-month old WT and Neu1-/- mice brain samples showed similar pattern for both neutral and acidic ganglioside. In these samples, -a series gangliosides, GM1 (Figure 3.4 A), GD1a (Figure 3.4 B), and –b series gangliosides, GD1b (Figure 3.4 C) , GT1b (Figure 3.4 D) were clearly detected.

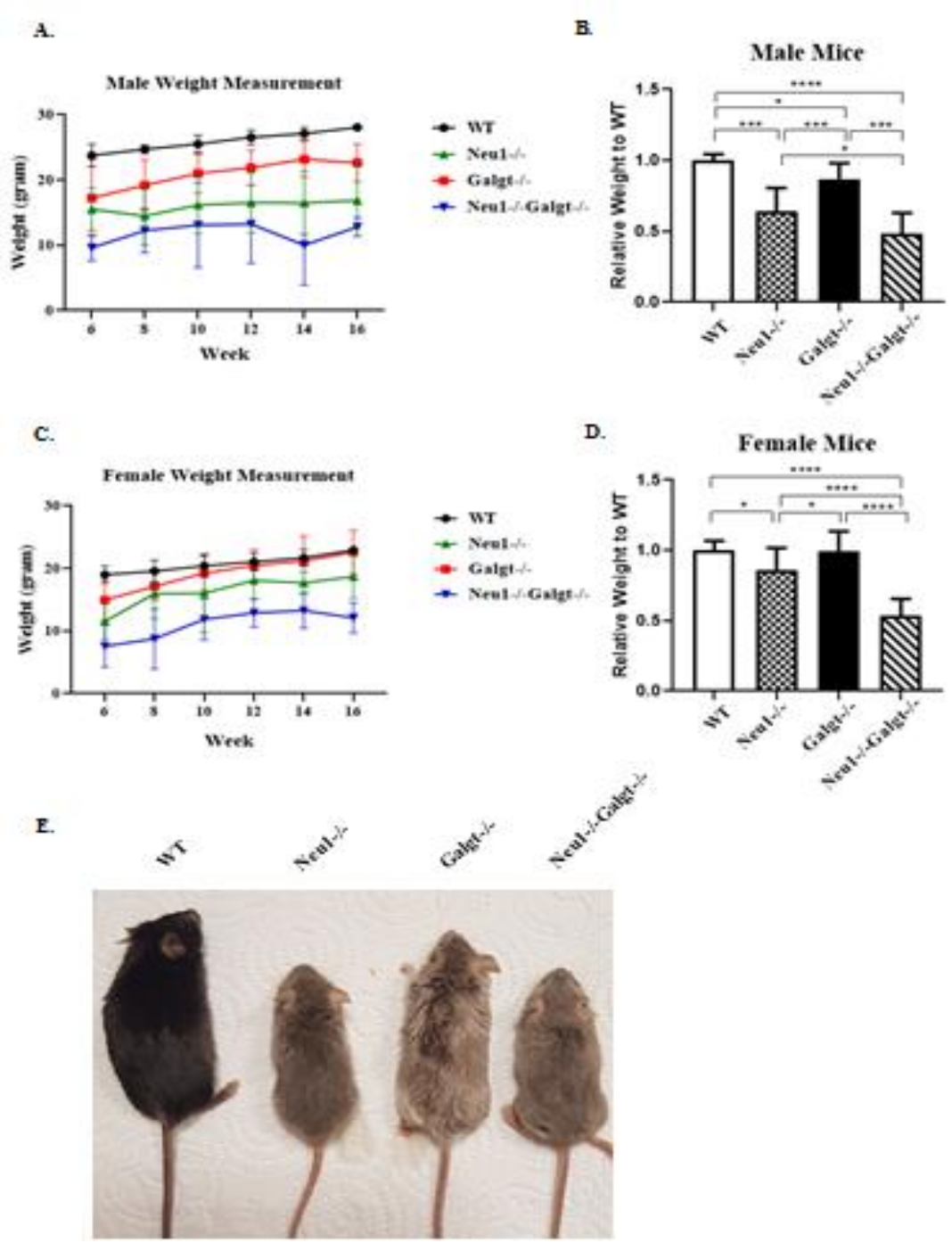

Figure 3.2. Weight measurements belonging to male (A) and female (C) WT, Neu1-/-,Galgt-/- and Neu1-/-Galgt mice from 6th week to 16th week. Relative weight ratio of male (B) and female (D) Neu1-/-, Galgt-/- and Neu1-/-Galgt mice to WT at the 16th week. Gross appearance of 4-month-old WT, Galgt-/-, Neu1-/- and Neu1-/-Galgt-/- mice from left to right (E). Data were reported as means ± SEM. One-way ANOVA statistic method was used to determine significancy of data (*p<0.05,**p<0.025, ***p<0.001 and ****p<0.0001)

However these gangliosides were not seen in 2-and 4-month old Galgt-/- and Neu1-/-Galgt-/- mice brain. This situation can be explained by absence of Galgt enzyme ,catalyzes synthesis of -o ,–a,–b and -c series complex ganglioside, in these mice groups. Althought no complex ganglioside determination in Galgt-/- and Neu1-/-Galgt-/- mice, abnormal expresion of LacCer (Figure 3.7),GM3 (Figure 3.5 A),GD3 (Figure 3.5 B) and o-Acetyl GD3 (Figure 3.5 C) gangliosides were detected. This result indicated that a compensation mechanism play role in the absence of Galgt gene and complex gangliosides. However abnormal expression of small gangliosides, GM3,GD3 and o-Acetyl GD3, was not detected as age-dependent manner so progressive accumulation was not valid for these mice groups (Figure 3.5 A-C). Since both GM3 and GD3 gangliosides exhibited decreased expression in 4-month-old Galgt-/- mice compared to 2-month-old counterpart (Figure 3.5 A-B). Additionally, no significant differences were detected between 2-and 4-month-old Neu1-/-Galgt-/- mice for GM3, GD3 and o-Acetyl GD3 ganglioside expression (Figure 3.5 A-C). Galgt-/- and Neu1-/-Galgt mice had elevated LacCer level in both 2-and 4-month-old group (Figure 3.5). This increase compared to WT and Neu1-/- mice could be the explanation for that Galgt enzyme has effect on LacCer. In normal conditions, GA2 is synthesized from LacCer by Galgt enzyme. In addition to that GM3 is also synthesized from LacCer. Galgt enzyme deficiency in Galgt-/- and Neu1-/-Galgt-/- mice could block GA2 synthesis from LacCer so this situation resulted in LacCer accumulation. Also elevated LacCer level could lead GM3 and GD3 accumulation in these mice. However no changes were detected in Neu1-/- mice compared WT so it could be said that Neu1 enzyme has no role on degredation of LacCer, *in vivo*. Progressive accumulation of LacCer was noted in which 4-month-old group had higher level of LacCer compared to 2-month-old group (Figure 3.5). In cerebellum region, clear GM1 (Figure 3.9 A), GD1a (Figure 3.9 B), GD1b (Figure 3.9 C),, and GT1b bands (Figure 3.9 D) were detected in 2- and 4-month old WT and Neu1-/- mice brain samples. Like in cortex, these bands,-a and –b series gangliosides, were not seen in 2-and 4-month old Galgt-/- and Neu1-/-Galgt-/- mice brain (Figure 3.9 A-D). Unlike cortex, only accumulated GD3 ganglioside was observed in 2-and 4-month-old Galgt-/- and Neu1-/-Galgt-/- mice (Figure 3.10). In cerebellum, no significant expression differences between genotypes were detected as age-dependent manner (Figure 3.9 A-D ; Figure 3.10). Similar to cortex, higher LacCer level was detected in Galgt-/- and Neu1-/-Galgt-/- mice compared to WT and Neu1-/- mice for both age group (Figure 3.12). No obvious effect of Neu1 on LacCer conversion to GA2 was noted in cerebellum, *in vivo.*

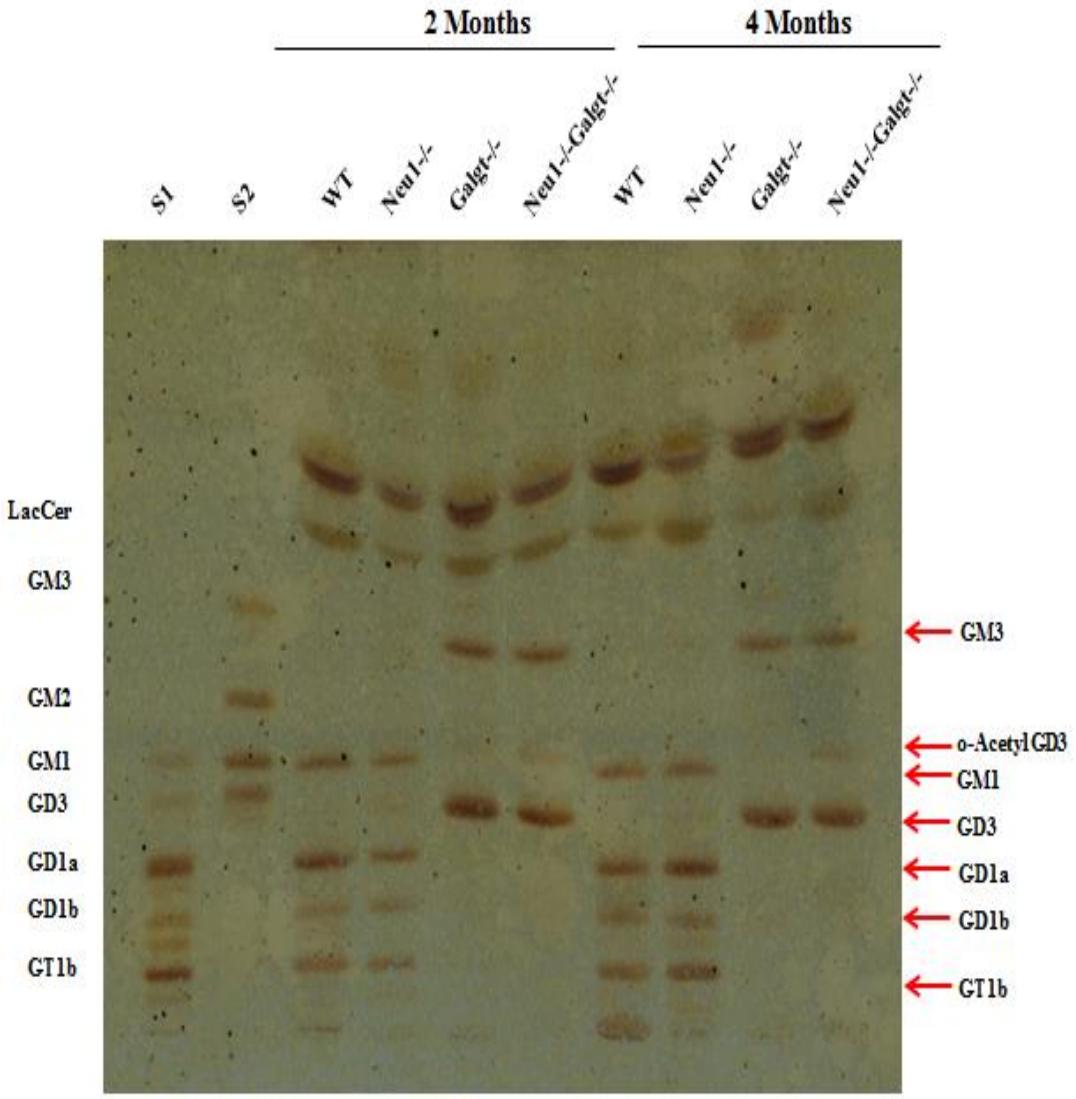

Figure 3.3. Orcinol stained Thin Layer Chromotography of acidic gangliosides from cortex of 2-month-old WT,Neu1-/-, Galgt-/- and Neu1-/-Galgt-/- mice. S1 included LacCer,GM1, GD3,GD1a, GD1b, GT1b as standard while S2 included GM3,GM2,GM1,GD3.

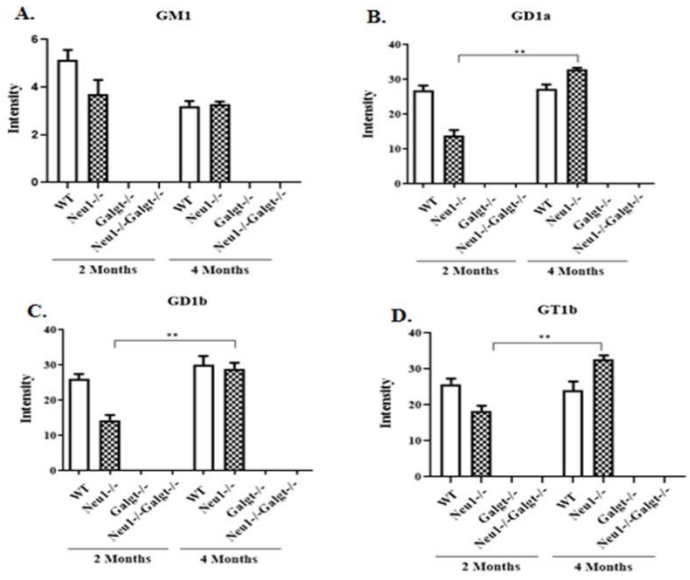

Figure 3.4. Acidic gangliosides' intensity quantitation of a-series gangliosides GM1 (A), GD1a (B), and b-series gangliosides GD1b (C), GT1b (D). (Band intensities were determined by ImageJ and p-values were determined by two-way-ANOVA analysis by GraphPad. Data are reported as mean ± SEM, n=3;**p<0,01)

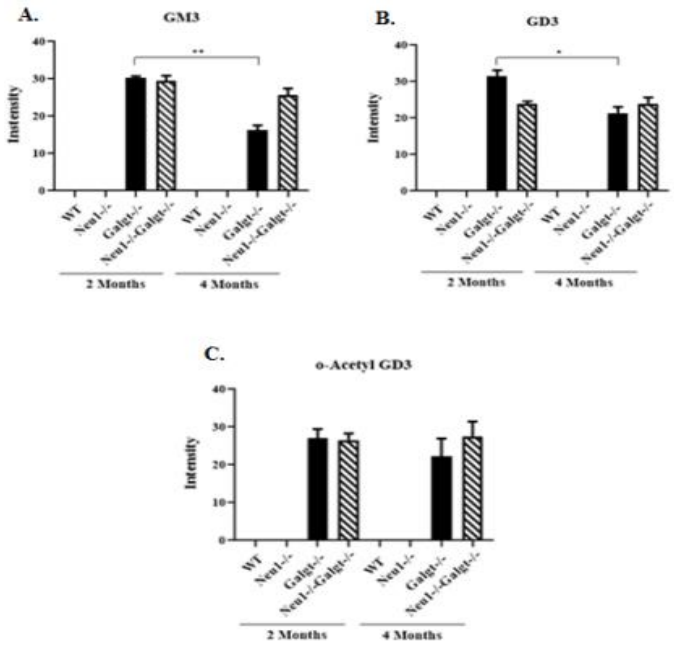

Figure 3.5. Acidic gangliosides' intensity quantitation of (A) GM3, (B) GD3, (C) o-Acetyl GD3. (Band intensities were determined by ImageJ and p-values were determined by two-way-ANOVA analysis by GraphPad. Data are reported as mean ± SEM, n=3;*p<0,05,**p<0,01)

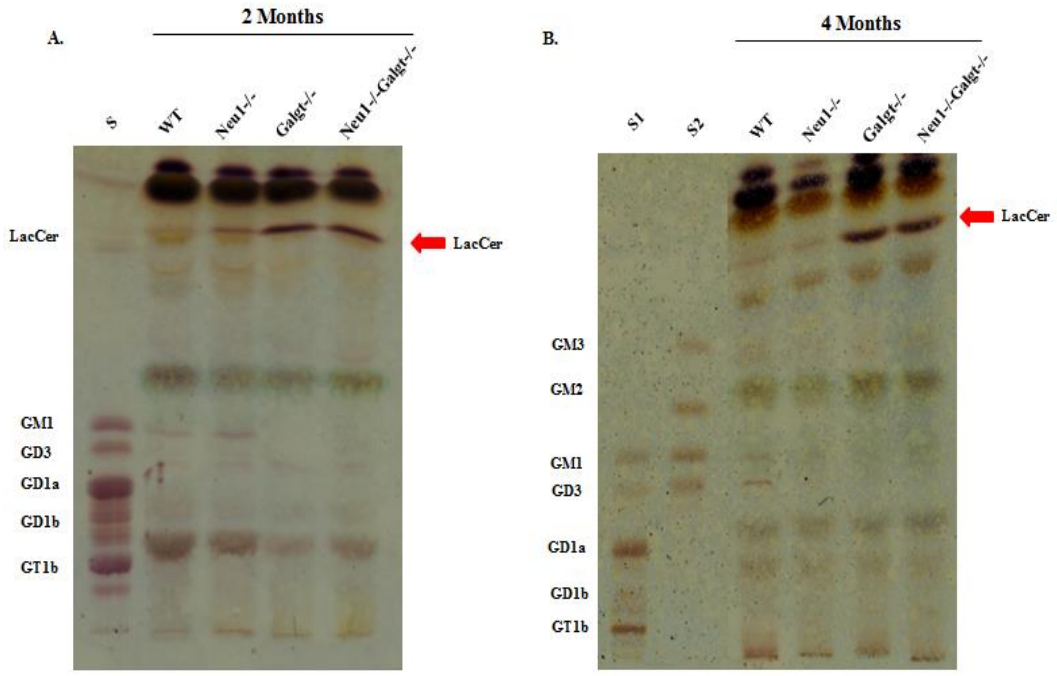

Figure 3.6. Orcinol stained Thin Layer Chromotography of neutral gangliosides from cortex of 2-month-old WT,Neu1-/-, Galgt-/- and Neu1-/-Galgt-/- mice (A) and 4-month-old WT,Neu1-/-, Galgt-/- and Neu1-/-Galgt-/- mice (B). S included LacCer,GM1, GD3,GD1a, GD1b, GT1b as standard while S and S1 were identical to each other, S2 included GM3,GM2,GM1,GD3 as standard

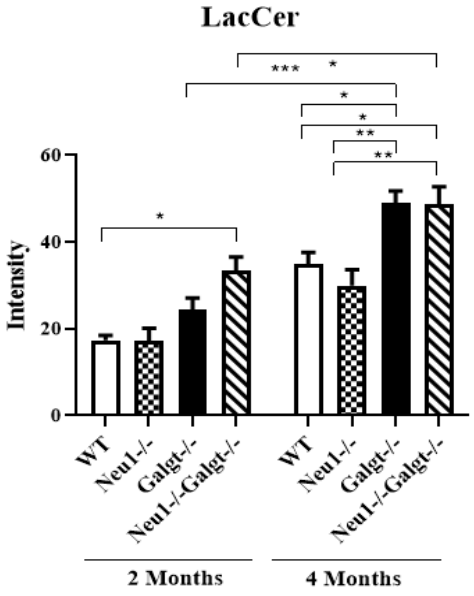

Figure 3.7. Neutral ganglioside LacCer intensity quantitation. (Band intensities were determined by ImageJ and p-values were determined by two-way-ANOVA analysis by GraphPad. Data are reported as mean ± SEM, n=3;*p<0,05,**p<0,01,***p<0,001

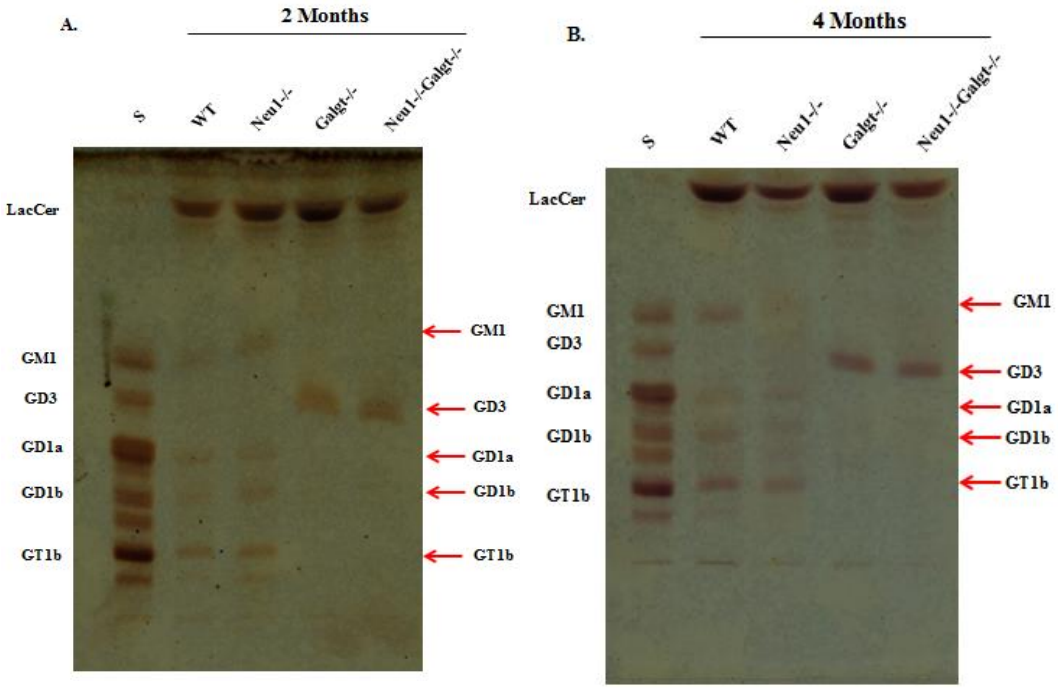

Figure 3.8. Orcinol stained Thin Layer Chromotography of acidic gangliosides from cerebellum of 2-month-old WT, Neu1-/-, Galgt-/- and Neu1-/-Galgt-/- mice

(A) and 4-month-old WT, Neu1-/-, Galgt-/- and Neu1-/-Galgt-/- mice (B). S included LacCer,GM1, GD3,GD1a, GD1b, GT1b as standard.

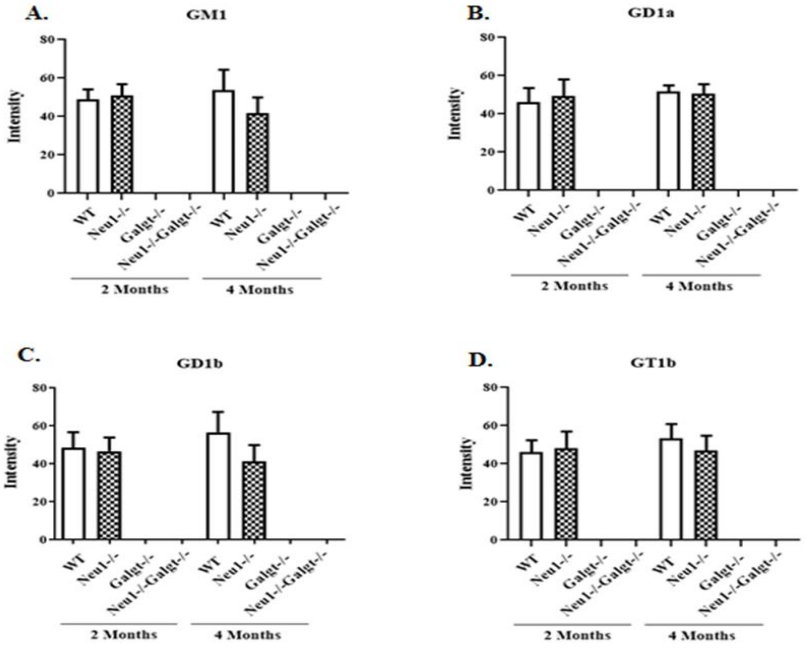

Figure 3.9. Acidic gangliosides' intensity quantitation of a-series gangliosides GM1 (A), GD1a (B) and b-series gangliosides GD1b(C), GT1b (D). (Band intensities were determined by ImageJ and p-values were determined by two-way-ANOVA analysis by GraphPad. Data are reported as mean ± SEM, n=3)

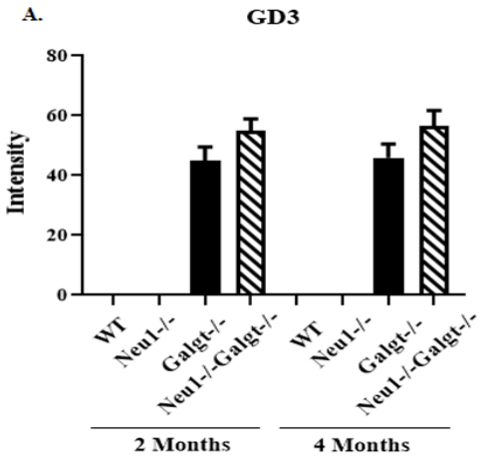

Figure 3.10. Intensity quantitation of acidic ganglioside GD3 (A). (Band intensities were determined by ImageJ and p-values were determined by two-way-ANOVA analysis by GraphPad. Data are reported as mean ± SEM n=3)

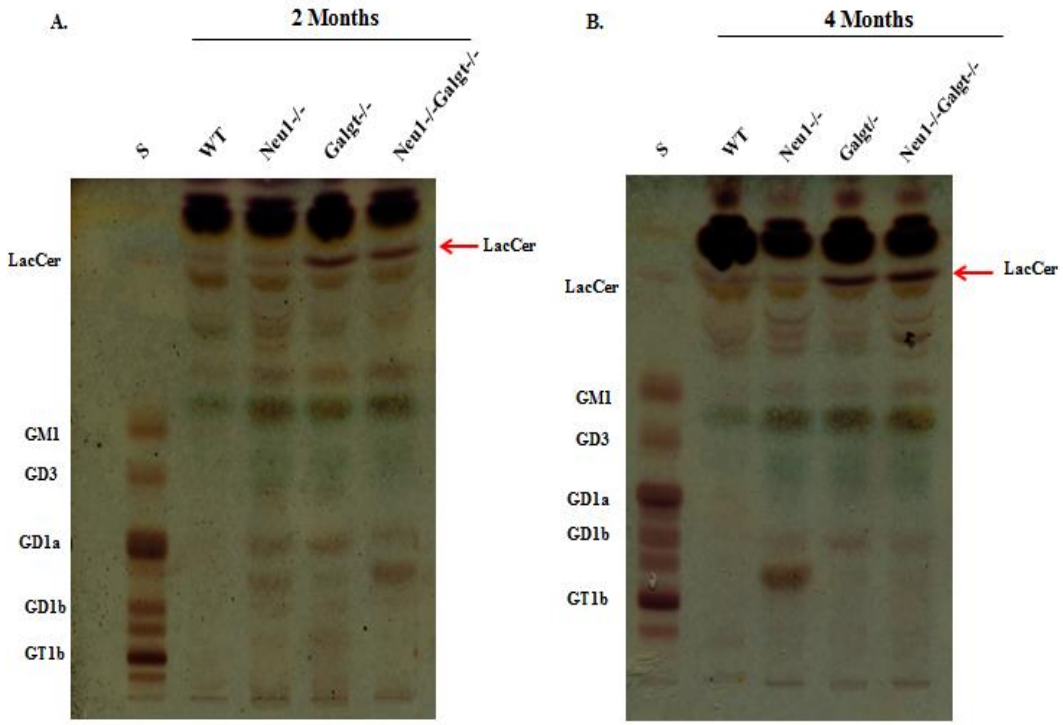

Figure 3.11. Orcinol stained Thin Layer Chromotography of neutral gangliosides from cerebellum (A) 2-month-old WT,Neu1-/-, Galgt-/- and Neu1-/-Galgt-/- mice (B) 4-month-old WT,Neu1-/-, Galgt-/- and Neu1-/-Galgt-/- mice. S included LacCer,GM1, GD3,GD1a, GD1b, GT1b as standard.

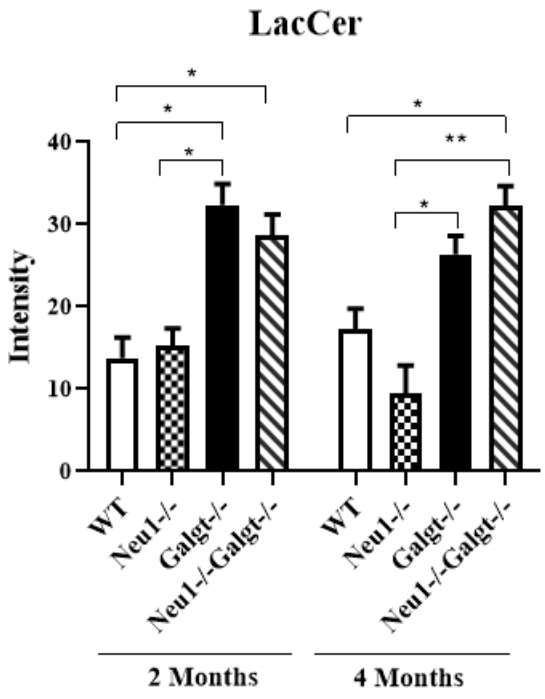

Figure 3.12. Neutral ganglioside LacCer intensity quantitation. (Band intensities were determined by ImageJ and p-values were determined by two-way-ANOVA analysis by GraphPad. Data are reported as mean ± SEM, n=3;*p<0,05,**p<0,01,***p<0,001)

Although major differences in the ganglioside pattern could be detected by Thin Layer Chromatography analysis, there were some limiations for this analysis. Gangliosides that were included in the standards could be noticed but other gangliosides that were not found in the standards could not be named. For these gangliosides more detailed analysis should be carried on. Additionaly, minor differences could not be detected by TLC method. Therefore LC/MS method may be applied to these samples for detailed analysis and clarify minor differences in terms of different brain regions. Moreover thalamus brain region could not be used for TLC analysis because of amount of this section. Therefore ganglioside pattern of thalamus could not be analyzed. Obtained results from other experiments belongs to thalamus, could be related with altered ganglioside pattern in that region. In order to analyse ganglioside pattern of different brain regions (cortex, cerebellum, and tahalmus), LC/MS method could be helpful.

3.4. DNA Fragmentation Assay

To understand if Neu1, Galgt or both gene deficiencies cause apoptosis in mice brain, DNA isolation and gel electrophoresis experiment was performed for 2- and 4-month-old WT,Neu1-/-,Galgt-/- and Neu1-/-Galgt-/- mice' brain cortex, cerebellum and thalamus regions.

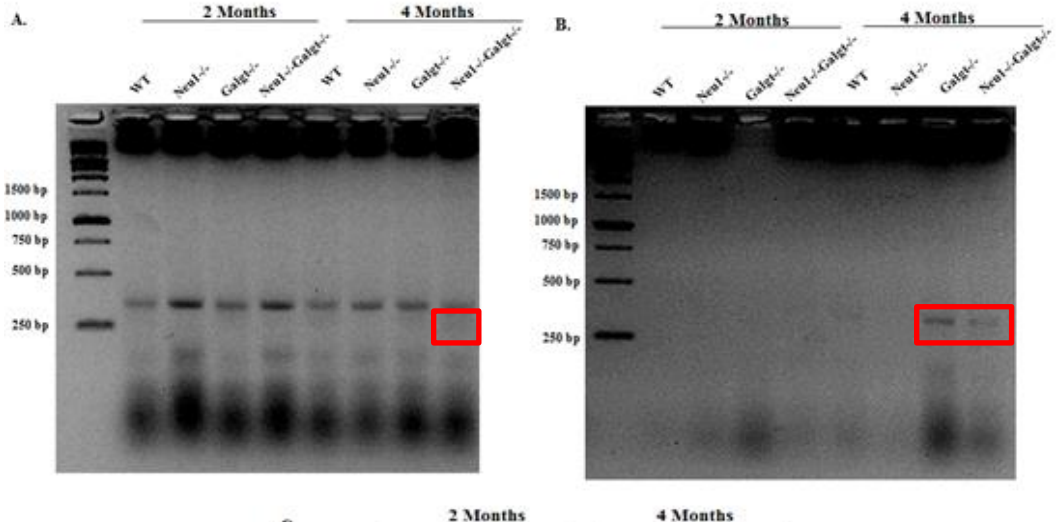

Figure 3.13. DNA fragmentation and agarose gel electrophoresis results for (A)Cortex, (B) Cerebellum (C) Thalmus region of 2-and 4-month-old WT,Neu1-/-,Galgt-/- and Neu1-/-Galgt-/- mice.

According to cortex region result, an extra band around 200 bp (indicated with red square) was seen in 4-month-old Neu1-/-Galgt-/- mice which was not found in another genotypes (Figure 3.13 A). This fragmented DNA could be the sign for apoptosis in the cortex region of 4-month-old Neu1-/-Galgt-/- mice.

In cerebellum result, 4-month-old Galgt-/- and Neu1-/-Galgt-/- mice had an extra band around 300 bp (indicated with red square). However no another bands were detected in other genotypes for 2-and 4-month old age groups (Figure 3.13 B). This result could be explained by the apoptotic role of GM3 and GD3 gangliosides which are highly expressed in both Galgt-/- and Neu1-/-Galgt-/- mice. Therefore DNA fragmentation of Galgt-/- and Neu1-/-Galgt-/- mice could indicate apoptosis in these mice.

In thalamus region, compared to other two regions, more different bands were detected for each genotype and age groups. Especially, 2-month-old Neu1-/-Galgt-/- mice had smear (Figure 3.13 C). This fragmented DNA in 2-month-old Neu1-/-Galgt-/- line could be a marker for apoptosis. In addition to that 2-month-old Neu1-/- mice and 4-month-old Neu1-/-Galgt-/- mice had a band in different location compared to their WT counterparts.

These results implied that Neu1-/-,Galgt-/- and Neu1-/-Galgt-/- mice shows different apoptotic pattern in different brain regions so more detailed investigations are

needed in order to understand how these gene deficiencies effect apoptotic pathway. In order to clarify apoptosis in these mice brain, relative gene expression analysis, Western Blot analysis and TUNEL assay were performed.

3.5. Relative Gene Expression Analysis

RT-PCR analysis was carried out to understand effect of single and double gene deficiency on apoptosis in mouse brain. For this aim, expression level of apoptotic markers that are subdivided as ER stress (ATF6, Calnexin, XBP1) , oxidative stress (SOD2, Catalase, Ttase1), anti-apaoptotic (Bcl-2, Bcl-XL) and apoptotic (Bax) were analyzed in cortex, cerebellum and thalamus regions of 2-and 4-month-old WT,Neu1-/-, Galgt-/- and Neu1-/-Galgt-/-mice.

ATF6 acts as a ER stress-regulated transmembrane transcription factor which activates transcription of ER molecules in unfolded/misfolded protein response (Sano and Reed 2013). In cortex, expression level of ATF6 decreased in 2-month-old Neu1-/-Galgt-/- mice compared to age-matched littermates but this decrease was statistically significant just only between 2-month-old Galgt-/- and Neu1-/-Galgt-/- mice (Figure 3.14 A). Increased expression level of ATF6 was detected in 2-month-old Galgt-/- mice among 2-month-old group and also this increase was significant compared to 4-month-old Galgt-/- (Figure 3.14 A). In 4-month-old mice group, decreased expression level of ATF6 was demonstrated in WT compared to age-matched Neu1-/- and Neu1-/-Galgt-/- mice (Figure 3.14 A). In cerebellum, 2-month-old Neu1-/-Galgt-/- mice displayed clear decreased expression level of ATF6 compared to age-matched littermates (Figure 3.14 B). 4-month-old WT mice had significantly decreased expression level of ATF6 compared to age-matched Neu1-/-, Galgt-/- and 2-month-old counterpart.In 4-month-old Neu1-/- mice, the expression level of ATF6 was significantly higher than both age-matched Galgt-/- and Neu1-/-Galgt-/- (Figure 3.14 B). In thalamus, 4-month-old mice exhibited significant increament in expression level of ATF6 compared to age-matched littermates and 2-month-old counterpart (Figure 3.14 C). Moreover 4-month-old Galgt-/- and Neu1-/-Galgt-/- mice had decreased ATF6 expression compared to 4-month-old Neu1-/- mice (Figure 3.14 C). Decrement in 4-month-old Neu1-/-Galgt-/- mice could be associated with Galgt enzyme deficiency.

Calnexin is Type I ER transmembrane protein that plays essential role in protein folding and quality control of folded protein so it is called ER chaperon (Araki and Nagata 2011). In cortex, 2-month-old Galgt-/- and Neu1-/-Galgt-/- mice had a slight increase in the expression level of of Calnexin compared to age-matched Neu1-/- mice and 4-month-old counterparts (Figure 3.15 A). In 4-month-old mice, WT mice displayed decreased expression level of Calnexin compared to littermates and 2-month-old counterpart (Figure 3.15 A). In cerebellum, decreased expression level of Calnexin was detected in 2-month-old Galgt-/- mice compared to age-matched Neu1-/- mice. Moreover this decrement was significant in comparison to 4-month-old Galgt-/- mice (Figure 3.15 B). In 4-month-old group, Neu1-/- mice exhibited higher expression level of Calnexin than age-matched littermates but statistically significant result was obtained only between WT and Neu1-/- mice (Figure 3.15 B). In thalamus increased expression

level of Calnexin was obtained in 2-month-old double knockout mice compared to control group. Elevated expression level of Calnexin was demonstrated in 4-month-old Neu1-/-Galgt-/- mice and it was statistically significant in comparison to 4-month-old Galgt-/-, WT and 2-month-old Neu1-/-Galgt-/- mice (Figure 3.15 C) .

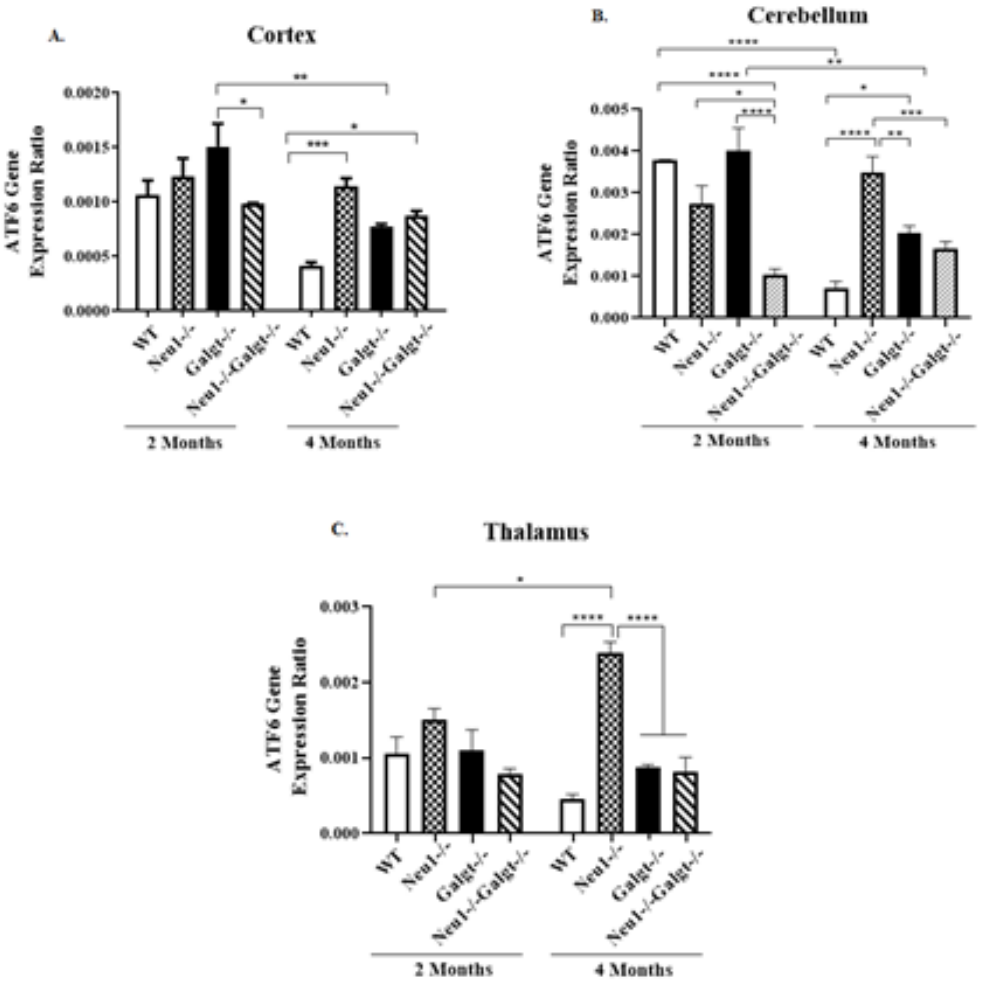
A.
Cortex
ATF6 Gene Expression Ratio
0.0020
0.0015
0.0010
0.0005
0.0000
WT
Neu1-/-
Galgt-/-
Neu1-/-Galgt-/-
2 Months
4 Months
B.
Cerebellum
0.005
0.004
0.003
0.002
0.001
0.000
C.
Thalamus
0.003
0.002
0.001
0.000

Figure 3.14. Expression ratio of ER Stress related ATF6 Gene in Cortex (A) Cerebellum (B) Thalamus (C) for 2- and 4-month-old WT, Neu1-/-, Galgt-/- and Neu1-/-Galgt-/- mice (△CT method was used for expression ratio determination and two-way-ANOVA analysis was used for p value determination via GraphPad. Data are reported as mean ± SEM, n=3; *p<0.05, **p<0.01, ***p<0.001, ****p<0.0001)

XBP-1 is a transcription factor which is cleaved by activated IRE1 during unfolded protein response stimulation (Wang et al. 2011). In cortex, 2-month-old Galgt-/- mice expressed higher level of XBP-1 compared to 2-month-old WT, Neu1-/- and Neu1-/-Galgt-/- mice (Figure 3.16 A). In 4-month-old mice increased exprssion level of XBP-1 was detected in Galgt-/- and Neu1-/-Galgt-/- mice compared to WT and Neu1-/- mice. Additionally, 4-month-old mice exhibited higher expression level of XBP-1 than 2-month-old counterpart (Figure 3.16 A). Although no significant changes were observed in cerebellum (Figure 3.16 B), 4-month-old Neu1-/-Galgt-/- mice displayed increased expression level of XBP-1 in comparison to 2-month-old counterpart in thalamus (Figure 3.16 C).

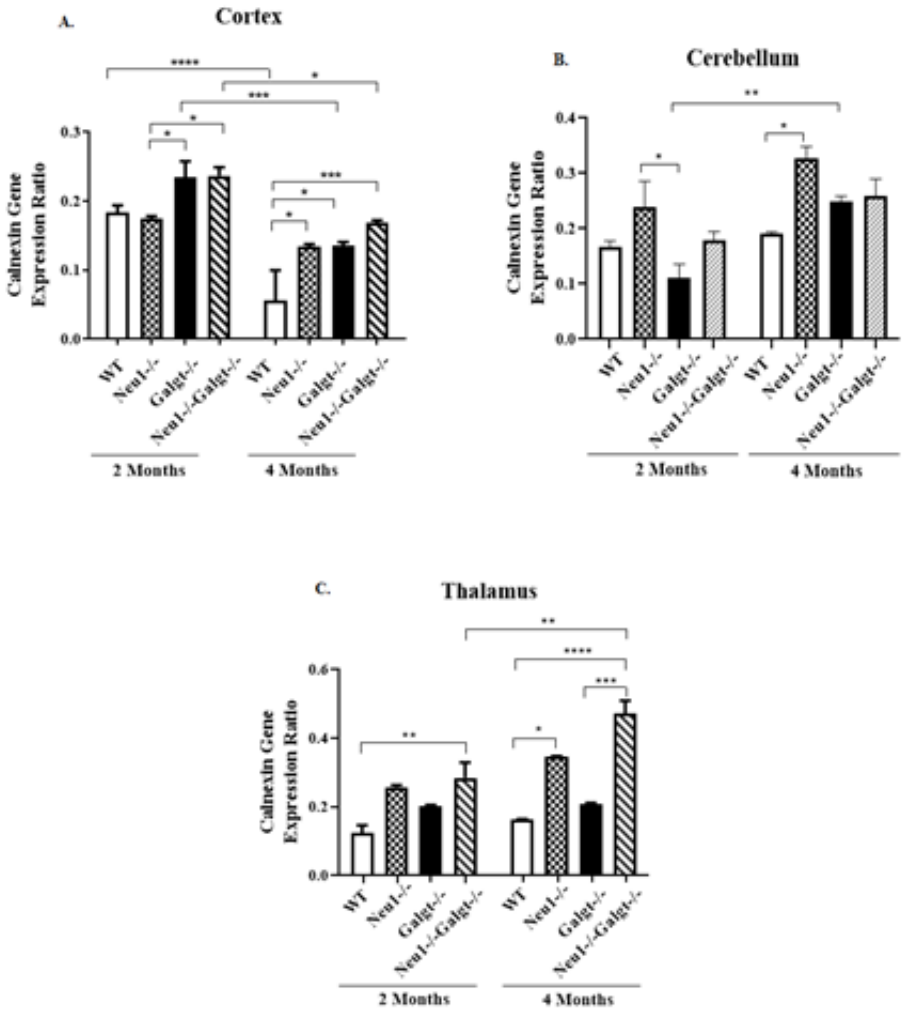

Figure 3.15.Expression ratio of ER Stress related Calnexin Gene in Cortex (A) Cerebellum (B) Thalamus (C) for 2- and 4-month-old WT, Neu1-/-, Galgt-/- and Neu1-/-Galgt-/- mice (△CT method was used for expression ratio determination and two-way-ANOVA analysis was used for p value determination via GraphPad. Data are reported as mean ± SEM, n=3; *p<0.05, **p<0.01, ***p<0.001, ****p<0.0001)

SOD2 could be called as anti-apoptotic marker against oxidative stress which clears mitochondrial ROS (Zorov et al.2014). In 2-month old mice group, expression level of SOD2 decreased in Neu1-/- compared to WT, Galgt-/- and Neu1-/-Galgt-/- mice (Figure 3.17 A). Also Neu1-Galgt-/- mice had higher level of SOD2 expression than WT. In 4-month-old mice group, dramatic decrease was observed in expression level of SOD2 compared to 2-month-old mice group (Figure 3.17 A). Therefore 4-month-old WT, Neu1-/-,Galgt-/- and Neu1-/-Galgt-/- showed significant decrease in expression level of SOD2 compared to 2-month-old counterparts (Figure 3.17 A). Additionally, SOD2 expression

level was increased in 4-month-old Neu1-/-Galgt-/- mice when compared to age-matched WT and Galgt-/- mice. Although there were no significant differences among 2-month-old mice for expression level of SOD2, clear differences were demonstrated in 4-month-old mice group in cerebellum (Figure 3.17 B). 4-month-old Neu1-/- mice displayed significantly increased expression level of SOD2 compared to age-matched littermates and 2-month-old Neu1-/-.

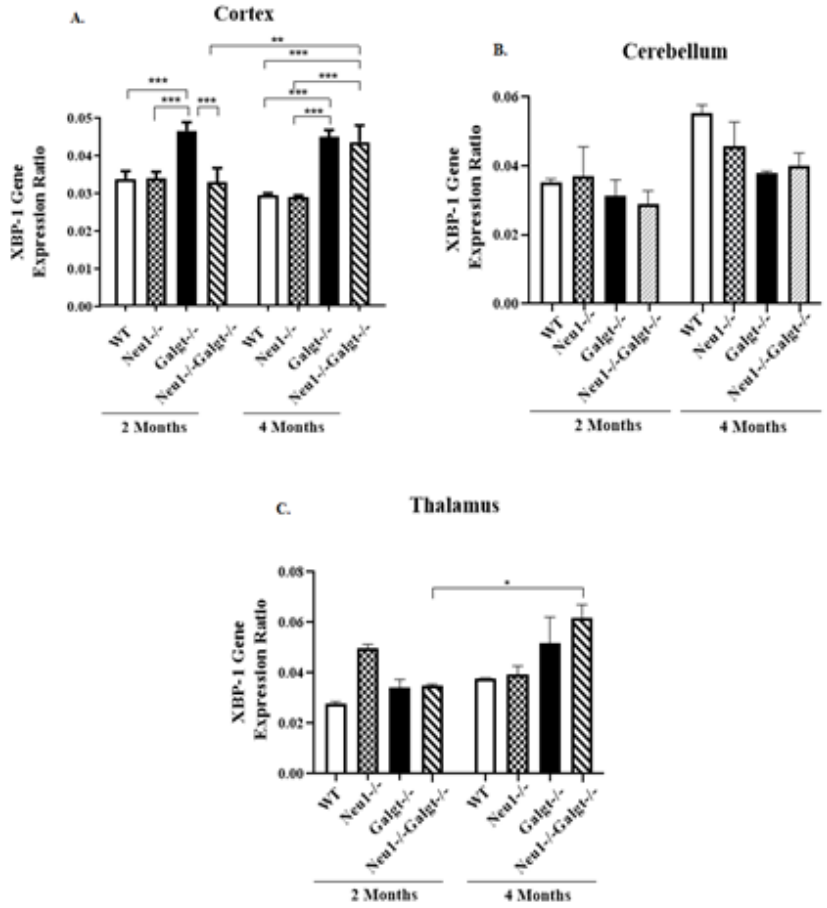

Figure 3.16. Expression ratio of ER Stress related XBP-1 Gene in Cortex (A) Cerebellum (B) Thalamus (C) for 2- and 4-month-old WT, Neu1-/-, Galgt-/- and Neu1-/-Galgt-/- mice (△CT method was used for expression ratio determination and two-way-ANOVA analysis was used for p value determination via GraphPad. Data are reported as mean ± SEM, n=3; *p<0.05, **p<0.01, ***p<0.001, ****p<0.0001

Moreover 4-mont-old Neu1-/-Galgt-/- mice had greater expression level of SOD2 than 2-month-old counterpart (Figure 3.17 B). 2-month-old mice group did not show any significant changes between genotypes in thalamus (Figure 3.17 C). In 4-month-old mice

group, Neu1-/- mice had significantly increased expression level of SOD2 compared to age matched littermates and 2-month-old counterpart (Figure 3.17 C).

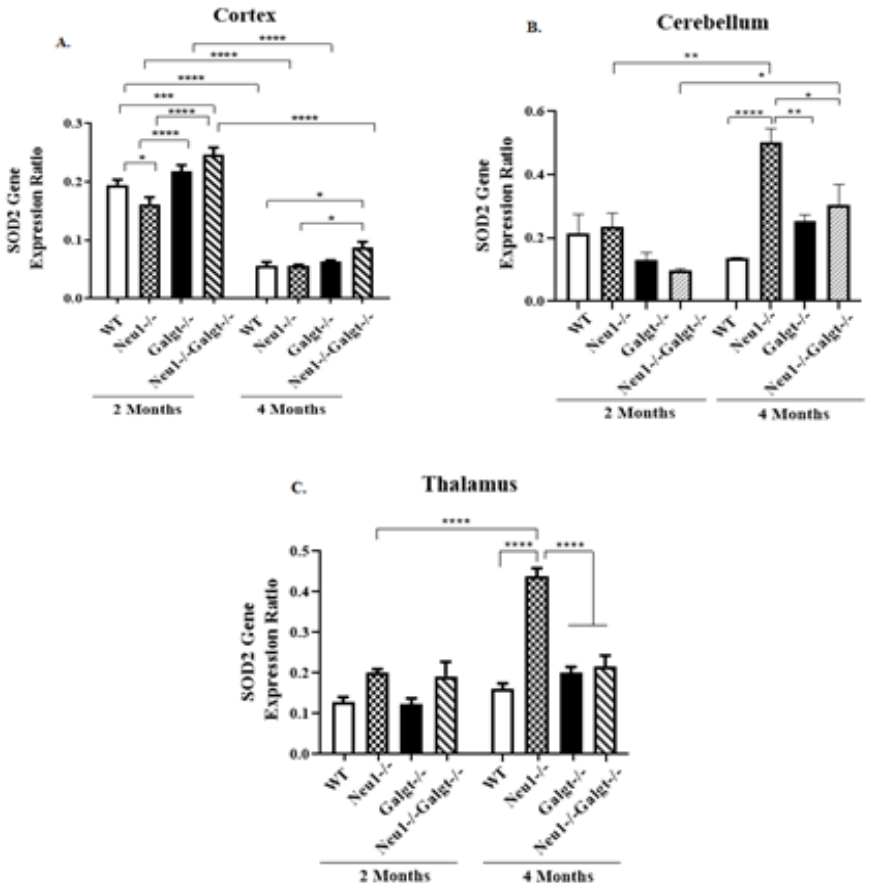

Figure 3.17. Expression ratio of oxidative stress related SOD2 Gene in Cortex (A) Cerebellum (B) Thalamus (C) for 2- and 4-month-old WT, Neu1-/-, Galgt-/- and Neu1-/-Galgt-/- mice (△CT method was used for expression ratio determination and two-way-ANOVA analysis was used for p value determination via GraphPad. Data are reported as mean ± SEM, n=3; *p<0.05, **p<0.01, ***p<0.001, ****p<0.0001)

As the one of the key enzyme which prevents oxidative damage by catalyzing hydrogen peroxide degradation to water and oxygen, Catalase protects cell from oxidative stress(Heck et al.2010). To examine cellular oxidative stress level, Catalase gene expression ratio was detected. In cortex region, the expression level of Catalase significantly increased in 2-month-old Galgt-/- mice compared to age-matched littermates and 4-month-old counterpart (Figure 3.18 A). In 4-month-old mice group, single and double knockout mice had clear increased expression level of Catalase compared to

control group. Additionally, expression level of Catalase slightly increased in 4-month old Neu1-/ -mice compared to 2-month-old counterpart (Figure 3.18 A). In cerebellum region, no statistically significant changes were detected for 2-month-old mice group (Figure 3.18 B). However increased expression level of Catalase was observed in 4-month-old Neu1-/- mice in comparison to age-matched WT mice (Figure 3.18 B). In thalamus region, only change was exhibited between 2-and 4-month-old WT mice in which increased expression level of Catalase was demonstrated in 4-month-old WT (Figure 3.18 C).

TTase1 is an essential player for antioxidant defense system (Heck et al.2010).In cortex, dramatic increase was demonstrated in the expression level of TTase1 for 2-month-old Neu1-/-Galgt-/- mice compared to age-matched littermates (Figure 3.19 A). Additionally, 2-month-old Galgt-/- mice had higher level of TTase1 expression than 2-month-old Neu1-/-mice. When TTase1 expression level was examined in 4-month-old mice group, significant decrement was observed in this group compared to younger group for each genotype. Therefore 4-month old control, single and double knockout mice group exhibited lower expression level of TTase1 compared to 2-month-old counterparts (Figure 3.19 A). In cerebellum, 2-month-old mice group did not display any significant changes among genotypes (Figure 3.19 B). Although only 4-month-oldd Neu1-/- had significantly increased expression level of Ttase1, slight changes were detected in 4-month-old Neu1-/-, Galgt-/- and Neu1-/-Galgt-/- compared to control group. In addition to that, increased expression level of TTase1 was noted in 4-month old Galgt-/- mice in comparison to 2-month-old counterpart (Figure 3.19 B). Even though, no significant changes were detected in 2-month-old mice group, expression level of TTase1 exhibited differences among 4-month-old mice group in thalamus (Figure 3.19 C). expression level of TTase1 decreased in 4-month-old WT mice compared to age-matched Galgt-/- and Neu1-/-Galgt-/- mice. Moreover 4-month-old double knockout mice had elevated level of TTase1 expression compared to single knockout, control mice and 2-month-old counterpart (Figure 3.19 C).

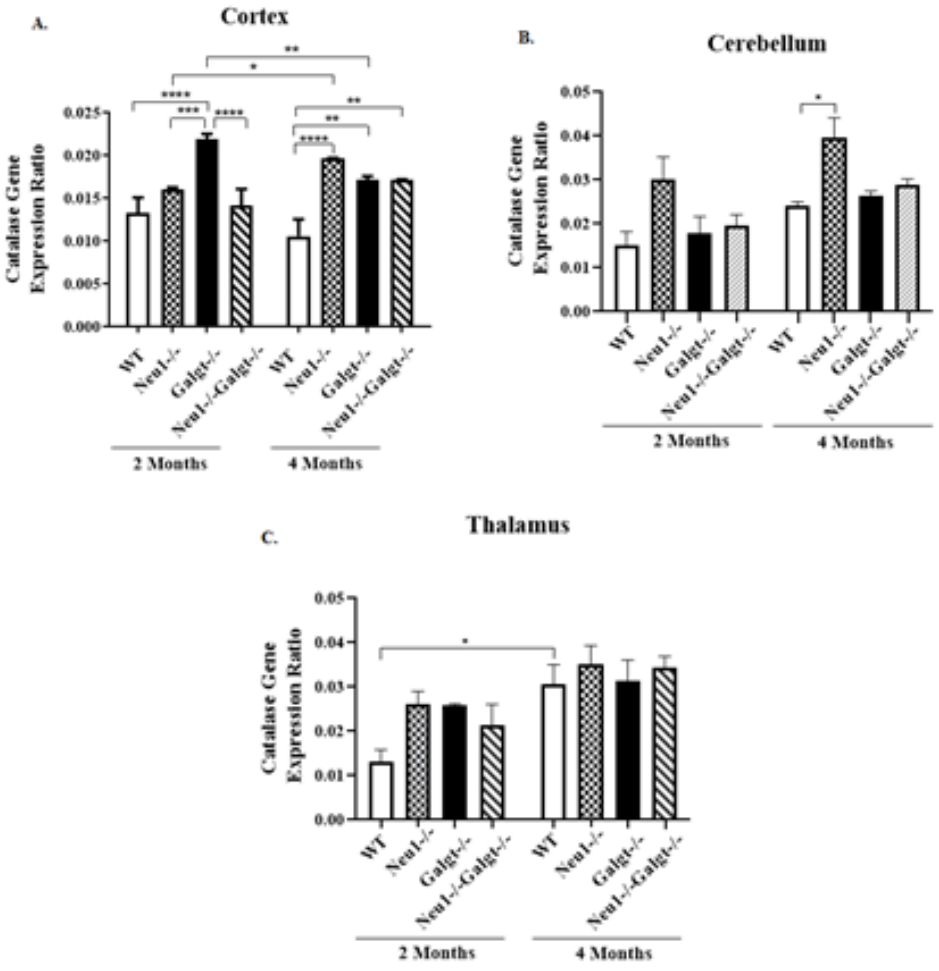
A.
Cortex
Catalase Gene Expression Ratio
0.025
0.020
0.015
0.010
0.005
0.000
****
***
****
**
*
**
**
****
WT
Neu1-/-
Galgt-/-
Neu1-/-Galgt-/-
2 Months
4 Months
B.
Cerebellum
Catalase Gene Expression Ratio
0.05
0.04
0.03
0.02
0.01
0.00
*
C.
Thalamus
Catalase Gene Expression Ratio
0.05
0.04
0.03
0.02
0.01
0.00
*

Figure 3.18. Expression ratio of oxidative stress related Catalase Gene in Cortex (A) Cerebellum (B) Thalamus (C) for 2- and 4-month-old WT, Neu1-/-, Galgt-/- and Neu1-/-Galgt-/- mice (△CT method was used for expression ratio determination and two-way-ANOVA analysis was used for p value determination via GraphPad. Data are reported as mean ± SEM, n=3; *p<0.05, **p<0.01, ***p<0.001, ****p<0.0001)

As one of the anti-apoptotic marker, Bcl-2 is found on the outer membrane of mitochondria and inhibits apoptotic proteins such as Bax and Bak (Cory and Adams 2002). . In cortex, expression level of Bcl-2 displayed significant increase in 2-month-old Galgt-/- mice compared to age-matched littermates and 4-month-old counterpart (Figure 3.20 A). 4-month-old Galgt-/- mice had increased level of Bcl-2 expression level among 4-month-old group but this increment was only statistically significant between WT mice (Figure 3.20 A). In cerebellum, 2-month-old Neu1-/- mice exhibited significantly increased level of Bcl-2 expression compared to age-matched littermates. Moreover 4-month-old Neu1-/- mice had higher level of Bcl-2 expression compared to 4-month-old control group (Figure 3.20 B). In thalamus, 2-month-old Neu1-/- demonstrated significantly increased level of Bcl-2 expression among age-matched littermates (Figure 3.20 C). Increased expression level of Bcl-2 was detected in 4-month-old WT mice compared to age-matched Galgt-/- and Neu1-/-Galgt-/- mice. Additionally, this increased Bcl-2 expression level was significant in 4-month-old WT mice compared to 2-month-old WT (Figure 3.20 C).

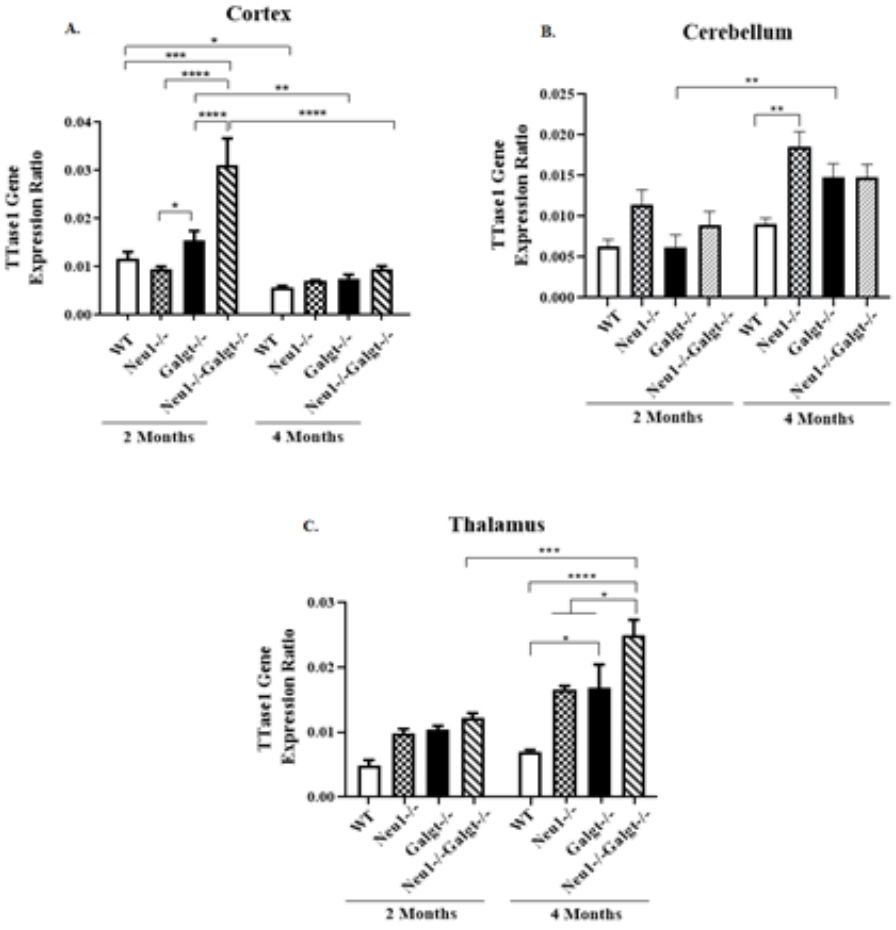

Figure 3.19. Expression ratio of oxidative stress related TTase1 Gene in Cortex (A) Cerebellum (B) Thalamus (C) for 2- and 4-month-old WT, Neu1-/-, Galgt-/- and Neu1-/-Galgt-/- mice (△CT method was used for expression ratio determination and two-way-ANOVA analysis was used for p value determination via GraphPad. Data are reported as mean ± SEM, n=3; *p<0.05, **p<0.01, ***p<0.001, ****p<0.0001)

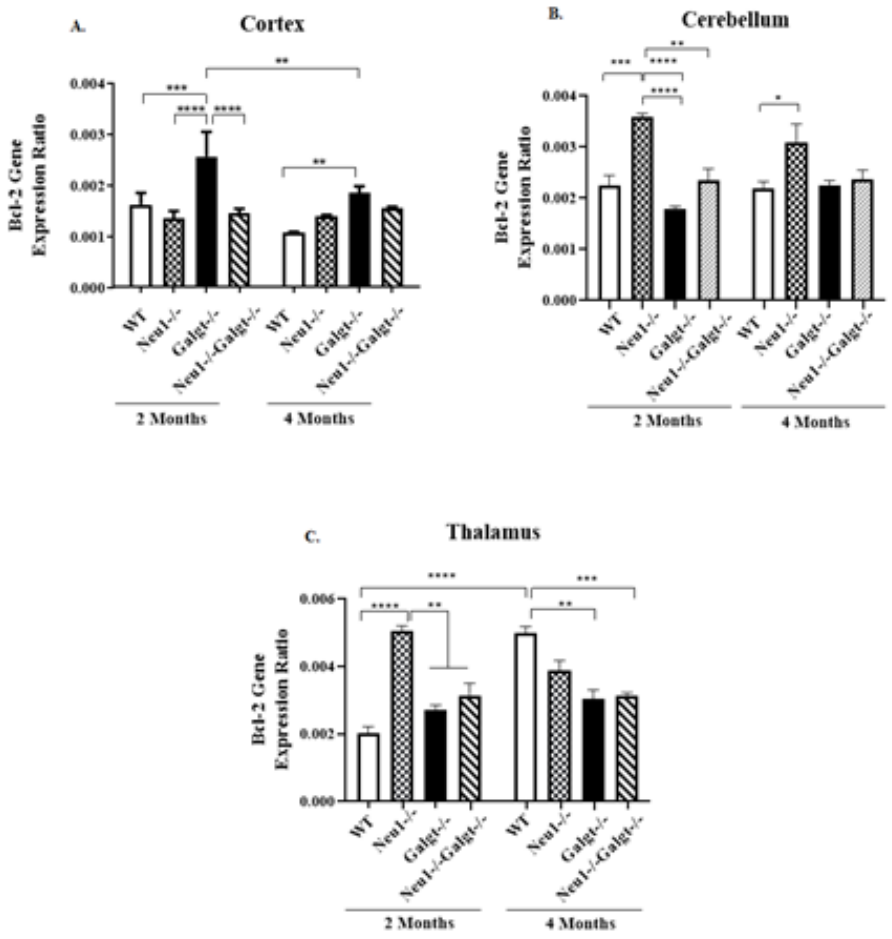

Figure 3.20. Expression ratio of anti-apoptotic Bcl-2 Gene in Cortex (A) Cerebellum (B) Thalamus (C) for 2- and 4-month-old WT, Neu1-/-, Galgt-/- and Neu1-/-Galgt-/- mice (△CT method was used for expression ratio determination and two-way-ANOVA analysis was used for p value determination via GraphPad. Data are reported as mean ± SEM, n=3; *p<0.05, **p<0.01, ***p<0.001, ****p<0.0001

As an inhibitor of cytochrome c release and caspase activation, Bcl-XL is an anti-apoptotic marker (Elmore 2007). In cortex, even though no significant changes were detected among the 2-month-old mice group, significantly different the expression levelof Bcl-XL were demonstrated in 4-month-old mice group (Figure 3.21 A). 4-month-old Neu1-/- mice had higher expression level of Bcl-XL than age-matched WT, Galgt-/- , Neu1-/-Galgt-/- mice and 2-month-old counterpart. Moreover decreased expression level of Bcl-XL was detected in 4-month-old WT mice compared to age-matched littermates (Figure 3.21 A). Although no significantly changed expression levels of Bcl-XL were noted in cerebellum (Figure 3.21 B), different Bcl-XL expression levels were evaluated among genotypes and age groups in the thalamus(Figure 3.21 C). Expression level of Bcl-

XL increased in 2-month-old Neu1-/- mice compared to 2-month-old WT and Galgt-/- mice. 4-month-old Neu1-/- mice exhibited increased level of Bcl-XL expression in comparison to age-matched WT and Neu1-/-Galgt-/- mice. Moreover 4-month-old Neu1-/-Galgt-/- mice showed significantly decreased expression level of Bcl-XL compared to age-matched Neu1-/- ,Galgt-/- mice and 2-month-old counterpart (Figure 3.21 C).

Bax is one of the apoptotic markers that is able to control mitochondrial voltage-dependent anion channel in which opening causes membrane potential loss and cytochrome c release from mitochondria (Shimizu et al1999). In cortex, significant difference was detected only between 2-and 4-month-old Galgt-/- mice. 2-month-old Galgt-/- mice exhibited increased expression level of Bax compared to 4-month-old counterpart (Figure 3.22 A).

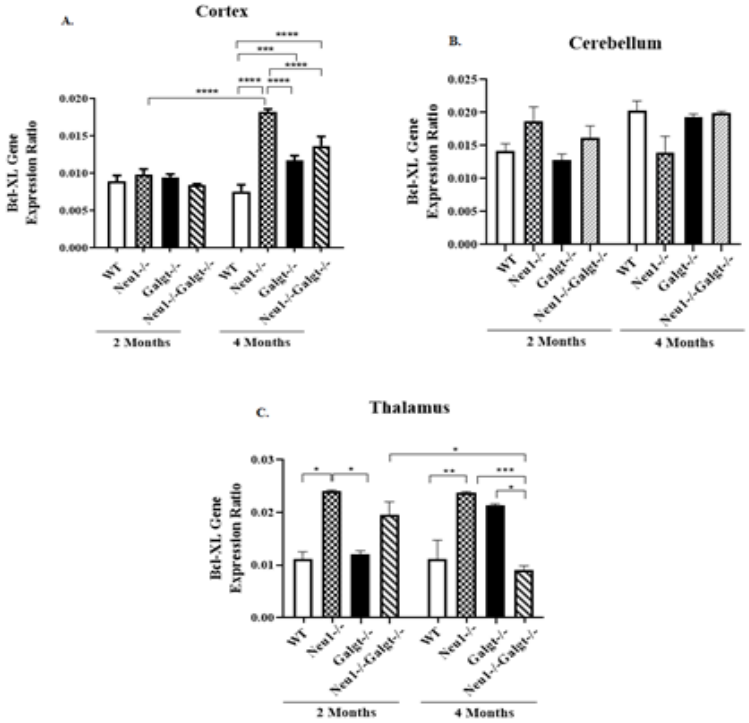

Figure 3.21. Expression ratio of anti-apoptotic Bcl-XL Gene in Cortex (A) Cerebellum (B) Thalamus (C) for 2- and 4-month-old WT, Neu1-/-, Galgt-/- and Neu1-/-Galgt-/- mice (△CT method was used for expression ratio determination and two-way-ANOVA analysis was used for p value determination via GraphPad. Data are reported as mean ± SEM, n=3; *p<0.05, **p<0.01, ***p<0.001, ****p<0.0001)

In cerebellum no significant changes were observed among 2-month-old mice group. 4-month-old Neu1-/- mice had significantly higher expression level of Bax than its age-matched littermates and 2-month-old counterpart (Figure 3.22 B). In thalamus, expression level of Bax did not show any significant changes among gentoypes and age groups(Figure 3.22 C).

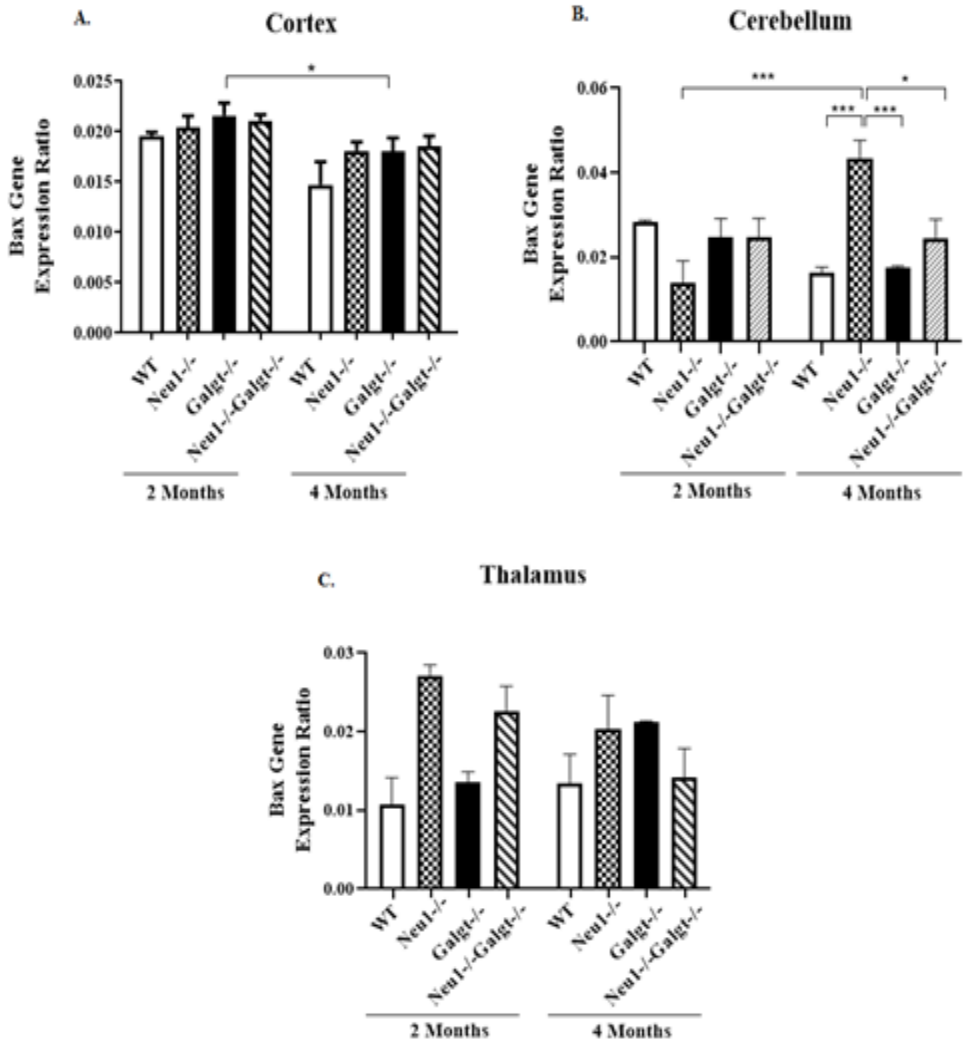

Figure 3.22. Expression ratio of apoptotic Bax Gene in Cortex (A) Cerebellum (B) Thalamus (C) for 2- and 4-month-old WT, Neu1-/-, Galgt-/- and Neu1-/-Galgt-/- mice (△CT method was used for expression ratio determination and two-way-ANOVA analysis was used for p value determination via GraphPad. Data are reported as mean ± SEM, n=3; *p<0.05, ***p<0.001)

3.6. Protein Level Analysis

Western Blot analysis in the single and double knockout mice showed importance of Neu1 and Galgt enzyme deficiency in distinct steps of apoptotic pathway. In order to detect apoptosis, apoptotic (Fas-Ligand, Caspase 3, Caspase 9) and ER stress markers' (BiP), expression was analyzed in cortex, cerebellum and thalamus regions of 2-and 4-month-old WT, Neu1-/-, Galgt-/- and Neu1-/-Galgt-/- mice.

Apoptosis was examined in two aspects that are intrinsic and extrinsic pathway. Fas-Ligand is one of the markers for extrinsic pathway (Locksley et al. 2001) and expression of this marker did not show any significant difference between genotypes and age groups (Figure 3.23 B). This result seems that change in ganglioside pattern and Neu1 enzyme deficiency did not affect extrinsic pathway of apoptosis.

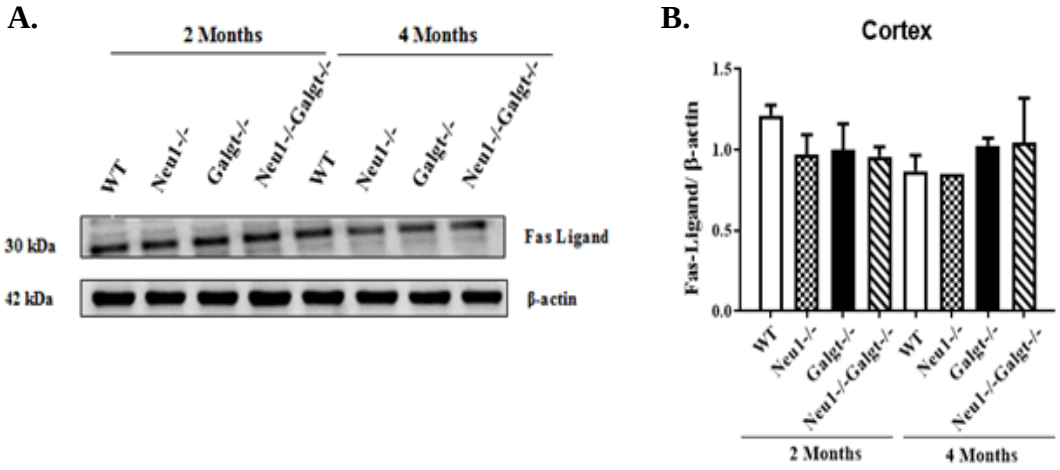

Figure 3.23. Western blot analysis of Fas-Ligand in cortex region for 2-and 4-month-old WT,Neu1-/-,Galgt-/- and Neu1-/-Galgt-/- mice. β-actin was internal control (A).Densitometry analysis relative to β-actin (B). (Band intensities were determined by ImageJ and p values were determined by two-way-ANOVA analysis by GraphPad. Data are reported as mean ± SEM, n=3)

As initiator Caspase of intrinsic pathway, Caspase 9 protein level was analyzed (Elmore 2007). Protein level of Caspase 9 significantly decreased in 2-month-old Galgt-/- mice compared to age-matched WT (Figure 3.24 B). When 2-month-ol Galgt-/- and Neu1-/-Galgt-/- mice were compared, increased level of cleaved Caspase 9 was detected in 2-month-old Neu1-/-Galgt-/- mice (Figure 3.24 B). Neu1 enzyme deficiency could result in this increase in Neu1-/-Galgt-/- mice. When 4-month-old mice groups were compared to control group, increased level of cleaved Caspase 9 was seen but that increases were not statictically significant (Figure 3.24 B).

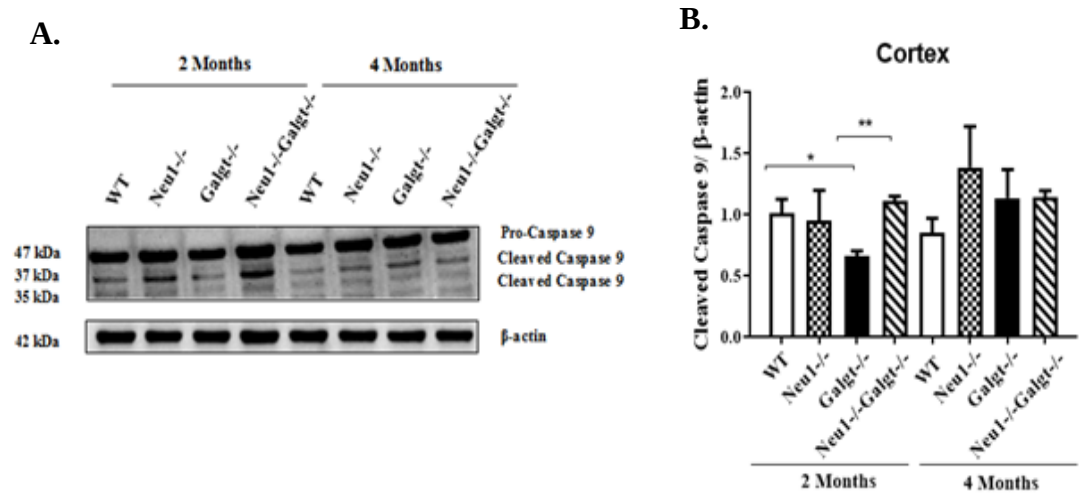

Figure 3.24. Western blot analysis of Caspase 9 in cortex region for 2-and 4-month-old WT, Neu1-/-, Galgt-/- and Neu1-/-Galgt-/- mice. β-actin was internal control (A) . Densitometry analysis of Cleaved Caspase 9 relative to β-actin (B).(Band intensities were determined by ImageJ and p values were determined by two-way-ANOVA analysis by GraphPad. Data are reported as mean ± SEM, n=3;*p<0,05,**p<0,01)

Caspase 3 is one of the executioner caspases and it plays essential role in the final step of apoptosis (Elmore 2007).According to the Western Blot result, slight but not significant differences were noticed between genotypes and age groups in cortex region (Figure 3.25 B).Although it was not statistically significant, 4-month old Galgt-/- mice exhibited increased Caspase 3 protein level compared to age matched Neu1-/- and Neu1-/-Galgt-/- mice (Figure 3.24 B).Increased cleaved Caspase 3 level in Galgt-/- mice could result from absence of GM1 ganglioside which has antiapoptotic role.

Extended ER Stress causes Unfolded Protein Response (UPR) and UPR regulates many different cellular fates so apoptosis is one of this regulated cellular fates (Gardner and Walter 2011). Owing to being key player of UPR, protein level of BiP was examined. Slight changes were detected in both 2-and 4-month old mice groups compared to control group (Figure 3.26 B). Although it was not statistically significant, 2-month-old Neu1-/-Galgt-/- showed increased protein level of BiP compared to age matched littermates. Similar result was found for 4-month-old mice group s(Figure 3.26 B). In that, increased BiP expression level was observed in Galgt-/- and Neu1-/-Galgt-/- mice. Therefore complex ganglioside deficit and Neu1 enzyme deficiency could cause ER stress in the mice brain.

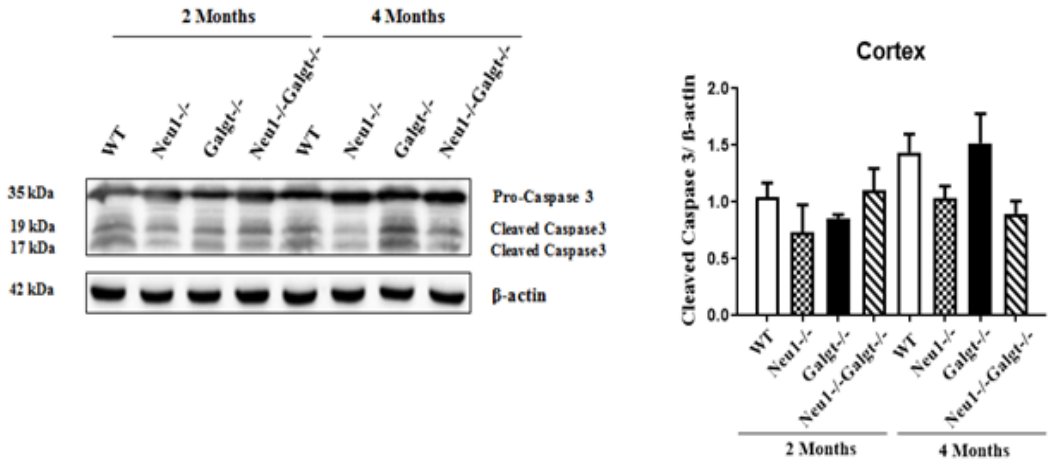

Figure 3.25. Western blot analysis of Caspase 3 in cortex region for 2-and 4-month-old WT, Neu1-/-, Galgt-/- and Neu1-/-Galgt-/- mice. β-actin was internal control (A). Densitometry analysis of Cleaved Caspase 3 relative to β-actin (B).(Band intensities were determined by ImageJ and p values were determined by two-way-ANOVA analysis by GraphPad. Data are reported as mean ± SEM, n=3)

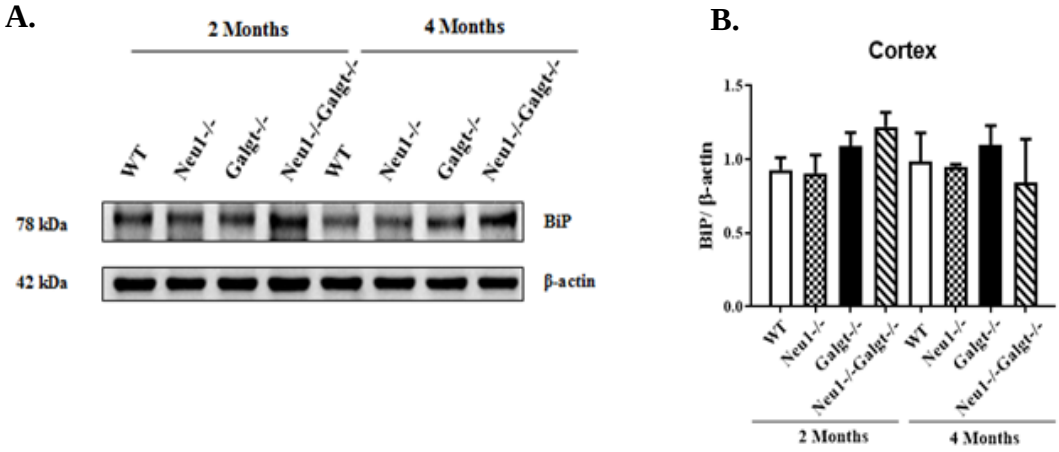

Figure 3.26. Western blot analysis of BiP in cortex region for 2-and 4-month-old WT, Neu1-/-, Galgt-/- and Neu1-/-Galgt-/- mice. β-actin was internal control (A). Densitometry analysis of BiP relative to β-actin (B).(Band intensities were determined by ImageJ and p values were determined by two-way-ANOVA analysis by GraphPad. Data are reported as mean ± SEM,n=3)

The protein level of Fas-Ligand slightly increased in 2-month-ol Neu1-/- mice compared to age-matched WT. However 2-month-old Neu1-/-Galgt-/- mice showed decreased protein level of Fas-Ligand in comparison to 2-month-old WT and Neu1-/- mice (Figure 3.27 B). That minor decrease could be explained by the deficient of *Galgt* gene in Neu1-/-Galgt-/- mice. Moreover, 4-month-old double knockout mice had decreased protein level of Fas-Ligand compared to age-matched WT and Galgt-/-(Figure 3.27 B).

A. **B.**

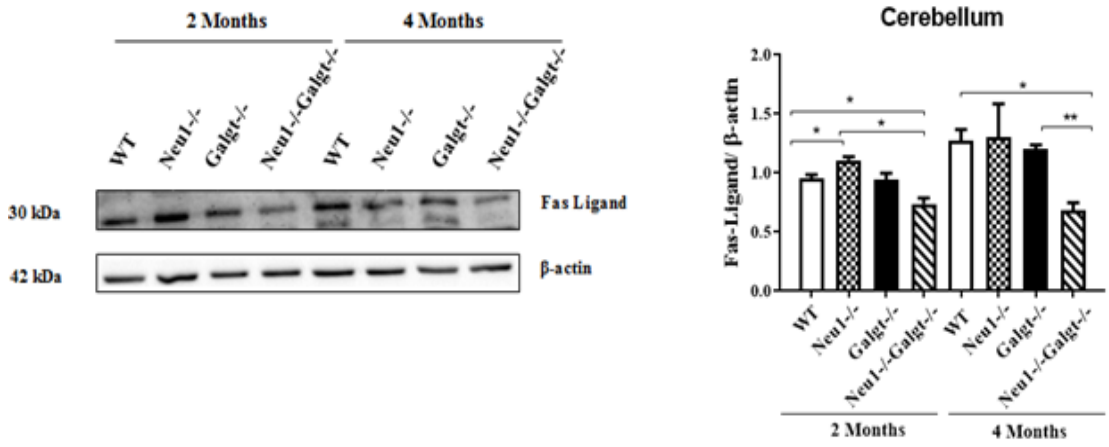

Figure 3.27. Western blot analysis of Fas-Ligand in cerebellum region for 2-and 4-month-old WT, Neu1-/-, Galgt-/- and Neu1-/-Galgt-/- mice. B-actin was internal control (A). Densitometry analysis of Fas-Ligand relative to β-actin (B).(Band intensities were determined by ImageJ and p values were determined by two-way-ANOVA analysis by GraphPad. Data are reported as mean ± SEM, n=3;*p<0,05,**p<0,01)

Increased protein level of cleaved Caspase 9 was detected in 2-month-old Neu1-/- mice in comparison to age-matched littermates but this increase was not statistically significant (Figure 3.28 B).Although it was not statistically significant, 2-month-old Neu1-/-Galgt-/- mice showed decreased protein level of cleaved Caspase 9 compared to age-matched WT and Neu1-/-. In 4-month-old group, single knockout mice had increased level of cleaved Caspase 9 compared to control group. However no significant change was detected in double knockout mice (Figure 3.28 B). Furthermore neither increased nor decreased Caspase 9 protein level was not observed as age-dependent manner.

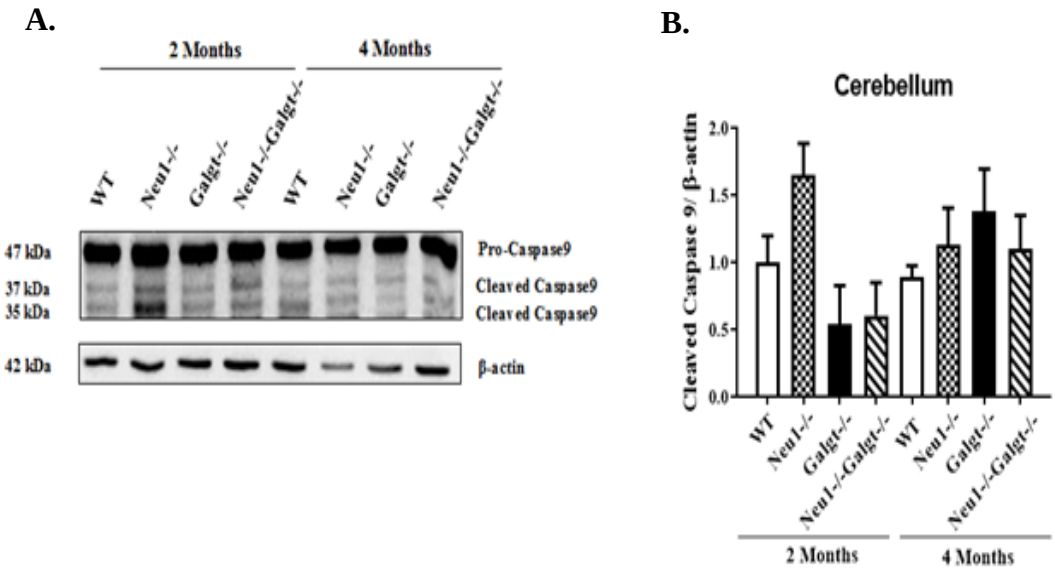

Figure 3.28. Western blot analysis of Caspase 9 in cerebellum region for 2-and 4-month-old WT, Neu1-/-, Galgt-/- and Neu1-/-Galgt-/- mice. β-actin was internal control (A) .Densitometry analysis of Cleaved Caspase 9 relative to β-actin(B).(Band intensities were determined by ImageJ and p values were determined by two-way-ANOVA analysis by GraphPad. Data are reported as mean ± SEM, n=3)

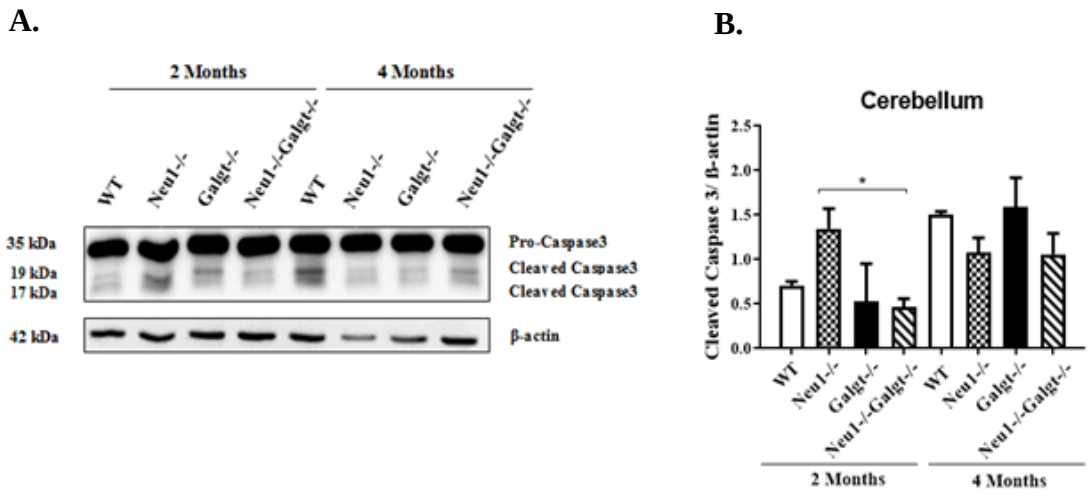

Figure 3.29. Western blot analysis of Caspase 3 in cerebellum region for 2-and 4-month-old WT, Neu1-/-, Galgt-/- and Neu1-/-Galgt-/- mice. β-actin was internal control (A). Densitometry analysis of Cleaved Caspase 3 relative to β-actin (B).(Band intensities were determined by ImageJ and p values were determined by two-way-ANOVA analysis by GraphPad. Data are reported as mean ± SEM, n=3;*p<0,05)

In 2-month-old mice group, double kockout mice had decreased level of cleaved Caspase 3 compared to Neu1-/- mice (Figure 3.29 B). However no significant changes between WT,Galgt-/- and Neu1-/-Galgt-/- were detected. In 4-month-old mice group, no change was evaluated between genotypes for cleaved Caspase 3 protein level (Figure 3.29 B)

BiP protein level analysis demonstrated that there was no significant change in 2-month-old mice group (Figure 3.30 B). In 4-month-old mice group, double knockout mice had decreased protein level of BiP compared to control group. Although it was not statistically significant, 4-month-old single knockout mice showed increased protein level of BiP in comparison to age-matched WT and double knockout mice(Figure 3.30 B).

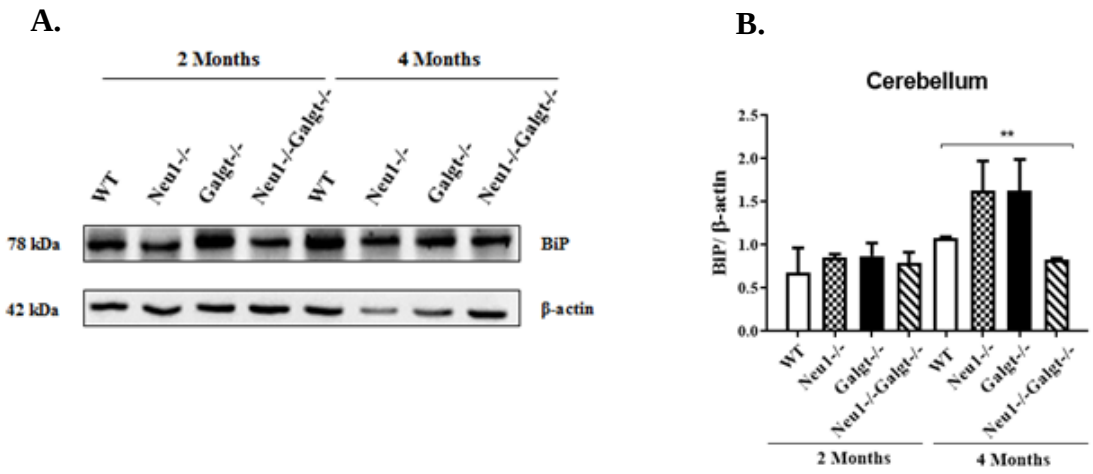

Figure 3.30. Western blot analysis of BiP in cerebellum region for 2-and 4-month-old WT, Neu1-/-, Galgt-/- and Neu1-/-Galgt-/- mice. β-actin was internal control (A) .Densitometry analysis of BiP relative to β-actin (B).(Band intensities were determined by ImageJ and p values were determined by two-way-ANOVA analysis by GraphPad. Data are reported as mean ± SEM, n=3;**p<0,01)

Protein level of Fas-Ligand did not show any significant difference between 2-month-old littermates (Figure 3.31 B). In 4-month-old mice, decreased protein level of Fas-Ligand was detected in single and double knockout mice compared to control group even though no statistically significant change was evaluated (Figure 3.31 B).

There were no significant differences between 2-month-old genotypes in terms of protein level of cleaved Caspase 9 (Figure 3.32 B). However cleaved Caspase 9 level of 4-month-old Neu1-/- mice showed slight increase compared to age-matched WT. Additionally 4-month-old Galgt-/- and Neu1-/-Galgt-/- mice had slight but not significant increase in the level of cleaved Caspase 9 compared to age-matched WT(Figure 3.32 B).

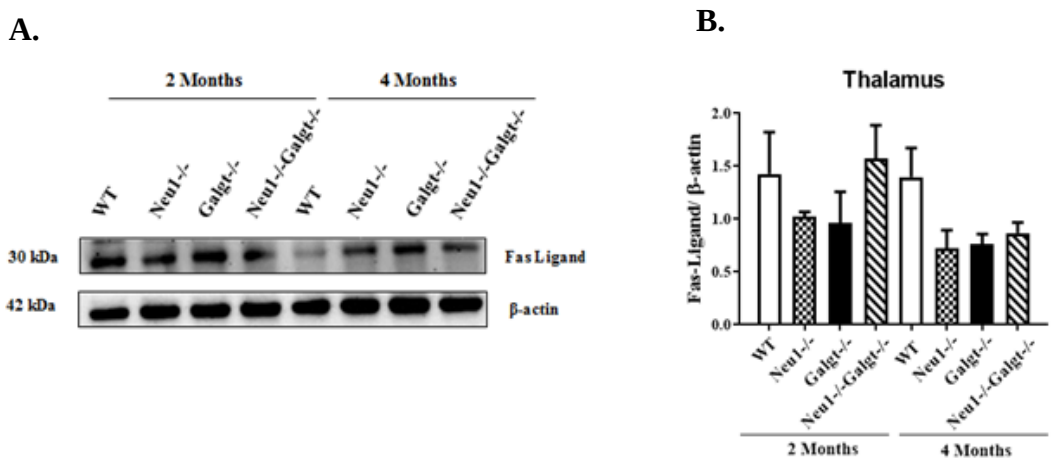

Figure 3.31. Western blot analysis of Fas-Ligand in thalamus region for 2-and 4-month-old WT, Neu1-/-, Galgt-/- and Neu1-/-Galgt-/- mice. β-actin was internal control (A). Densitometry analysis of Fas-Ligand relative to β-actin (B).(Band intensities were determined by ImageJ and p values were determined by two-way-ANOVA analysis by GraphPad. Data are reported as mean ± SEM, n=3)

Protein level of cleaved Caspase 3 showed minor differences in 2-month-old mice group (Figure 3.33 B). Although it was not statistically significant, increased level of cleaved Caspase 3 was observed in 2-month-old Galgt-/- and Neu1-/-Galgt mice compared to age-matched WT and Neu1-/- littermates (Figure 3.33 B). In 4-month-old mice group, level of cleaved Caspase 3 did not exhibit any changes except increased protein level in Galgt-/-mice (Figure 3.33 B).

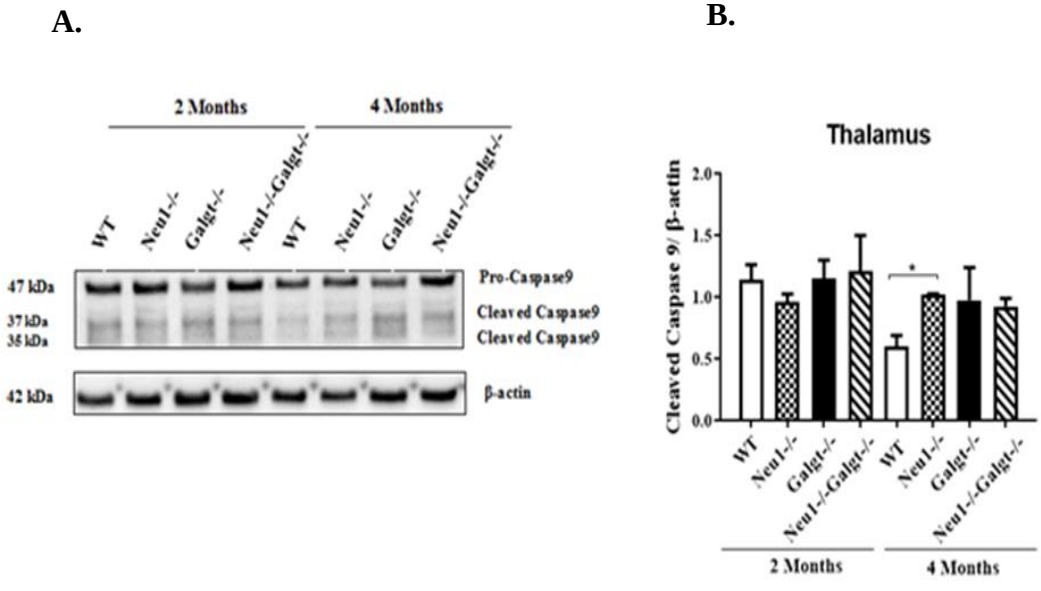

Figure 3.32. Western blot analysis of Caspase 9 in thalamus region for 2-and 4-month-old WT, Neu1-/-, Galgt-/- and Neu1-/-Galgt-/- mice. β-actin was internal control (A) Densitometry analysis of Cleaved Caspase 9 relative to β-actin (B).(Band intensities were determined by ImageJ and p values were determined by two-way-ANOVA analysis by GraphPad. Data are reported as mean ± SEM, n=3;*p<0,05)

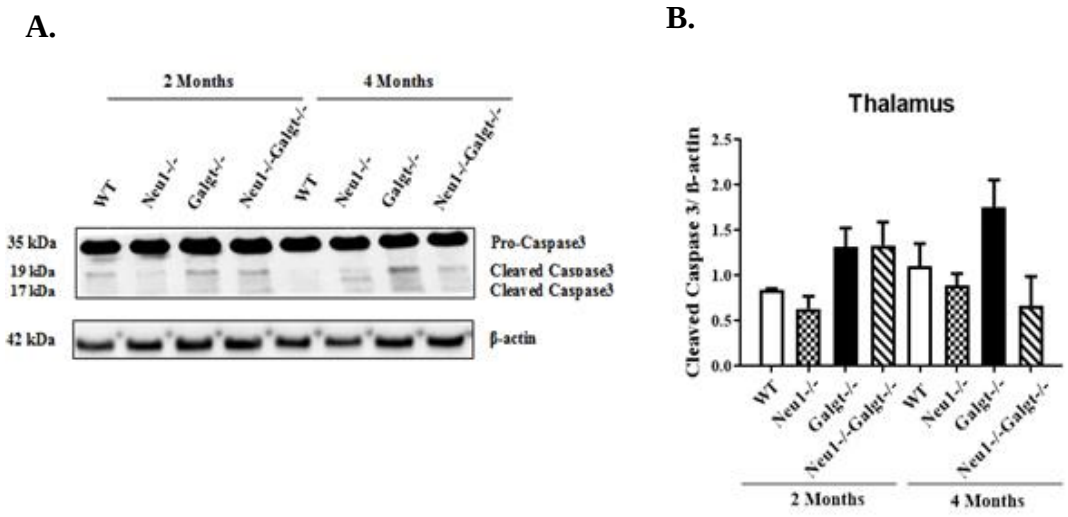

Figure 3.33. Western blot analysis of Caspase 3 in thalamus region for 2-and 4-month-old WT, Neu1-/-, Galgt-/- and Neu1-/-Galgt-/- mice. β-actin was internal control (A).Densitometry analysis of Cleaved Caspase 3 relative to β-actin (B).(Band intensities were determined by ImageJ and p values were determined by two-way-ANOVA analysis by GraphPad. Data are reported as mean ± SEM, n=3)

Protein level of BiP was significantly increased in 2-month-old Galgt-/- mice compared to Neu1-/-Galgt-/- mice (Figure 3.34 B). In addition to that increased protein level of BiP was detected in 4-month-old Neu1-/- mice compared to age-matched Neu1-/-Galgt-/- mice (Figure 3.34 B). That increase in 2-month-old Galgt-/- and 4-month-old Neu1-/- mice could be associated with ER stress in these mice.

A. **B.**

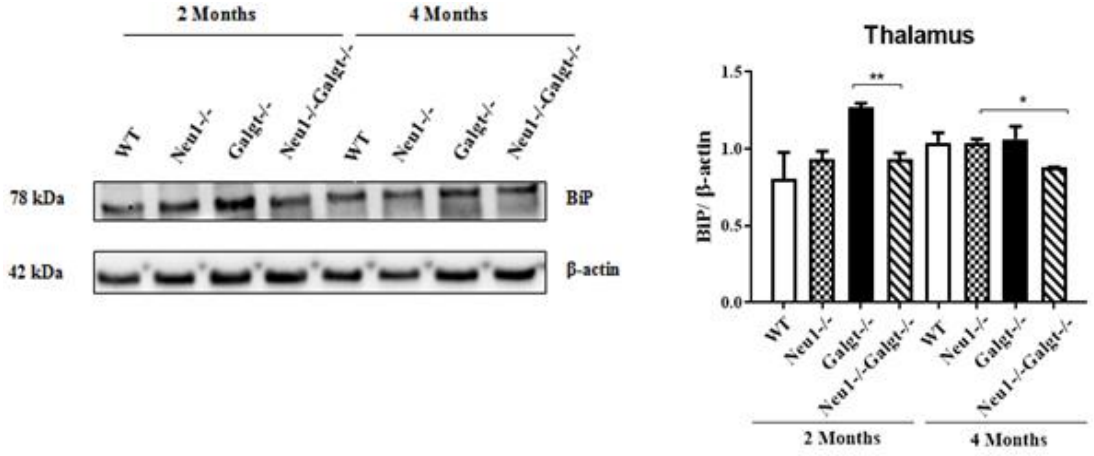

Figure 3.34. Western blot analysis of BiP in thalamus region for 2-and 4-month-old WT, Neu1-/-, Galgt-/- and Neu1-/-Galgt-/- mice. β-actin was internal control (A). Densitometry analysis of BiP relative to β-actin (B).(Band intensities were determined by ImageJ and p values were determined by two-way-ANOVA analysis by GraphPad. Data are reported as mean ± SEM, n=3;*p<0,05,**p<0,01)

3.7. Histologic Stainings

3.7.1.Hemotoxylin-Eosin Staining

In order to analyse if absence of -a and –b series ganglioside or Neu1 deficiency affect brain histology, Hemotoxylin-Eosin staining was performed . For this aim 10 μm thickness coronol sections of cortex and cerebellum regarding 2-and 4-month-old WT,Neu1-/-,Galgt-/- and Neu1-/-Galgt-/- mice were used.

In cortex, 2- and 4-month-old WT mice had normal histologic structure (Figure 3.35 A; Figure 3.36 A). However moderate edema was observed in both 2-and 4-month-old Neu1-/- mice. Additionally disorganization was detected in cortex structure and dilatation in veins was noted with edema. Degenerative findings were noticed in neurons and glial cells for Neu1-/- mice (Figure 3.35 B; Figure 3.36 B). When compared to Neu1-/- mice, less edema was observed in 2-and 4-month-old Galgt-/- mice brain. Cellular edema and minimal dilatation in veins were detected (Figure 3.35 C; Figure 3.36 C).

However the most dramatic symptoms were detected in 2-and 4-month-old Neu1-/-Galgt-/- mice brain compared to age-matched littermates. Cortex had the most degenerative structure. Cellular death, high level edema, dilations in veins and vacuolization were significant findings for Neu1-/-Galgt-/- mice. Number of the cell in certain area was the least compared to other groups(Figure 3.35 D; Figure 3.36 D).

In hippocampus, the main three layers, stratum polyforma, stratum pyramidate, stratum moleculare, were detected in 2-and 4-month-old WT mice (Figure 3.35 E; Figure 3.36 E). Normal morphological features of these layers were seen in WT mice. On the other hand, vein dilatation and intense edema were noted in white matter of Neu1-/- mice in both age groups (Figure 3.35 F; Figure 3.36 F). 2-and 4-month-old Galgt-/- mice exhibited karyolysis and degeneration in the cell. Moreover edema and vein dilatation were also seen in Galgt-/- mice group (Figure 3.35 G; Figure 3.36 G). 2-and 4-month-old Neu1-/-Galgt-/- mice displayed cell death, high level of edema, dilatation in vein and vacuolated structure in large area. Additionally total cell in the certain area was significantly decreased in Neu1-/-Galgt-/- mice group(Figure 3.35 H; Figure 3.36 H).

In thalamus, 2-and 4-month-old WT mice had normal histologic structure in thalamic nucleus and thalamic neurons (Figure 3.35 I; Figure 3.36 I). Although thalamic nucleuses were seen in Neu1-/- mice, edema was noted as cellular and tissual level for both age groups. Dilatation in veins and cell clearance were observed in Neu1-/- mice group (Figure 3.35 J; Figure 3.36 J).2-and 4-month-old Galgt-/- mice showed edema and intense dilatation in veins (Figure 3.35 K; Figure 3.36 K). Both 2-and 4-month-old Neu1-/-Galgt-/- mice displayed dramatic cell death, dilatation in veins and higher vacuolization (Figure 3.35 L; Figure 3.36 L).

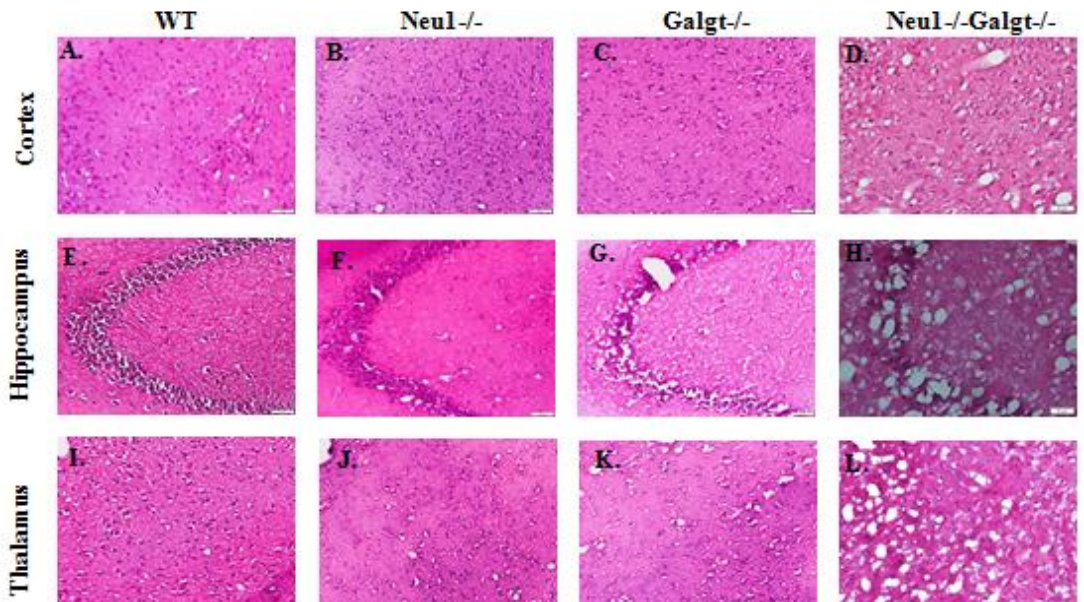

Figure 3.35. Brain pathalogy of 2-month-old mice. H&E staining was performed for cortex sections (A, B, C,and D, respectively), hippocampus sections (E, F, G, and H, respectively), thalamus sections (I, J,K, and L, respectively) and cerebellum sections (M, N, O and P,respectively) of WT, Neu1-/-, Galgt-/- and Neu1-/-Galgt-/- mice.Size bars : 100 μm

In cerebellum, normal white and gray matter distribution was seen in 2-and 4-month-old WT. Three layers, stratum moleculara, stratum gangliosum, stratum granulosum, were detected in cerebellar cortex. In gangliosum layer, Purkinje cells, axon and dendrite initiation were noted. WT mice displayed uniform distribution of Purkinje cells (Figure 3.35 M; Figure 3.36 M). 2-and 4-month-old Neu1-/- mice had minimal edema, dilation in veins. Moreover cellular edema and clearance symptoms were noticed in Purkinje cells of Neu1-/- mice (Figure 3.35 N; Figure 3.36 N). Similar findings were noted in Galgt-/- mice for both age groups (Figure 3.35 O; Figure 3.36 O). Both white and gray matter of 2-and 4-month-old Neu1-/-Galgt-/- mice had intense edematous changes. In addition to that increased Purkinje cell death was detected in Neu1-/-Galgt-/- mice compared to other groups (Figure 3.35 P; Figure 3.36 P). However 4-month old Neu1-/-Galgt-/- mice had dramatic Prukinje cell death compared to 2-month-old counterparts and age-matched littermates. Moreover Neu1-/-Galgt-/- mice group was the most affected group in terms of karyolysis neuron (Figure 3.35 P; Figure 3.36 P)

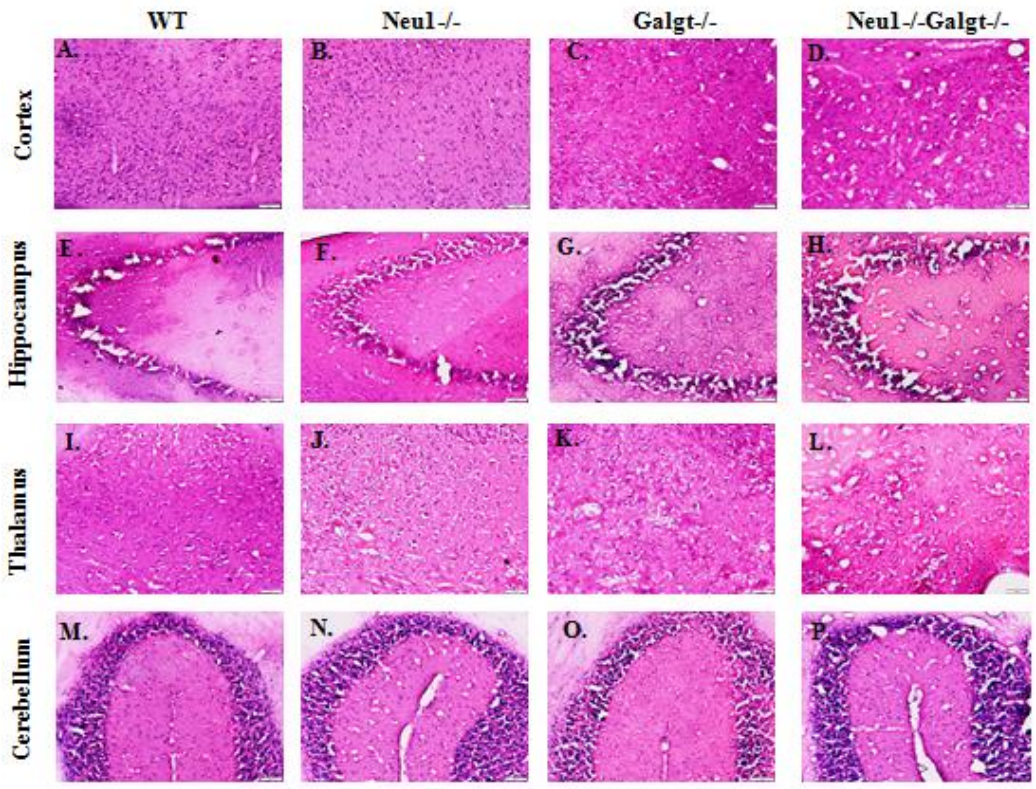

Figure 3.36. Brain pathalogy of 4-month-old mice. H&E staining was performed for cortex sections (A, B, C,and D, respectively), hippocampus sections (E, F, G, and H, respectively), thalamus sections (I, J,K, and L, respectively) and cerebellum sections (M, N, O and P,respectively) of WT, Neu1-/-, Galgt-/- and Neu1-/-Galgt-/- mice .Size bars : 100 μm

3.7.2. Cresyl Echt Violet Staining

To examine neuron structure, 10 μm coronol sections of 2-and 4-month-old WT,Neu1-/-,Galgt-/- and neu1-/-Galgt-/- cortex and cerebellum regions were stained with Cresyl Echt stain.

In 2-and 4-month-old WT mice, degeneration were not observed in neuron structure of cortex, hippocampus, thalamus and cerebellum. Additionally 2-and 4-month-old mice exhibited normal formation of Nissl granules (Figure 3.37 and Figure 3.38 A,E,I,and M). 2-and 4-month-old Neu1-/- and Galgt-/- mice had locally karyolysis (Figure 37 and Figure 3.38 B,C,F,G,J,K,N,and O). However 2-and 4-month-old Neu1-/-Galgt-/- mice displayed intense karyolysis and increased degenerative cells number (Figure 3.37 and Figure 3.38 D,H,L,and P)

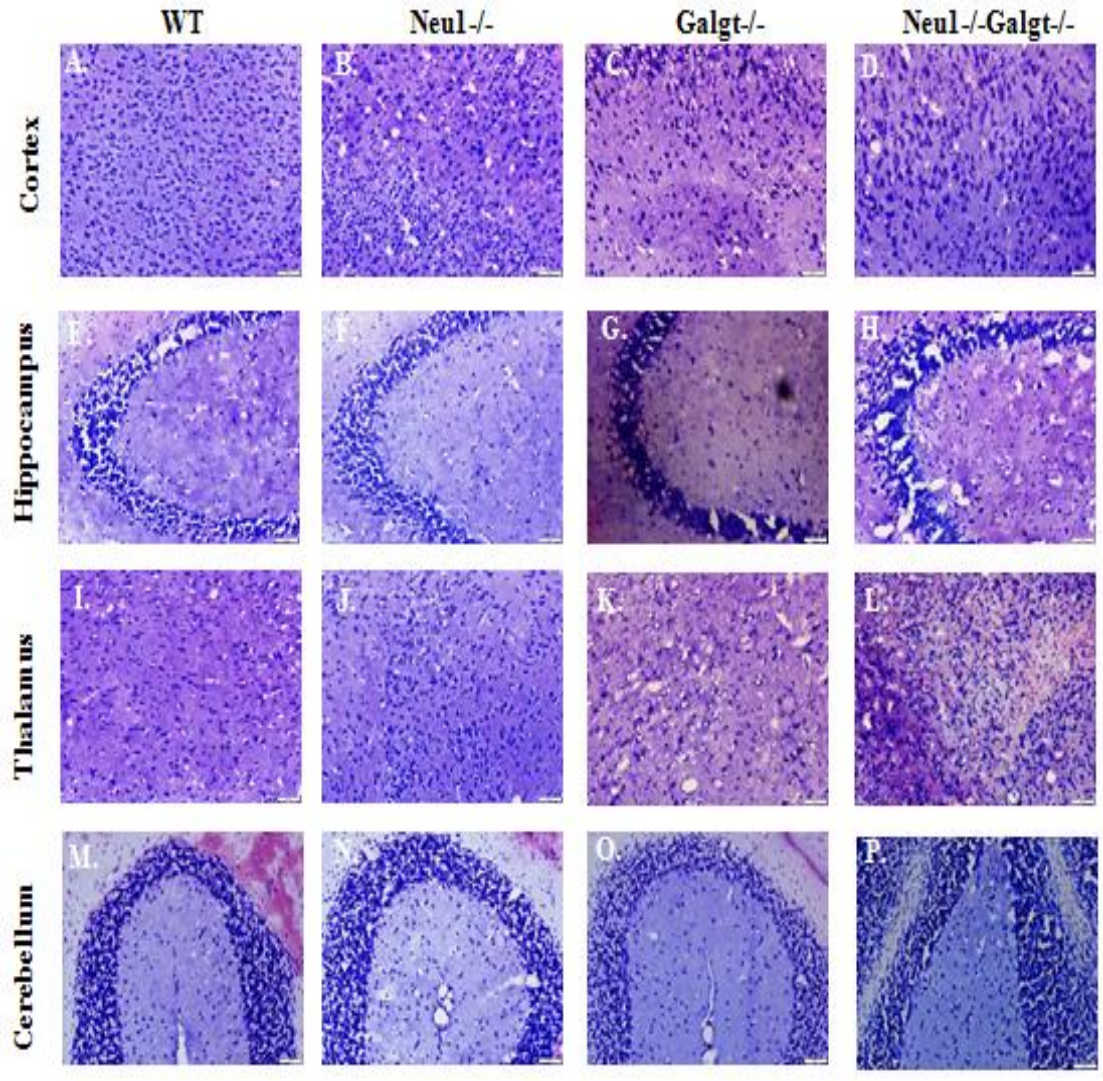

3.37. Neuron structure analysis of 2-month-old mice. Cresyl-Echt Violet staining was performed for cortex sections (A, B, C,and D, respectively), hippocampus sections (E, F, G, and H, respectively), thalamus sections (I, J,K, and L, respectively) and cerebellum sections (M, N, O and P,respectively) of WT, Neu1-/-, Galgt-/- and Neu1-/-Galgt-/- mice .Size bars : 100 μm

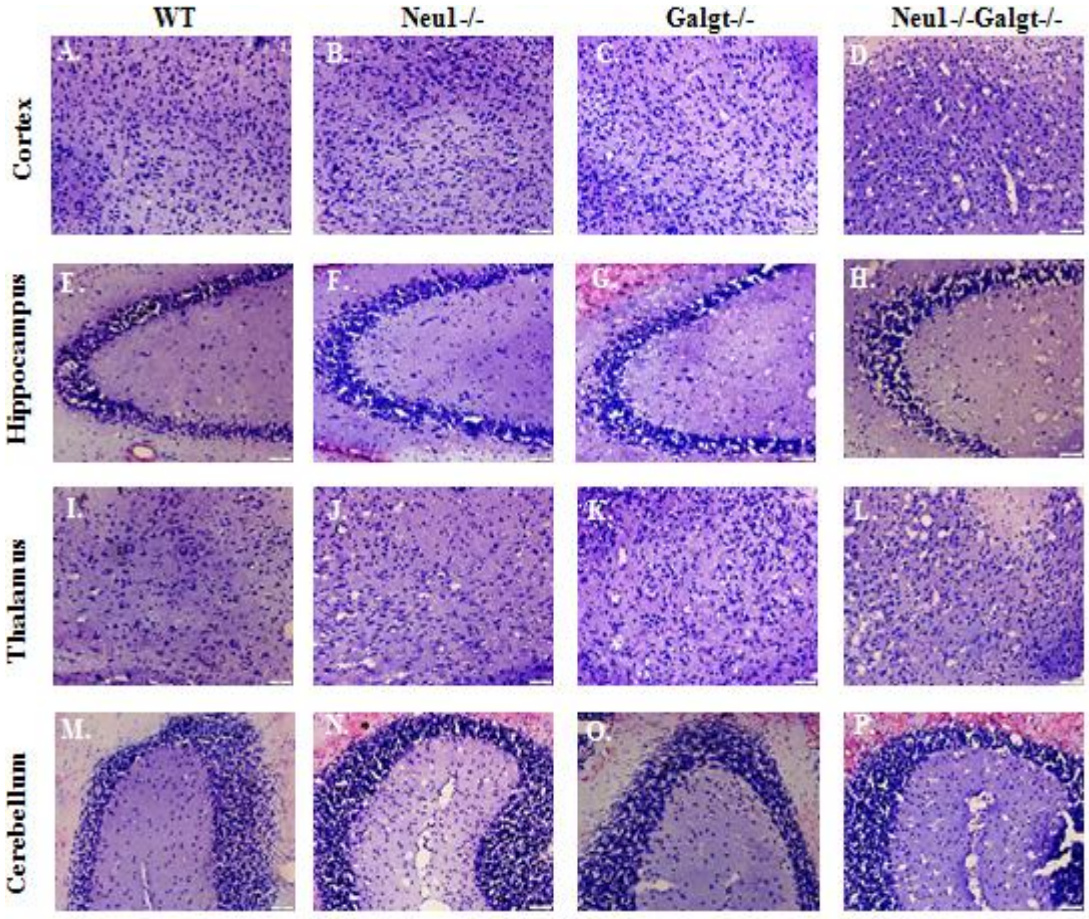

Figure 3.38. Neuron structure analysis of 4-month-old mice. Cresyl-Echt Violet staining was performed for cortex sections (A, B, C,and D, respectively), hippocampus sections (E, F, G, and H, respectively), thalamus sections (I, J,K, and L, respectively) and cerebellum sections (M, N, O and P,respectively) of WT, Neu1-/-, Galgt-/- and Neu1-/-Galgt-/- mice. Size bars : 100 μm

3.7.3. Periodic acid-Schiff Stain (PAS) Staining

In order to detect glycosphingolipid accumulation in WT,Neu1-/-, Galgt-/- and Neu1-/-Galgt-/- mice, Periodic acid-Schiff staining was performed by 10 μm coronol sections belongs to 2-and 4-month-old mice.

Glycosphingolipid accumulation was not detected in cerebellar cortex, hippocampus,thalamus and cerebellum of 2-and 4-month-old WT mice (Figure 3.39 and Figure 3.40 A,E,I,and M). In 2-and 4-month-old Neu1-/- mice ,locally accumulated glycosphingolipid was noticed (Figure 3.39 and Figure 3.40 B,F,J,and N). When compared to Neu1-/- mice, 2-and 4-month-old Galgt-/- mice had less glycosphingolipid

accumulation (Figure 3.39 and Figure 3.40 C,G,K and O). Cellular organization disruption that was related to the highest glycosphingolipid accumulation was detected in Neu1-/-Galgt-/- mice group (Figure 3.39 and Figure 3.40 D,H,L,and P).

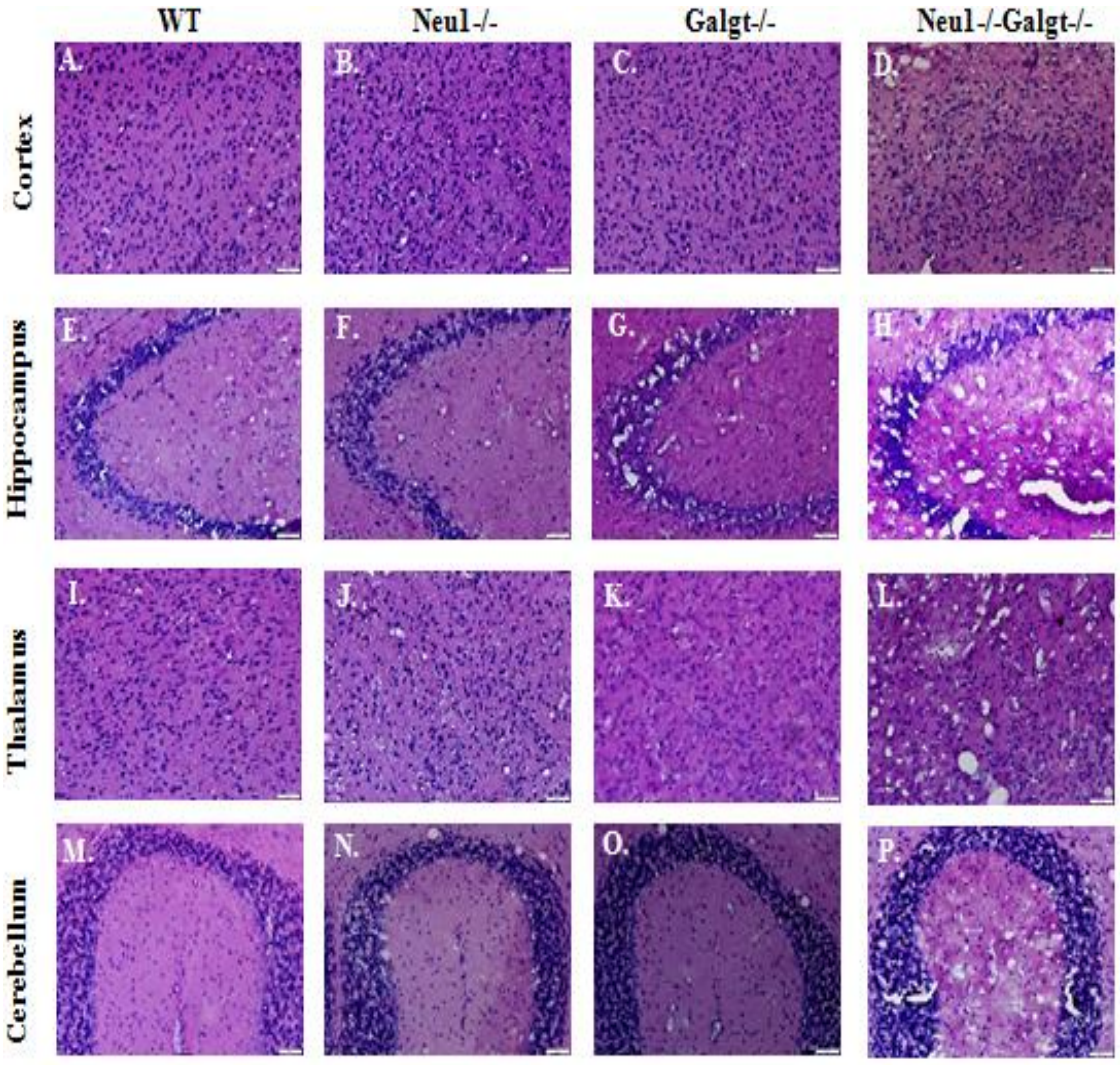

Figure 3.39. Glycolipid accumulation analysis of 2-month-old mice. PAS staining was performed for cortex sections (A, B, C,and D, respectively), hippocampus sections (E, F, G, and H, respectively), thalamus sections (I, J,K, and L, respectively) and cerebellum sections (M, N, O and P,respectively) of WT, Neu1-/-, Galgt-/- and Neu1-/-Galgt-/- mice .Size bars : 100 μm

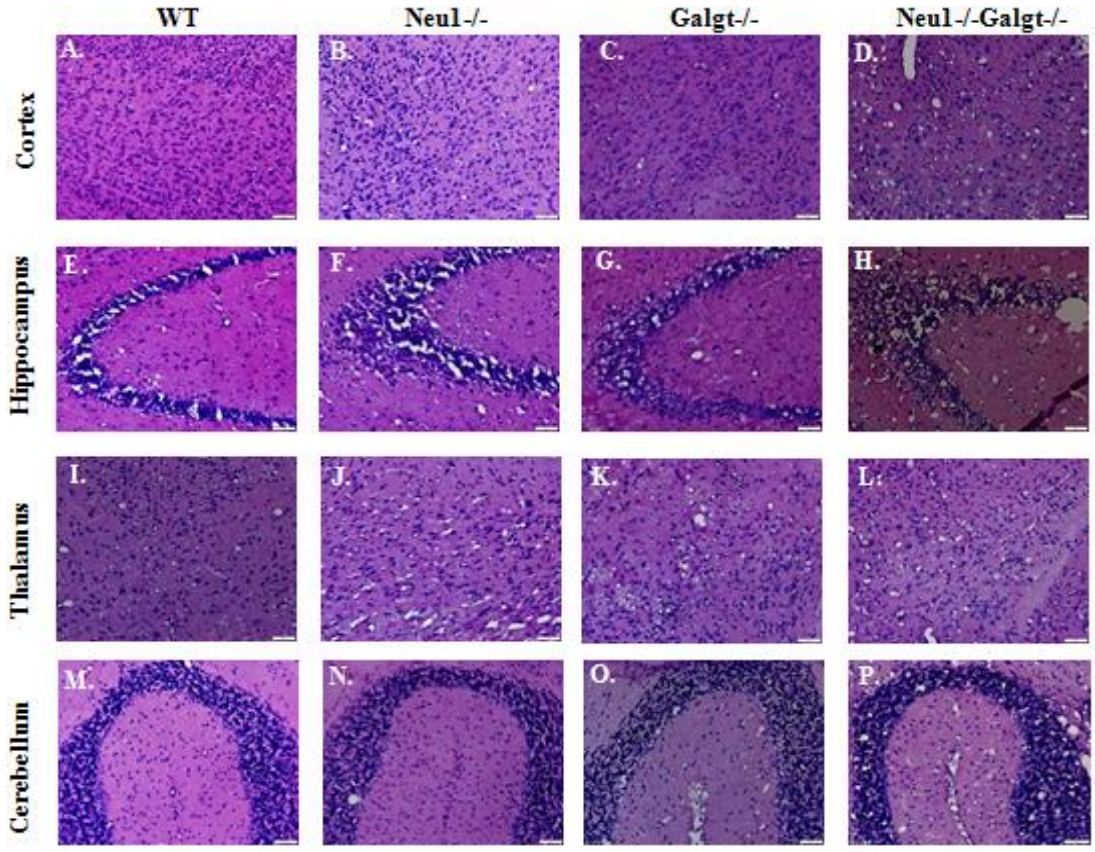

Figure 3.40. Glycolipid accumulation analysis of 4-month-old mice. PAS staining was performed for cortex sections (A, B, C,and D, respectively), hippocampus sections (E, F, G, and H, respectively), thalamus sections (I, J,K, and L, respectively) and cerebellum sections (M, N, O and P,respectively) of WT, Neu1-/-, Galgt-/- and Neu1-/-Galgt-/- mice. Size bars : 100 μm

3.7.4.Luxol Fast Blue Staining

Luxol Fast Blue staining was done from 10 μm coronol sections of 2-and 4-month-old WT ,Neu1-/-,Galgt-/- and Neu1-/-Galgt-/- mice to indicate demyelinated region in the mouse brain,

Demyelinaziton was not noticed in cerebellar cortex, hippocampus, thalamus and cerebellum of 2-and 4-month-old WT mice (Figure 3.41 and Figure 3.42 A,E,I,and M). In Neu1-/- mice brain, minimal partially demyelinazation was observed (Figure 3.41 and Figure 3.42 B,F,J,and N). However in Galgt-/- mice, noticeable demyelination was seen

especially in corpus collosum region (Figure 3.41 and Figure 3.42 C,G,K and O). Demyelinatin of Galgt-/- mice brain was greater than Neu1-/- mice brain and demyelination of Neu1-/-Galgt-/- mice brain was less than Galgt-/- mice but higher than Neu1-/- mice (Figure 3.41 and Figure 3.42 D,H,L,and P). Therefore significant effect of Galgt on demyelination was noted in Neu1-/-Galgt-/- mice. In addition to that, noticed demyelination in Neu1-/- mice compared to WT, could be the sign for importance of Neu1 on myelination process in mouse brain.

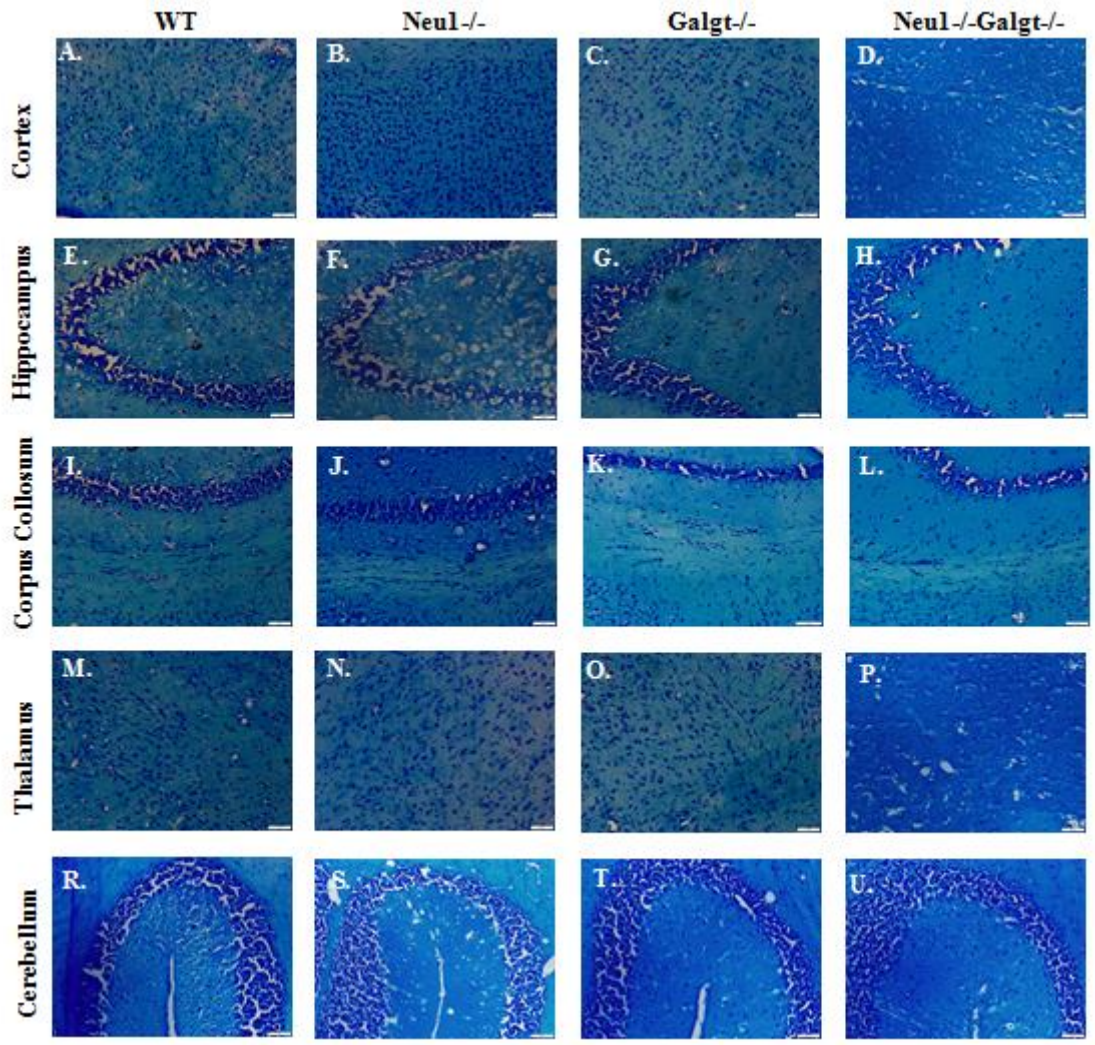

Figure 3.41. Demyelination analysis of 2-month-old mice. Luxol Fast Blue staining was performed for cortex sections (A, B, C,and D, respectively), hippocampus sections (E, F, G, and H, respectively), corpus collosum sections (I, J,K, and L, respectively) ,thalamus sections (M, N, O and P,respectively) and cerebellum sections (R,S,T and U, respectively) of WT, Neu1-/-, Galgt-/- and Neu1-/-Galgt-/- mice .Size bars : 100 μm

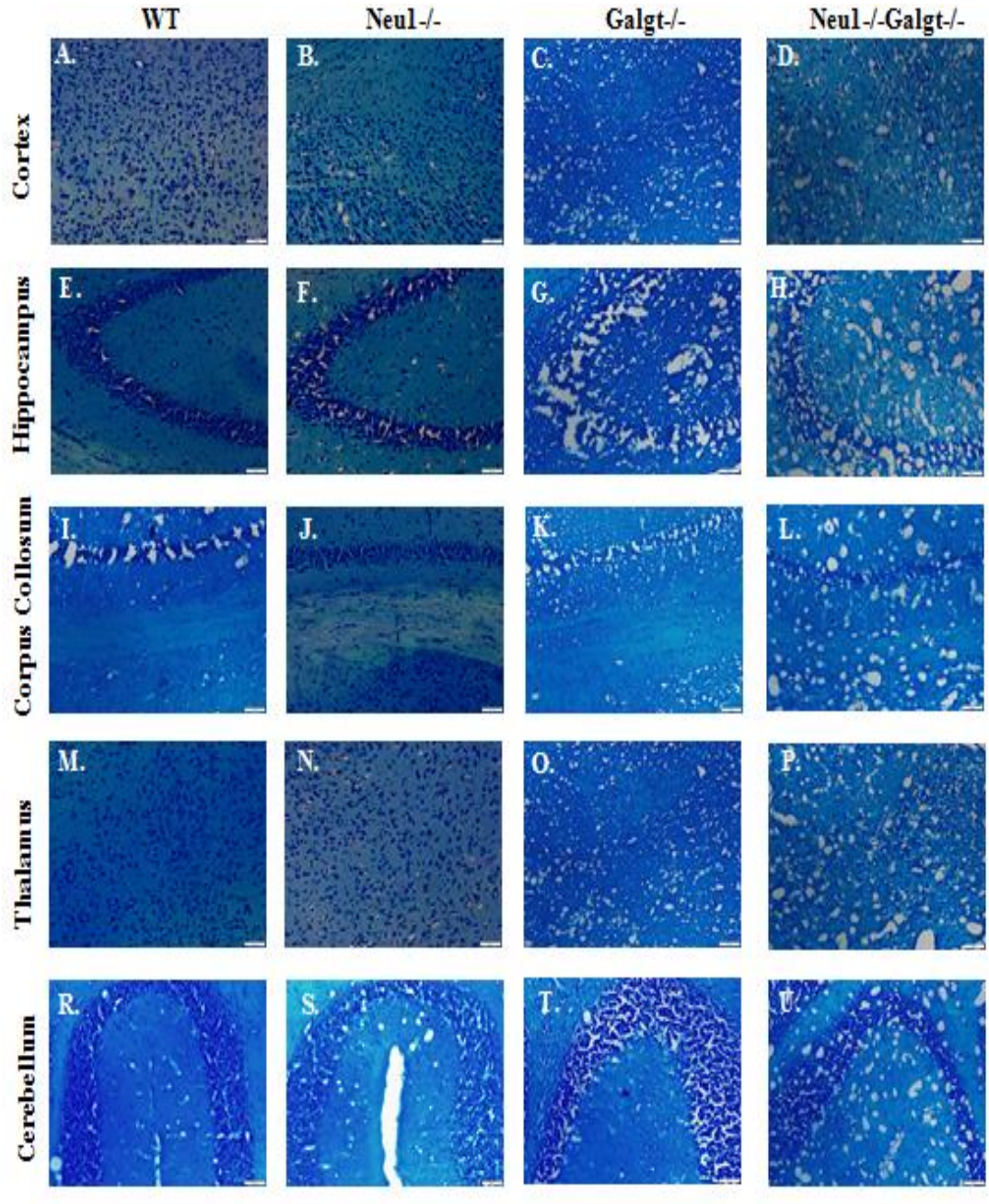

Figure 3.42. Demyelination analysis of 4-month-old mice. Luxol Fast Blue staining was performed for cortex sections (A, B, C,and D, respectively), hippocampus sections (E, F, G, and H, respectively), corpus collosum sections (I, J,K, and L, respectively) ,thalamus sections (M, N, O and P,respectively) and cerebellum sections (R,S,T and U, respectively) of WT, Neu1-/-, Galgt-/- and Neu1-/-Galgt-/- mice .Size bars : 100 μm

3.8. Immunostainings

3.8.1. Anti-CNPase Staining

In order to analyse if single and double deficiency of Neu1 and Galgt affect oligodendrocytes, immunostaining with CNPase antibody was performed in 10 μm coronal sections cortex and cerebellum from 4-month-old WT, Neu1-/-, Galgt-/- and Neu1-/-Galgt-/- mice.

In cortex, single and double knockout mice had decreased CNPase intensity compared to control group (Figure 3.43 C). The most significant CNPase positive cell number loss was detected in Galgt-/- mice. Reduction in CNPase intensity was noted as approximately 44%, 92% and 78% in Neu1-/- , Galgt-/- and Neu1-/-Galgt-/- mice respectively compared to control group. Oligodendrocyte reduction can be associated with demyalinazation and according to these results effect of Galgt deficiency on oligodendrocytes could be seen obviously. Deficiency of Galgt showed its apperant effect on double knockout mice among oligodendrocyte compared to Neu1 deficiency(Figure 3.43 C). Consistent results with Luxol Fast Blue staining were obtained in CNPase analysis

In cerebellum, Neu1-/- and Neu1-/-Galgt-/- mice exhibited significant decrease compared WT and Galgt-/- mice (Figure 3.43 D). The most obvious CNPase positive cell number loss was detected in Neu1-/-Galgt-/- mice (Figure 3.43 D). CNPase intensity reduction was found as approximately 57% in Neu1-/- mice, 20% in Galgt-/- mice, 67% in Neu1-/-Galgt-/- mice compared to WT.

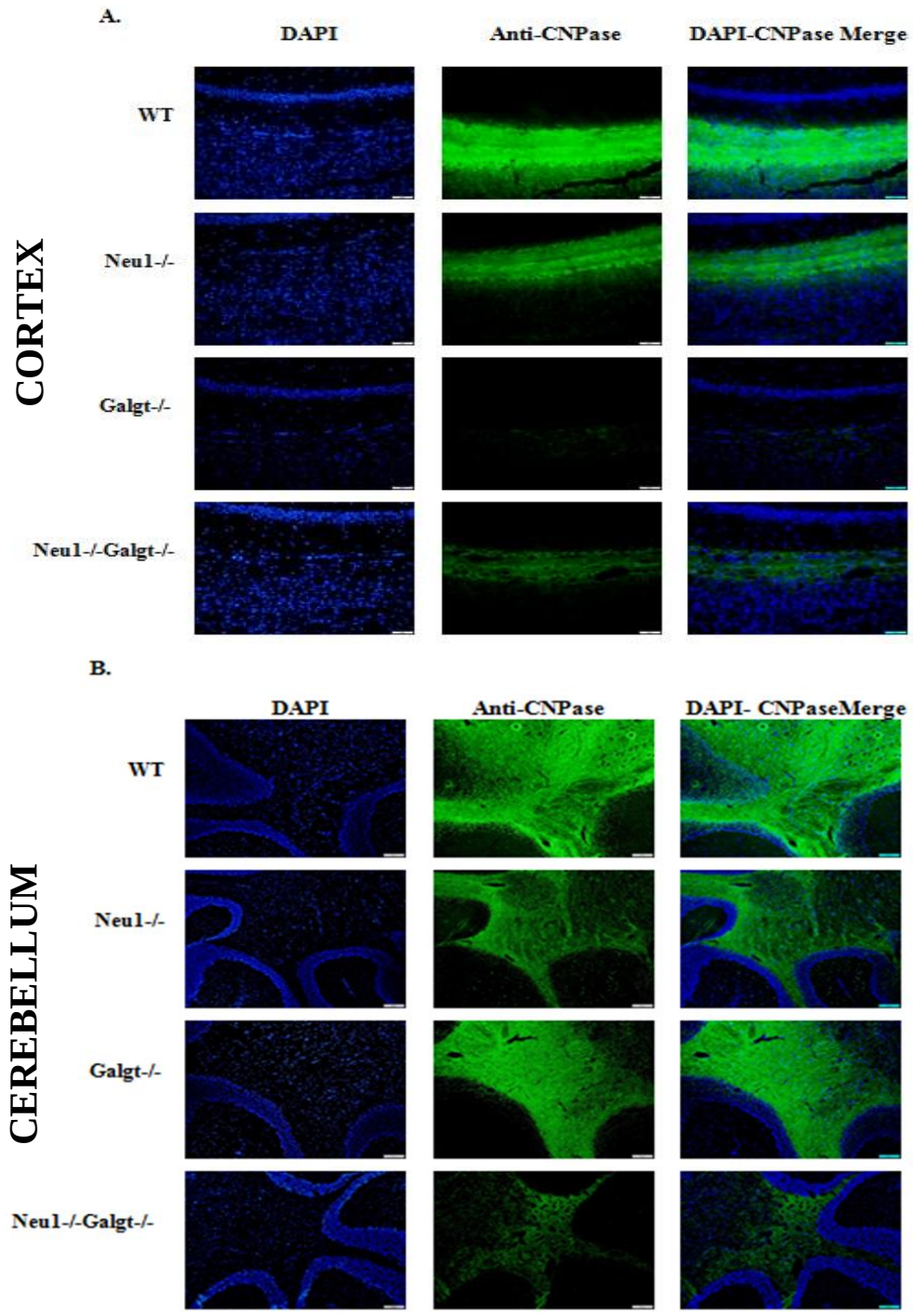

Figure 3.43. Oligodendrocyte detection by anti-CNPase immunostaining for cortex (A) cerebellum region (B) of 4-month-old WT, Neu1-/-, Galgt-/-,Neu1-/-Galgt-/- mice. Quantification of oligodendrocytes in the cortex (C) and cerebellum (D). Size bars: 100 µm. CNPase intensity of samples was normalized to WT. Intensities were determined by ImageJ and one-way ANOVA was used for statistical analysis. The data are reported as the mean ± SEM, n=3; *p<0.05, **p<0.025 ,***p<0,01and ****p<0.001)

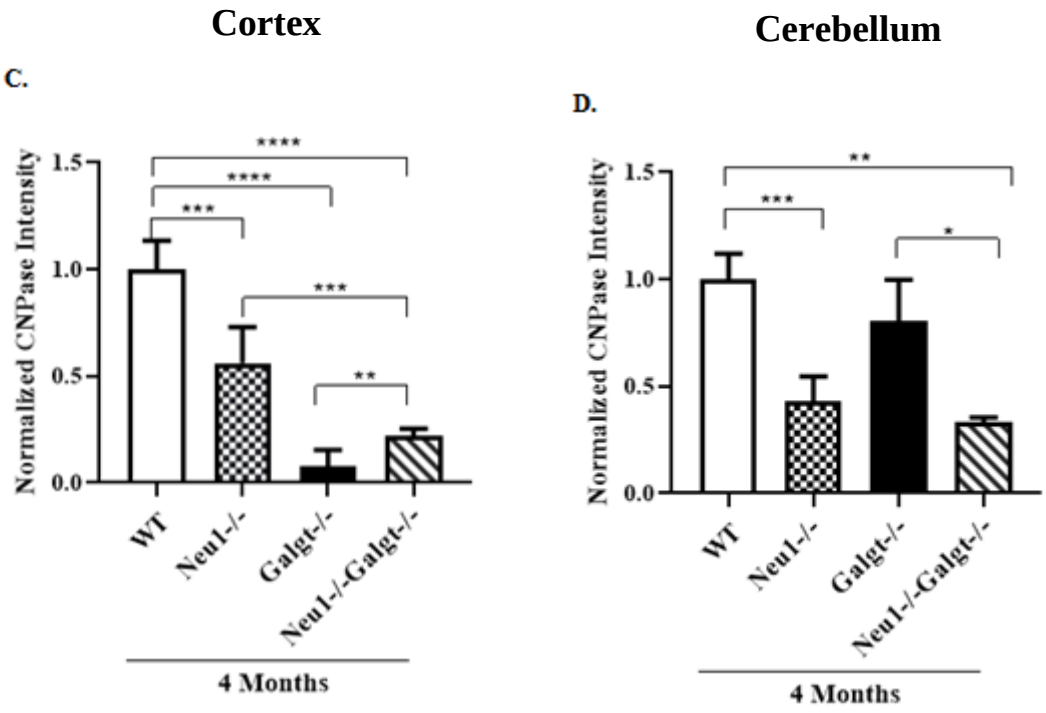

Figure 3.43(cont.)

3.8.2.Anti-NeuN Staining

To detect neuron cell number in cortex,thalamus, hippocampus and cerebellum of 4-month-old WT, Neu1-/-, Galgt-/- and Neu1-/-Galgt-/- mice, immunostiaing was done with anti-NeuN antibody.

Although significant change were detected in cortex, thalamus and hippocampus regions of Neu1-/- and Galgt-/- mice compared to WT, effect of these genes deficiencies was not observed in Neu1-/-Galgt-/- mice. There were no significant changes in cerebellum region among genotypes for neuronal density (Figure 3.44 U). Reduction of NeuN-positive neurons was demonstrated as 70% in cortex (Figure 3.44 R), and 81% in hippocampus (Figure 3.44 S) , 84% in thalamus (Figure 3.44 T), in Neu1-/- mice compared to WT. Galgt-/- mice exhibited reduced NeuN-positive neurons in cortex approximately 69% (Figure 3.44 R), 78% in hippocampus (Figure 3.44 S) and 87% in thalamus (Figure 3.44 T) compared to WT. However there was increased neuronal density in Neu1-/-Galgt-/- mice as 73% in cortex (Figure 3.44 R), 63% in hippocampus (Figure 3.44 S) and 80% in thalamus (Figure 3.44 T)compared to Neu1-/- and Galgt-/- mice.

These results could be explained by distinct impact of Neu1 and Galgt genes on neuronal death which could be supported by TUNEL assay result however double deficiency of these genes did not show similar or combined effect on Neu1-/-Galgt-/- mice' neuronal density. This situation could be the sign for a presence of neuroprotective behavior or compensatory mechanism on the brain in the absence of both Neu1 and Galgt genes.

3.8.3. TUNEL Assay

To detect impact of Galgt and Neu1 enzyme deficiency in neuronal death via apoptosis, TUNEL assay (PROMEGA-DeadEnd^{TM} , Madison, USA)was performed by using 10 μm coronal sections of 4-month-old WT,Neu1-/-,Galgt-/- and Neu1-/-Galgt-/- mice brain. In the principle of this kit, free 3'-OH end of DNA is enzymatically labeled in order to detect DNA strand breaks. In the case of apoptosis, new free 3'-OH ends are generated results in DNA fragmentation. However in normal conditions, nuclei do not include detectable 3'-OH ends of DNA. Therefore apoptotic and non-apoptotic situation can be differentiated each other by using this kit.

In cortex, Neu1-/- and Neu1-/-Galgt-/- mice had noticable TUNEL positive neurons compared to WT and Galgt-/- mice. Neu1-/- mice exhibited approximately 6 fold increased TUNEL positive neurons while Neu1-/-Galgt-/- mice had 7 fold inceased TUNEL positive neurons compared to WT (Figure 3.45 C).

In cerebellum, although slight changes were noticed in both single and double knockout mice, significant increase in TUNEL postive neurons was detected only in Galgt-/- mice (2,3 fold increase) compared to control group (Figure 3.45 D).

In hippocampus, elevated number of TUNEL positive neurons was detected in both Galgt-/- and Neu1-/-Galgt-/- mice. Compared to WT, 7 fold changes was noted in Galgt-/- mice while 9 fold change was detected in Neu1-/-Galgt-/- mice (Figure 3.46 C).

Significant increase in TUNEL positive neurons was noticed in thalamus of Neu1-/- and Neu1-/-Galgt-/- mice group. Change in TUNEL positive neurons was approximately 3 fold in Neu1-/- and 5 fold in Neu1-/-Galgt-/- mice (Figure 3.46 D).

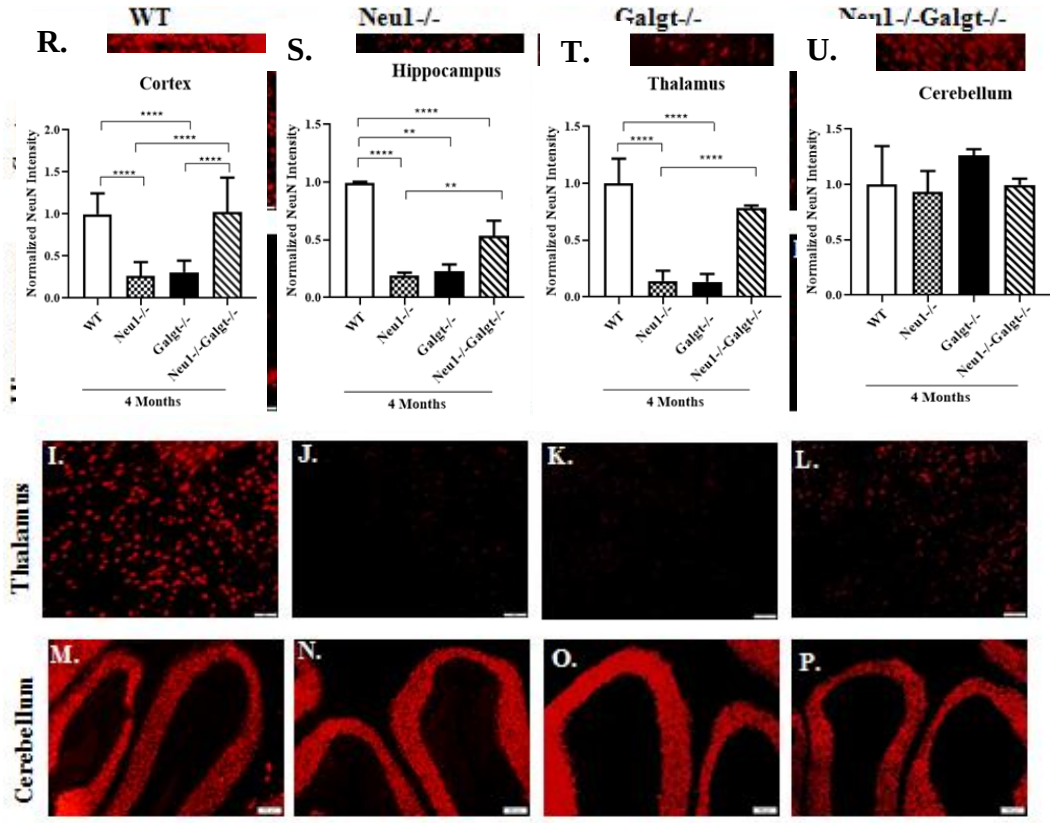

Figure 3.44. Neuron number analysis by anti-NeuN immunostaining for cortex (A, B,C, and D, respectively), hippocampus (E, F, G, and H, respectively), thalamus (I, J, K, and L, respectively) and cerebellum (M, N, O and P, respectively) of 4-month-old WT, Neu1-/-, Galgt-/- and Neu1-/-Galgt-/- .Quantification of neuronal density for cortex (R), hippocampus (S), thalamus (T) cerebellum (U). Size bars: 100 μm. NeuN intensity of samples was normalized to WT. Intensities were determined by ImageJ and one-way ANOVA was used for statistical analysis. The data are reported as the mean ± SEM, n=3; *p<0.05, **p<0.025 ,***p<0,01 and ****p<0.001)

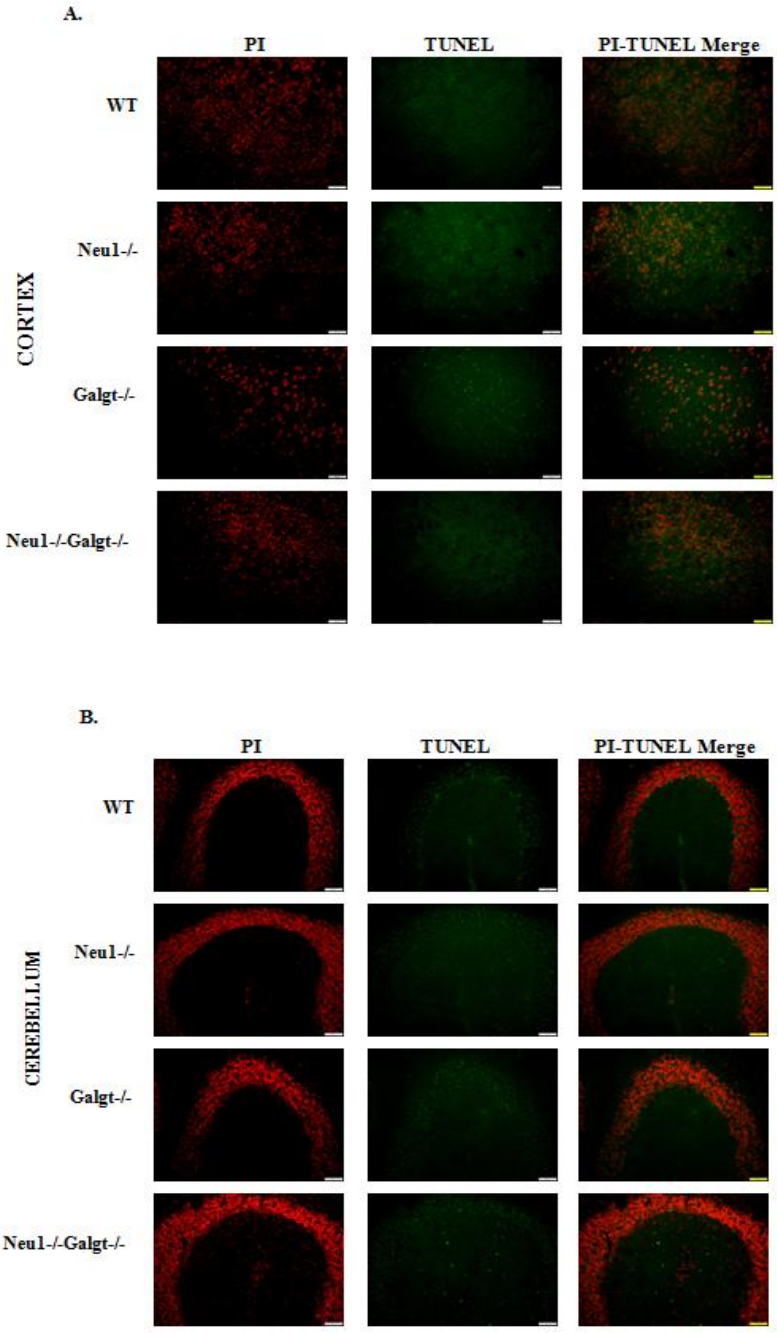

Figure 3.45. Apoptosis detection by the TUNEL assay for cortex (A) and cerebellum (B) section of 4 month-old WT,Neu1-/-,Galgt-/-,and Neu1-/-Galgt-/- mice. Apoptosis was detected with Terminal deoxynucleotidyl transferase (TdT) as green while nuclei were stained with Propidium iodide (PI) as red. Quantification of TUNEL positive neurons in cortex (C) and cerebellum (D). Size bars: 100 μm. TUNEL intensity of samples was normalized to WT. Apoptosis was determined with colocolization of green and red stain as yellow in Image J program and one-way ANOVA was used for statistical analysis. The data are reported as the mean ± SEM, n=3; *p<0.05, **p<0.025 ,***p<0,01and ****p<0.001)

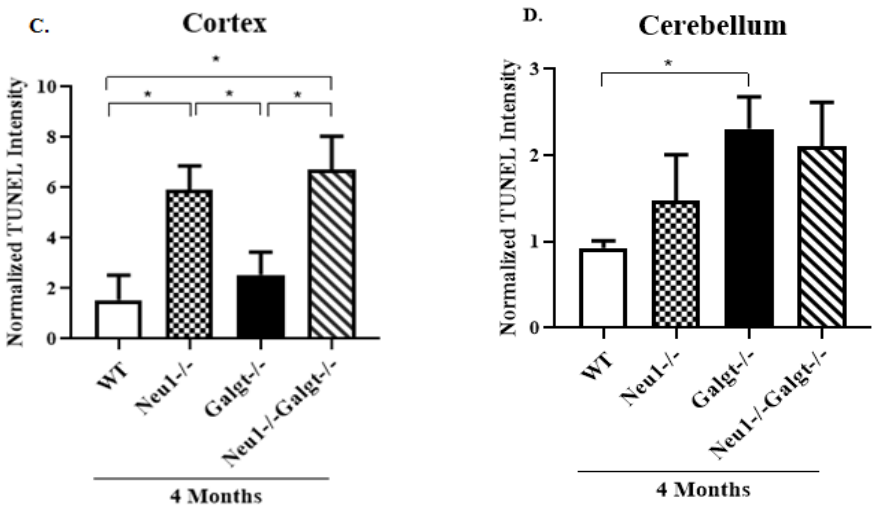

Figure 3.45(cont.)

3.9.Behavioral Analysis

3.9.1.Rotarod Test

In Rotarod Test, aim was to understand changed ganglioside content and Neu1 enzyme deficiency in the brain of mice either has an effect on motor activity or not. For this aim, time spend on the accelerating rod was measured and recorded for each mice. When looked at the duration on the rod, 2-month-old Neu1-/-Galgt-/- had decresed time compared to age matching WT mice (55%), Neu1-/- mice (59%) and Galgt-/- mice (52%) (Figure 3.47). In single knockout mice, age-related changes were not detected. In 4-month-old group, double knockout mice displayed significant decrease in time spending on rod compared to WT as 94% , Neu1-/- as 96%, Galgt-/- as 94% (Figure 3.47). Result of 4-month-old double knockout mice showed that these mice spend the least time on accelerating rod among whole experiment mice. These results had indicated that two gene deficiency affected locomotor activity of mice progressively.

Decreased locomotor activity could be correlated with altered ganglioside pattern and Neu1 deficiency in brain, especially in cerebellum region. Moreover Purkinje cell death detection by H&E staining in 4-month-old Neu1-/-Galgt-/- mice could be the evidence for impairment in motor activity and balance of this mice.

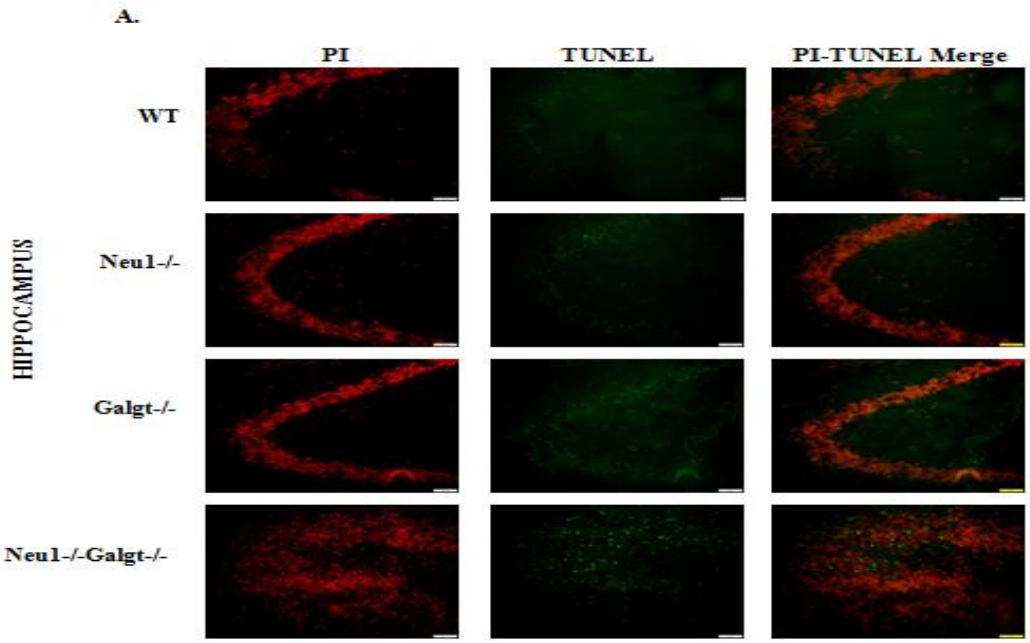
A.
PI
TUNEL
PI-TUNEL Merge
WT
Neu1-/-
Galgt-/-
Neu1-/-Galgt-/-
HIPPOCAMPUS

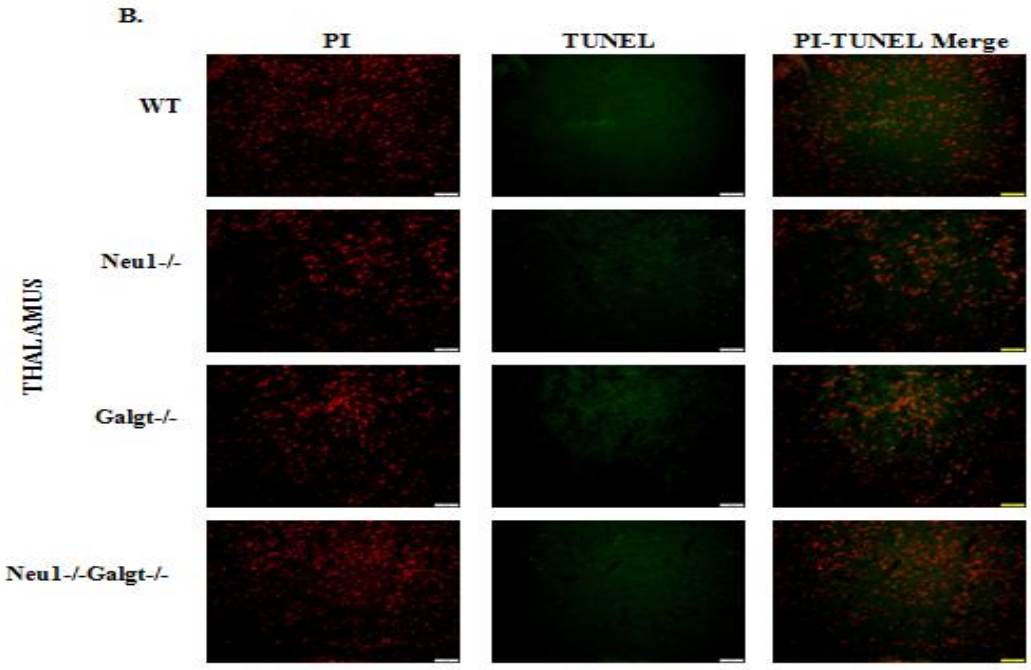

Figure 3.46. Apoptosis detection by the TUNEL assay for hippocampus (A) and thalamus (B) section of 4 month-old WT,Neu1-/-,Galgt-/-,and Neu1-/-Galgt-/- mice. Apoptosis was detected with Terminal deoxynucleotidyl transferase (TdT) as green while nuclei were stained with Propidium iodide (PI) as red. Quantification of TUNEL positive neurons in hippocampus (C) and thalamus (D). Size bars: 100 μm. TUNEL intensity of samples was normalized to WT. Apoptosis was determined with colocolization of green and red stain as yellow in Image J program and one-way ANOVA was used for statistical analysis. The data are reported as the mean ± SEM, n=3; *p<0.05, **p<0.025 ,***p<0,01 and ****p<0.001)

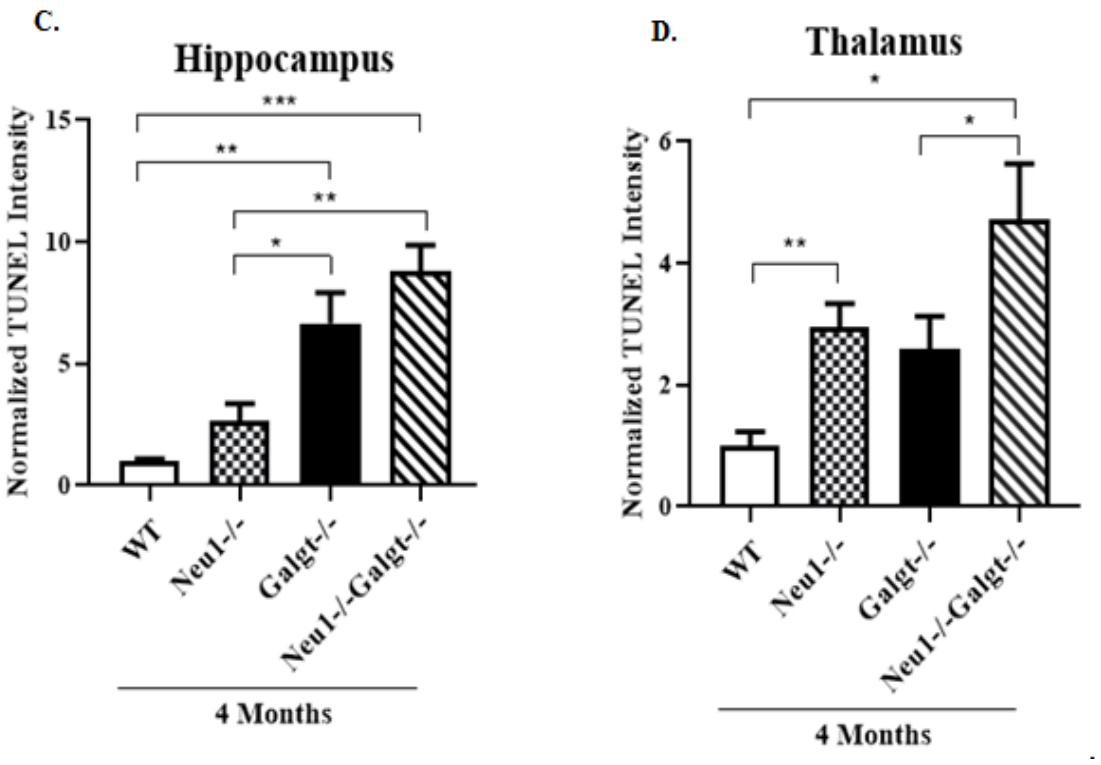

Figure 3.46 (cont.)

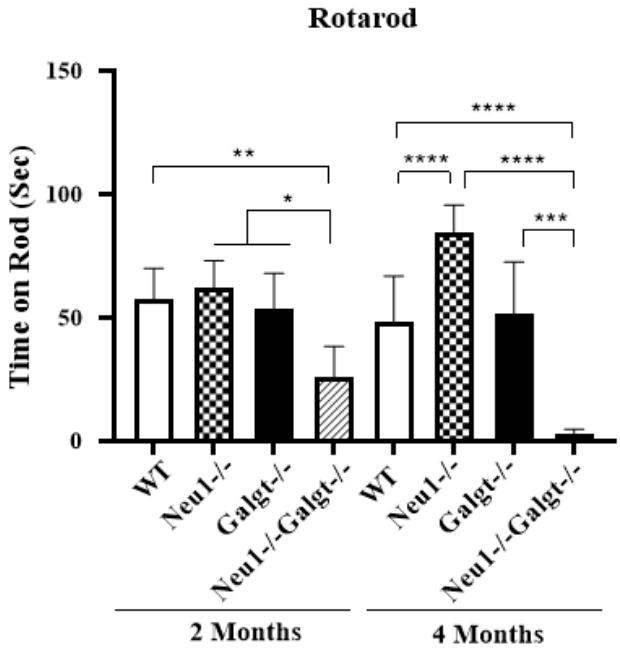

Figure 3.47. Time spend on accelerating rod of 2- and 4-month-old WT, Neu1-/- , Galgt-/- and Neu1-/-Galgt-/- mice. Before the test, mice were trained on the rod for coordination and runnıng and then each mouse was tested as three times for the experiment. Two-way-ANOVA statistical analysis was applied for p values determination in GraphPad. Data were reported as means ± SEM, n=6; p<0,05 **p<0,01, ***p<0,001, ***p<0,0001

3.9.2. Limb Grip Strength Measurement Test

In this behavioral analysis, understanding of altered ganglioside pattern and Neu1 enzyme deficiency effect on nerve-muscle function and muscle strength as age-dependent manner was aimed. For this purpose mice were allowed to grab bar with their forelimb and grip strength of 2-and 4-month-old WT, Neu1-/-, Galgt-/- and Neu1-/-Galgt-/- mice were recorded. According to forelimb grip strength results, 2-and 4-month-old WT, Neu1-/- and Galgt-/- mice did not exhibit significant changes compared to each other (Figure 3.48).

However 1.4 fold decreased forelimb grip strength was detected in 2-month-old double knockout mice compared to age-matched control group.4-month-old double knockout mice displayed significant decrease in forelimb grip strength when compared to aged-matched littermates (1.8 fold in WT, 1.6 fold in Neu1-/- and Galgt-/-) (Figure 3.48). On the other hand, significant difference was not observed between 2-and 4-month old Neu1-/-Galgt-/- mice which indicated that two gen deficiencies did not affect nerve-muscle function as age-dependent manner. Therefore decrement of grip strength in double knockout mice could be explained by combined effect of Neu1 and Galgt deficiency on nerve-muscle functions

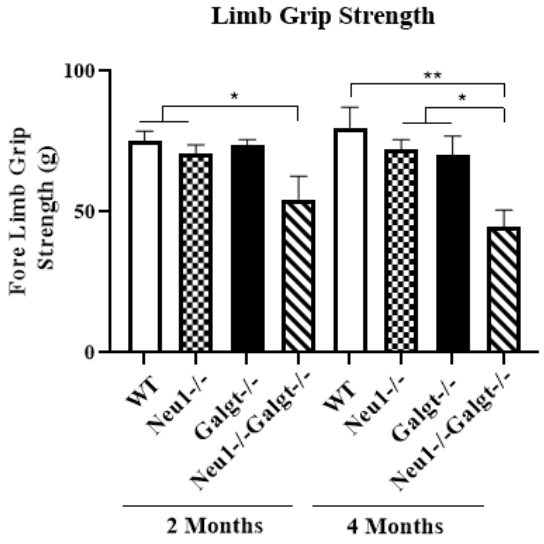

Figure 3.48. Fore limb grip strentg of 2- and 4-month-old WT, Neu1-/- , Galgt-/- and Neu1-/-Galgt-/- mice.Each mouse was subjected to test as three time and average of these three measurement was used. Two-way-ANOVA statistical analysis was applied for p values determination in GraphPad. Data were reported as means ± SEM, n=6; p<0,05 **p<0,01

3.9.3.Passive Avoidance Test

In order to detect if complex ganglioside absent and Neu1 enzyme deficiency causes impairment in learning and memory related with impairment in hippocampus, passive avoidance test was done. 2-and 4-month-old WT,Neu1-/-,Galgt-/-, Neu1-/-Galgt-/- mice were tested during three day and third day scores (re-entering time to dark box after taking electrical shock in second day) were used to evaluate mice' learning and memory capabilities. Latency time to re-enter the dark box of 2-month-old WT, Neu1-/-, Galgt-/- and Neu1-/-Galgt-/- mice: 260 ± 39s, 130 ± 28s, 294 ± 6s, 234 ± 42s (Figure 3.49). In 2-month-old group, significant differences were detected in which Neu1-/- mice had the lowest latency time compared to age-matched littermates (Figure 3.49). In 4-month-old group, almost all WT mice avoided to enter dark box (295 ± 5s). On the other hand Neu1-/- (36 ± 4s) and Neu1-/-Galgt-/- (69 ± 4s) mice exhibited impairment in learning and memory compared to WT and Galgt-/- mice (234 ± 65s). Obvious decrement was detected in Neu1-/- and Neu1-/-Galgt-/- mice compared to WT (Figure 3.49). Similar to 2-month-old group, 4-month-old Neu1-/- mice had lower latency time than 4-month-old Galgt-/-mice. Additionally, age-related defect on learning/memory was observed in 4-month-old Neu1-/- and Neu1-/-Galgt-/- mice compared to 2-month-old counterparts. 4-month-old Neu1-/- and Neu1-/-Galgt-/- mice displayed significant decrease in re-entered time to the dark box. According to this result, effect of Neu1 enzyme deficiency on hippocampus and learning/memory function of mice could be noted.

3.9.4.Open Field Test

Open Field test aimed to evaluate if altered ganglioside pattern and Neu1 enzyme deficiency affect anxiety like behavior, sedation and locomotor activity of single and double knockout mice. For this aim, behavior of 2-and 4-month-old WT, Neu1-/-,Galgt-/- and Neu1-/-Galgt-/- mice in 5 minute period were recorded and analyzed. In this test, two distinct results were obtained: spent time in center and walked total distance. According to time in center evaluation, 2-and 4-month-old Neu1-/- and Neu1-/-Galgt-/- mice spent significantly decreased time compared to age-matched WT and Galgt-/- mice (Figure 3.50 A). In 2-month-old group mice' spending time in the center was following:

16 ± 2s in WT, 1,8 ± 1s in Neu1-/-, 6 ± 0,7s in Galgt-/-, 1,12± 0,8s in Neu1-/-Galgt-/-. 4-month-old mice group scores' was like 8 ± 1s in WT, 1,5 ± 0,7s in Neu1-/-, 4 ± 1,4s in Galgt-/-, 0 ± 0s in Neu1-/-Galgt-/- (Figure 3.50 A) .

Especially decreased spent time in the center result for Neu1-/-Galgt-/- mice could be associated with Neu1 gene deficiency. Since Neu1-/- mice tend to spend less time in the center compared to Galgt-/- mice. On the other hand, 4-month-old Neu1-/-Galgt-/- mice spent almost no time in the center and this could be the evidence for the progressive effect of double gene deficiency on anxiety-like behavior.

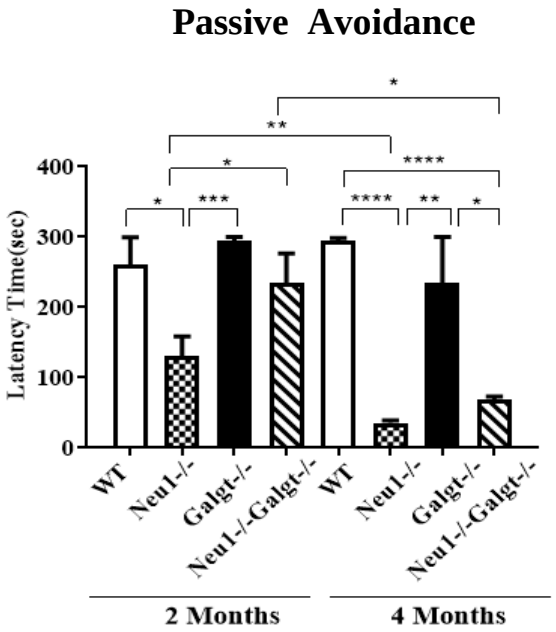

Figure 3.49. Latency time to enter the dark box in the third day of Passive avoidance test for 2-and 4-month-old WT, Neu1-/-, Galgt-/-, Neu1-/-Galgt mice. 300 seconds latency time indicated that mice did not enter the dark box. Two-way-ANOVA statistical analysis was applied for p values determination in GraphPad. Data were reported as means ± SEM, n=6; p<0,05 **p<0,01 ***p<0,001, ***p<0,0001

In walked total distance results indicated that both 2-and 4-month-old Neu1-/-, Galgt-/- and Neu1-/-Galgt-/- mice walked less than WT mice (Figure 3.50 B). In 2-month-old mice group, walked distance decreased in double knockout mice compared to WT as 4 fold and Galgt-/- as 3 fold but no significant difference was noted between Neu1-/- and Neu1-/-Galgt-/- mice (Figure 3.50 B). Additionally, Galgt-/- mice walked longer distance in comparison to Neu1-/- and Neu1-/-Galgt-/- mice. In 4-month-old mice group, double

knockout mice showed significantly decreased distance compared to age-matched littermates as following: 6 fold decrease compared to WT, 2 fold decrease compared to Neu1-/- and 3.4 fold decrease compared to Galgt-/- mice (Figure 3.50 B) . Like in younger group, Galgt-/- mice walked more than 4-month-old Neu1-/- and Neu1-/-Galgt-/- mice (Figure 3.50 B). This result about 2-and 4-month old Galgt-/- mice demonstrated that Galgt-/- mice did not show impairments in locomotor activity for these age groups. Moreover decreased walked distance in both 2-and 4-month-old Neu1-/-Galgt-/- mice could be related with combined effect of Neu1 and Galgt gene on cerebellum region results in impaired locomotor activity.

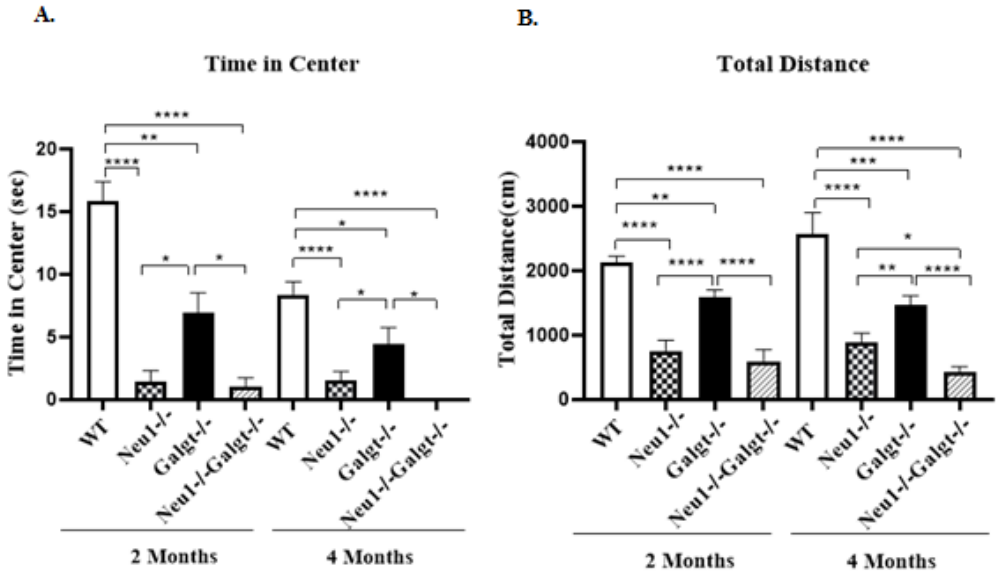

Figure 3.50.Open Field analysis for 2-and 4-month old WT, Neu1-/-, Galgt-/- and Neu1-/-Galgt-/- mice. Anxiety-related behavior was detected by spent time in the center (A) and locomotor activity of mice were tested by walked total distance through 5 minutes (B). Two-way-ANOVA statistical analysis was applied for p values determination in GraphPad. Data were reported as means ± SEM, n=6; p<0,05 **p<0,01 ***p<0,001, ***p<0,0001

3.10. Urine TLC Analysis

Urine TLC analysis was done to detect oligosaccharide pattern in single and double knockout mice. It is known that secretion of oligosaccharides into the urine is seen in Neu1 deficiency. There are two bands (Band 1 and Band 2) on urine TLC for diagnosis of sialidosis or GM1 gangliosidosis (Mutze et al.2017).These bands represents the oligosaccharide accumulation. In this experiment, presence of these bands and intensity of them were analyzed (bands were indicated with red arrows in Figure 3.51). Because of having Neu1 deficiency in these experiment mice groups, oligosaccharide accumulation was analyzed.

Oligosaccharide accumulutaion was detected in both 2 and 4 months-old Neu1-/- and Neu1-/-Galgt-/- mice urine but not in WT and Galgt-/- mice urine. Intensity of these two bands showed differences in 2 and 4 months-old age mice groups. Significant change was not observed among 2 and 4 months-old Neu1-/- mice but intensity of Band 1 and Band 2 increased in older group of Neu1-/-Galgt-/- mice compared to younger group (Figure 3.51 A and B). When compared to 2 months-old Neu1-/- and Neu1-/-Galgt-/- mice urine samples, more accumulated oligosaccharide was detected in Neu1-/- mice urine (Figure 3.51 A and B). In 4 months-old Neu1-/- mice urine, Band1 intensity was significantly higher than age matched Neu1-/-Galgt-/- mice urine (Figure 3.51 A). However Band 2 was more intense in 4 months-old Neu1-/-Galgt-/- mice urine compared to 4 months-old Neu1-/- mice urine (Figure 3.51 B).

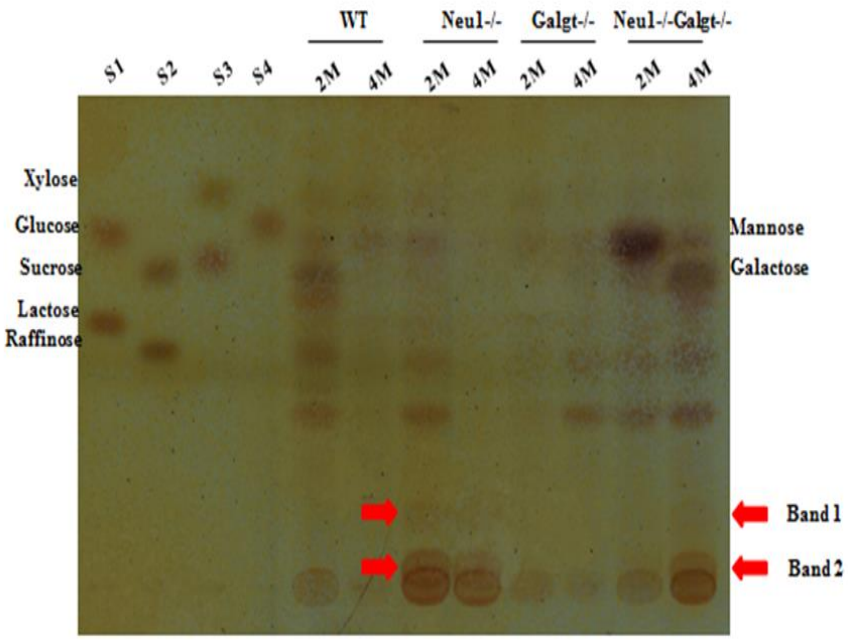

Figure 3.51. Orcinol stained Thin Layer Chromatography for urine samples of 2 and 4-month-old WT,Neu1-/-,Galgt-/-, Neu1-/-Galgt-/- mice. Red arrows show Band 1 and Band 2 that are oligosaccharides . (S1; Glucose and Lactose, S2; Sucrose and Raffinose, S3; Xylose and Galactose and S4; Mannose)

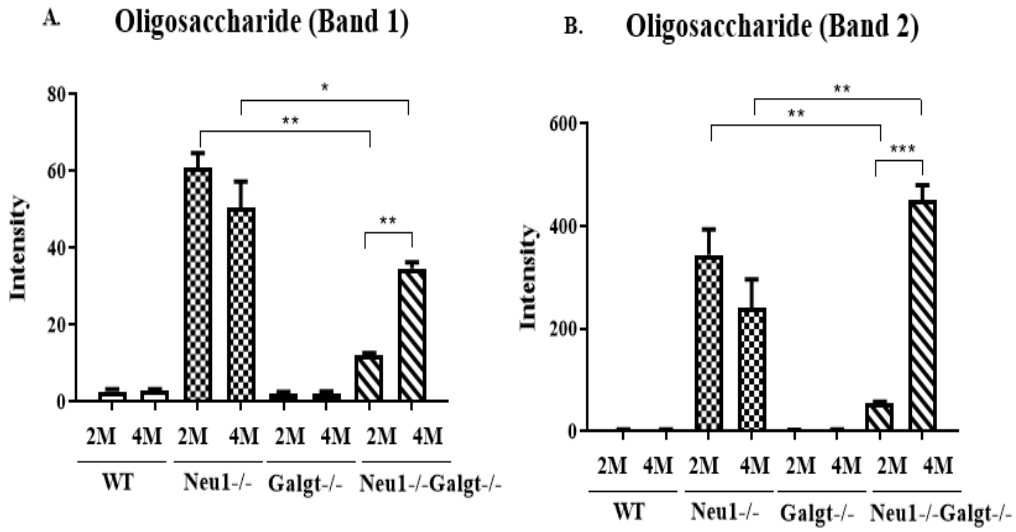

Figure 3.52. Intensity measurement of Band 1(A) and Band 2(B) from urine samples of 2 and 4-month-old WT,Neu1-/-,Galgt-/-, Neu1-/-Galgt-/- mice (Intensity measurement of bands was done by ImageJ software and two-way-ANOVA statistical analysis was applied for p-values determination in GraphPad. Data were reported as means ± SEM, n=3; p<0,05 **p<0,01, ***p<0,001, ***p<0,0001).

CHAPTER 4

DISCUSSION

Lysosomal storage diseases are rare genetic diseases and impairment or defect in lysosomal enzyme activity, cofactor protein or lysosomal protein transportation causes accumulation of specific substrate following secondary ganglioside or lipid accumulation in lysosome. There are more than 40 distinct lysosomal storage diseases and they can be categorized according to accumulated substrate type LSDs (Breiden and Sandhoff 2020). Sialidosis is the member of Glycoproteinoses which is characterized by sialic acid-containing substrate accumulation. In this disease lysosomal Neu1 deficiency results in elevated levels of GM3,GD3, GM4 and LM1 in visceral organs but not in brain. In vitro studies revealed that GM3 is a substrate of Neu1but effect of Neu1 on other accumulated gangliosides still unknown. Sialidosis patients suffer from progressive muscle and central nervous system deterioration, visceromegaly. There is no specific cure or therapies for sialidosis until now LSDs (Breiden and Sandhoff 2020).

As sialylated glycosphingolipids, gangliosides are essential compound of central nervous system that have rol in cell–cell recognition, signal transduction, growth, and motility. In ganglioside biosynthesis pathway, any defects in hydrolase, synthesis enzyme or sphingolipid activator proteins cause Gangliosidoses LSDs (Breiden and Sandhoff 2020). Such defects in lysosomal function result in storage of gangliosides and glycosphingolipids. GM2 Gangliosidoses (including Tay-Sachs disease, Sandhoff disease, GM2AP deficiency) and GM1 Gangliosidoses are subgroups of Gangliosidoses.

In ganglioside synthesis pathway, β-1,4-N- acetylgalactosaminyltransferase (Galgt) plays an essential role to catalyze synthesis of complex gangliosides (Takamiya K.,et al 1996). In Galgt deficiency, only simple gangliosides, LacCer, GM3 and GD3, are synthesized and progressive neurological degenerations are observed due to complex ganglioside absence.

Neu1-/- mice is used as model for Sialidosis Type II characterized as progressive accumulation of oligosaccharide in urea, lysosomal expansion in the nervous system, systemic organs and also in muscle and cartilage (de Geest et al.2002). β-1,4-N-acetylgalactosaminyltransferase deficient mice, Galgt-/-, is accepted as model for Hereditary Spastic Parapliegia and Parkinson's disease (Bhuiyan et al. 2019). Motor impairments, progressive neuropathies, strial dopamine depletion, alpha synuclein accumulation are some of the symptoms that are observed in that mice model . Neu1-/-Galgt-/- double knockout mice model was firstly generated in our laboratory for this study to investigate combined biological roles of Neuraminidase 1 and N-acetylgalactosaminyltransferase enzymes in glycolipid metabolism. In order to understand if double deficiency of Neu1 and Galgt enzymes have progressive effect on mice brain, 2-and 4-month-old WT,Neu1-/-,Galgt-/- and Neu1-/-Galgt-/- mice were analyzed.

For each biochemical analysis at least three different mice brain were used. Collected soft mice brains were analyzed in Thin Layer Chromotography for brain ganglioside analysis, RT-PCR for relative gene expression analysis, Western Blot for protein expression analysis, DNA Fragmentation assay for cleaved DNA,apoptosis, analysis. Paraformaldehyde fixed brain tissues were used in immunohistochemical analysis and histological analysis. Brain urine samples were subjected to oligosaccharide analysis in order to detect accumulated oligosaccharides in urine. Six different mice were used in each behavioral tests, rotarod, limb grip strength, and passive avoidance, open field, to evaluate effect of altered ganglioside pattern on motor coordination, muscle

strength, memory and anxiety-like behaviors respectively. Additionally,WT,Neu1-/-,Galgt-/- and Neu1-/-Galgt-/- mice were weighted during 16 weeks in every two week.

Like in sialidosis type II patients, Neu1-/- mice have symptoms of disease at birth and loss of weight at the end of their life span (6 to 7-month-old age). Additionally Neu1-/- mice have smaller gross appearance and swollen body compared to WT (de Geest 2002).However no phenotypic symptoms associated with Galgt enzyme deficiency were noted in previous studies. Similar to previous observations, Neu1 mice were smaller than WT and these mice loss weight progressively (Figure 3.2). Dramatic differences between WT and Galgt mice were not detected. However most dramatic results in both loss weight and gross appearance were noted in Neu1-/-Galgt-/- mice compared to age-matched littermates(Figure 3.2 A and C). Significant weight loss was indicated in the Neu1-/-Galgt mice and this result could explain the sudden death of these mice at the age of 4-month.

Thin Layer Chromatography is used to separate compounds (oligosaccharides ,lipids,etc.) according to their molecular weight and polarity on the stationary phase with the help of mobile solvent. In this study, TLC was used to analyze ganglioside pattern of single and double knockout mice compared to control group and standards. In this experiment cortex and cerebellum region of 2-and 4-month-old WT,Neu1-/-,Galgt-/- and Neu1-/-Galgt-/- mice brain were used. Before this experiment, ganglioside pattern of Neu1-/-(with reduced neuraminidase-1 activity) mice brain was demonstrated (Seyrantepe at al.,2015). Therefore this study was unique for ganglioside analysis of Neu1-/- (complete knockout) and Neu1-/-Galgt-/- mice brain.

In cortex ,WT and Neu1-/- mice showed similar ganglioside pattern for both 2- and 4-month old mice (Figure 3.3). While GM1,GD1a,GD1band GT1b acidic gangliosides were examined in cortex of 2-and 4-month-old WT and Neu1-/- mice, these gangliosides were not found in cortex of both 2-and 4-month-old Galgt-/- and Neu1-/-Galgt-/- mice (Figure 3.4). Absence of these complex gangliosides had been revealed in Galgt-/- mice in earlier studies (Takamiya et al.1996). Moreover Neu1-/- mice displayed progressive accumulation of GD1a,GD1b,and GT1b gangliosides in 4-month-old group compared to 2-month-old group (Figure 3.4). However there was no significant difference between WT and Neu1-/- mice for both age groups among GM1,GD1a,GD1band GT1b gangliosides(Figure 3.4).

As previously showed, elevated GM3,GD3, and o-Acetyl GD3 level were observed in cortex of both 2-and 4-month-old Galgt-/- mice compared to age matched

WT and Neu1-/- mice (Figure 3.5). Interestingly, progressive accumulations of these gangliosides were not noted in 4-month-old Galgt-/- mice compared to 2-month-old counterpart. Similar to Galgt-/- mice, 2-and 4-month-old Neu1-/-Galgt-/- mice had increased GM3,GD3, and o-Acetyl GD3 level compared to age-matched littermates (Figure 3.5). Noticeable accumulation of these gangliosides was not observed in cortex of 4-month-old Neu1-/-Galgt-/- mice compared to 2-month-old counterpart (Figure 3.5). 4-month could not be enough to detect progressive accumulation of simple ganglioside. If life time of mice would have be longer, progressive accumulation could be determined clearly. Therefore altered ganglioside pattern of Neu1-/-Galgt-/- mice could be explained by Galgt gene deficiency but additional effect of Neu1 on ganglioside metabolism was not discovered. Even though it was known that GM3 is substrate of Neu1, any noticeable effect of Neu1 on brain GM3 was not recorded. If it would have had effect on GM3 degradation, accumulated GM3 could be noticed in Neu1-/- mice and elevated GM3 accumulation could be found in Neu1-/-Galgt-/- double knockout mice compared to Galgt-/- mice.

In cerebellum, similar results to cortex were exhibited (Figure 3.8). GM1,GD1a,GD1b,and GT1b acidic gangliosides were observed only in 2-and 4-month old WT and Neu1-/- mice but no significant differences were detected among WT and Neu1-/- mice and age-dependent accumulation was not noted in both genotype (Figure 3.9). Unlike cortex, only accumulated GD3 was seen in Galgt-/- and Neu1-/-Galgt mice (Figure 3.10). This result could be the evidence for specific distribution of ganglioside among brain regions. However in TLC, thalamus region could not be analyzed because amount of thalamus was not enough to isolate gangliosides. Therefore ganglioside pattern of thalamus region could not be revealed. Obtained results of thalamus region from other experiments could be associated with altered ganglioside pattern of this region. Additionally minor differences in the ganglioside pattern between genotypes could not be detected by TLC method. Only major differences and gangliosides that are found in the stabdard could be analyzed by this method. To solve these problems, more detailed analysis should be performed and LC/MS analysis might be the solution.

Apoptosis was studied in different lysosomal storage disorders' animal model. For example mitochondira-mediated apoptosis in neuronal cells was detected in animal model of GM1 gangliosidosis due to elevated level of GM1 in the lipid rafts of mitochondria-associated ER membranes (MAM) (Sano et al.2009). In the death receptor activated situation which trigger apoptosis, movement of gangliosides toward mitochondria was

observed (Rippo et al.2000). Additionally, mitochondria and GD3 interaction resulting cytochrome c release and Caspase-3 activation was also indicated (Garcia-Ruiz et al. 2002). In another study, relation of GD3 and CD95/Fas-mediated apoptosis in lymphocytes was revealed (Malorni et al.2007). Additionally, protective effects of gangliosides on apoptosis was studied. Protective effect of GM1 gangliosides against the apoptosis in the developing mouse brain was detected (Saito et al.2007). Moreover, effect of sialidases on different cells was studied. Overexpression of NEU1 resulted in increased sensitivity to apoptosis while knockout of NEU1 resulted opposite in murine melanoma cell (Kato et al.2001) Increased sensitivity to apoptotic stimuli ,both extrinsic (Fas-mediated apoptosis) and intrinsic, in cancer cells were noted in the NEU2 overexpressed situation with the reduced GM3 level. (Kato et al.2001;Nath et al.2018). Involvement of NEU3 in apoptosis was demonstrated in skeletal muscle differentiation (Anastasia et al.2008). Overexpression of NEU3 suppressed apoptosis in human colon cancer by increased Bcl-2 protein and decreased caspase expression whereas silencing of NEU3 caused apoptosis with decreased Bcl-XL expression (Kato et al.2006). Relation of NEU4 and mitochondrial alterations leading to cell death via GD3 degradation was demonstrated (Sorice et al.2009)

Relation of apoptosis with gangliosides and silidases were noted in previous studies. In this study, it was investigated whether absence of –a and –b series of gangliosides (increased GM3 and GD3 accumulation) in mouse brain have any effect on apoptosis with contribution of Neu1.

In the case of apoptosis, endonuclease activation is seen in the cell which results in DNA fragments generation and presence of DNA fragments are used as apoptosis marker (Wyllie et al.1980). Agarose gel electrophoresis to observe fragmented DNA in Sandhoff mouse brain indicated discrete DNA bands at 180-200 bp intervals (Huang et al.1997). In order to determine apoptosis presence, DNA fragmentation assay could be the first step. To understand if Neu1 and Galgt enzyme deficiency leads to apoptosis or not in mice brain , 2-and 4-month old WT, Neu1-/-, Galgt-/- and Neu1-/-Galgt-/- mice' cortex,cerebellum and thalamus regions were subjected to DNA fragmentation assay.

In the results of cortex region, an extra band was observed only in the lane of 4-month-old Neu1-/-Galgt-/- mice (Figure 3.13 A). No obvious bands were detected in other genotypes. This result could the sign for apoptosis presence in the 4-month-old Neu1-/-Galgt-/- mice.

In the cerebellum analysis, 4-month-old Galgt-/- and Neu1-/-Galgt-/- mice exhibited extra band but other genotypes did not (Figure 3.13 B). Presence of fragmented DNA in these group could be related with the lack of complex gangliosides in Galgt-/- and Neu1-/-Galgt-/- mice. Additionally, apoptosis could be though as age-dependent manner owing to having extra band only in 4-month-old mice group.

In the thalamus analysis, more different bands were detected in each individual lanes compared to cortex and cerebellum analysis (Figure 3.13 C). 2-and 4-month old Neu1-/-Galgt-/- mice had more obvious bands in corresponding lanes. Especially, smear pattern was observed in 2-month-old Neu1-/-Galgt-/- mice which could be the evidence for apoptosis in that mice (Figure 3.13 C). According to these results, combined effect of Neu1 and Galgt enzymes on apoptosis was evaluated in thalamus region. Being the simplest method for apoptosis detection, complete implication for apoptosis could not be done by DNA fragmentation assay. Therefore more detailed analysis (mRNA level by RT-PCR and protein expression level by Western Blot) were performed to elucidate impact of Neu1 and Galgt enzymes on apoptotis.

Relative mRNA expression level analysis was performed to validate effect of single and double gene deficiency on apoptosis as different manner that are apoptotic, antiapoptotic, oxidative stress, and ER stress on cortex, cerebellum and thalamus regions of 2-and 4-month-old WT,Neu1-/-,Galgt-/- and Neu1-/-Galgt-/- mice. Following gene expression levels were determined: Bax as apoptotic marker, Bcl-2, Bcl-XL as antiapoptotic markers, Catalase, SOD2, TTase1 as oxidative stress markers, ATF6, Calnexin, XBP1 as ER stress markers.

Presence of oxidative stress, ER stress, UPR and relation of these cellular stresses with apoptosis was studied in different lysosomal storage disorders. For example elevated nitric oxide synthase and nitrotyrosine was noted in both GM1 and GM2 gangliosidoses (Jeyakumar et al.2003) and increased ROS level was detected in Fabry disease models (Shen et al. 2008). Niemann-Pick and Gaucher disease fibroblast samples showed enhanced oxidative stress (Deganuto et al.2007; Reddy et al. 2006) However UPR activation was not shown in wide range of LSDs. Gaucher mouse model had no evidence for UPR activation (Farfel-Becker et al.2009) .Activated UPR was observed in mouse model of GM1 gangliosidosis in the brain but UPR was not detected in the spinal cord tissue from sialidosis mouse model (Tessitore et al.2004).

In ER stress analysis, ATF6, Calnexin, and XBP-1expression levels were studied. ATF6 is transmembrane molecule that regulates transcription of ER molecules in

unfolded/misfolded protein response while Calnexin acts as a chaperon molecule for protein folding in ER (Araki and Nagata 2011). XBP1 is a transcription factor that is activated under ER stress condition (Wang et al. 2011). Increased expression of these genes is associated with presence of ER stress in the cell. In cortex, increased expression level of ATF6 was observed in Neu1-/- and Galgt-/- mice compared to WT in both ages (Figure 3.14 A). Additionally 4-month-old double knockout mice showed elevated ATF6 expression compared to WT but this increment could be explained by the Neu1-/- deficiency in that mice (Figure 3.14 A). Higher Calnexin expression was noted in 2-month-old Galgt-/- and Neu1-/-Galgt-/- mice (Figure 3.15 A). Moreover expression level of Calnexin was higher in 4-month-old single and double knockout mice compared to WT (Figure 3.15 A). However when expression levels of Calnexin were compared older mice group had lower level than younger group. Increased XBP-1 expression was detected in 2-month-old Galgt-/- mice and 4-month-old Galgt-/- and Neu1-/-Galgt-/- mice (Figure 3.16 A). Therefore increased expression level of Calnexin and XBP-1 could be related with Galgt enzyme deficiency in that region.In cerebellum, higher expression level of ATF6 was noticed in 2-month-old Galgt-/-and 4-month-old Neu1-/- mice but effect of Neu1 and Galgt deficiency was not detected in double knockout mice (Figure 3.14 B). Since decreased ATF6 expression was noted in both 2-and 4-month-old Neu1-/-Galgt-/- mice (Figure 3.14 B). Both 2-and 4-month-old Neu1-/- mice exhibited higher Calnexin expression and this increase could lead elevation of Calnexin expression in Neu1-/-Galgt-/- mice (Figure 3.15 B). No significant changes were detected for expression level of XBP-1 among genotypes and age groups(Figure 3.16 B).In thalamus, 4-month-old Neu1-/- mice displayed increased expression level of ATF6 compared to age-matched littermates(Figure 3.14 C). Enhanced Calnexin expression was obtained in both 2-and 4-month-old Neu1-/-Galgt-/- mice and this increment could be associated with Neu1 deficiency (Figure 3.15 C). Since Calnexin expression level slightly increased in Neu1-/- mice. Higher expression level of XBP-1 was detected in 4-month-old Neu1-/-Galgt-/- mice compared to 2-month-old Neu1-/-Galgt-/- mice (Figure 3.16 C).

For oxidative stress analysis, expression levels of antioxidant defense mechanism members (Catalase, SOD2, and TTase1) were detected. In cortex region, 4-month-old single and double knockout mice showed increased Catalase expression level compared to control group (Figure 3.18 A). However, TTase1 expression level decreased in 4-month-old single and double knockout mice (Figure 3.19 A). Similar to TTase1 expression level, clear decrease was observed in SOD2 expression level of 4-month-old

mice group compared to younger group (Figure 3.17 A). According to these results, conclusive interpretation could not be done for oxidative stress in cortex region. In cerebellum, 4-month-old Neu1-/- mice exhibited increased expression level of Catalase (Figure 3.18 B). Similar to Catalase expression level, increased expression level of TTase1 and SOD2 was detected in 4-month-old Neu1-/- mice (Figure 3.19 B and Figure 3.17 B). These results could indicate presence of oxidative stress in cerebellum of Neu1-/- mice which also causes elevated oxidative stress in Neu1-/-Galgt-/- mice.In thalamus, no significant change was noted in Catalase expression level (Figure 3.18 C). Increased expression level of TTase1 was observed in 4-month-old single and double knockout mice compared to WT (Figure 3.19 C). Also 4-month-old Neu1-/- mice had higher expression level of SOD2 than age-matched littermates (Figure 3.17 C). These results could be explained by increased oxidative stress in Neu1-/- mice that elevates oxidative stress in Neu1-/-Galgt-/- mice. Bcl-2 and Bcl-XL play role in inhibition of cytochrome c relase from mitochondria so they are named as anti-apoptotic marker. In cortex, 2-and 4-month-old Galgt-/- mice exhibited increased Bcl-2 expression level (Figure 3.20. A). However expression level of Bcl-XL increased only in 4-month-old Neu1-/- mice (Figure 3.21 A). It could be concluded that anti-apoptotic gene expression levels show distinct pattern in cortex region of single knockout mice group. In cerebellum, elevated expression level of Bcl-2 was seen in 2-and 4-month-old Neu1-/- mice (Figure 3.20 B) whereas no significant differences were noted in expression level of Bcl-XL (Figure 3.21 B). Therefore decreased anti-apoptotic response could be mentioned for Galgt-/- and Neu1-/-Galgt mice. In thalamus, 2-month-old Neu1-/- mice showed clear increase in expression level of Bcl-2 (Figure 3.20 C). Moreover compared to WT, Galgt-/- and Neu1-/-Galgt-/- mice had decreased expresion level of Bcl-2 in older mice group (Figure 3.20 C). Like in Bcl-2 expression, 2-month-old Neu1-/- mice displayed elevated Bcl-XL expression (Figure 3.21 C). Increased Bcl-XL expression was observed also in 4-month-old Neu1-/- mice (Figure 3.21 C). Similar to expression level of Bcl-2 result, obvious decrease was detected in 4-month-old Neu1-/-Galgt-/- mice. Like in cerebellum, Galgt and Neu1-/-Galgt mice showed decreased anti-apoptotic marker expression in thalamus (Figure 3.20 C; Figure 3.21 C).

Bax controls mitochondrial voltage-dependent channel and cytochrome c is released from mitochondria in the case of this channel opening (Shimizu et al1999). Therefore released cytochrome c causes activation of apoptosis initiator marker Caspase 9. In cortex, noticeable expression level of Bax difference was observed between 2-and

4-month-old Galgt-/- mice in which younger Galgt-/-mice group had increased expression level of Bax (Figure 3.22 A). In cerebellum, significantly elevated level of Bax expression was examined in 4-month-old Neu1-/- mice among older mice group (Figure 3.22 B). In thalamus obvious expression level of Bax differences were not observed (Figure 3.22 C).

Although UPR activation was not noticed in Neu1-/- spinal cord samples in previous study, 2-and 4-month old- cortex,cerebellum and thalamus sample of Neu1-/- mice showed altered ER Stress and UPR in this study (Tessitore et al.2004). In the same study, normalization of mRNA level of ER stress marker was detected when GM1 gangliosidosis mice (β-Gal-/- / Galgt-/-) crossed with Galgt-/- mice. However ER stress and UPR of Galgt-/- mice was not examined in the single knockout condition. Therefore normalization of ER stress and UPR level in spinal cord sample of β-Gal-/- / Galgt-/- was associated with absence of GM1 ganglioside in double knockout mice. According to that result, it was suggested that GM1 accumulation could cause UPR and neuronal apoptosis (Tessitore et al.2004). In our study, effect of Galgt enzyme in the brain of 2-and4-month-old age mice group was indicated and it might be concluded that altered ganglioside pattern showed its impact in different brain region as different manner.

In order to obtain conclusive results, protein levels of apoptotic markers (Fas-Ligand, Caspase 9, Caspase 3) and ER stress marker (BiP) were analyzed by Western Blot method in cortex,cerebellum and thalamus region of 2-and 4-month old WT,Neu1-/-,Galgt-/- and Neu1-/-Galgt-/- mice. Therefore mRNA level of genes could be related with corresponding protein levels. Fas-Ligand is the key mediator of extrinsic pathway of apoptosis. Caspase 9 is named as initiator caspase which is activated by cytochrome c release from mitochondria. Caspase 3 is known as executioner caspase which has role in the final step of apoptosis. Prolonged ER stress can result in apoptosis so BiP protein level was analyzed to have information about ER stress associated apoptosis in mice group (Gardner and Walter 2011).

In cortex, no obvious differences were noticed in Fas-Ligand protein level among genotypes and age groups (Figure 3.23 B). Therefore single and double enzyme deficiencies could not be correlated with extrinsic pathway of apoptosis. Decreased cleaved Caspase 9 level was detected in 2-month-old Galgt-/- mice (Figure 3.24 B) but this result could not be linked to Bax (causes cytochrome c release and Caspase 9 activation) expression level in which increased Bax expression was noted in 2-month-old Galgt-/- mice. No significant changes in cleaved Caspase 9 were observed in 4-month-old mice group (Figure 3.24 B). Although it was not significant, 4-month-old Galgt-/-

mice exhibited slightly increased protein level of cleaved Caspase 3 (Figure 3.25 B). Increased Caspase 3 could be correlated with increased GD3 expression in Galgt-/- mice which triggers cytochrome c release and Caspase-3 activation.Protein level of BiP did not exhibit noticable changes among genotypes but 2- month-old Galgt-/- and Neu1-/-Galgt-/- mice had increased protein level of BiP which was not significant (Figure 3.26 B).

In cerebellum, decreases protein level of Fas-Ligand was noted in both 2-and 4-month-old Neu1-/-Galgt-/- mice (Figure 3.27 B). This result could be explained by the combined effect of Neu1 and Galgt deficiency on this mice group. Therefore it could be mentioned that decreased response of apoptosis to extrinsic pathway was observed in double knockout mice group. Insignificant changes were detected in protein level of cleaved Caspase 9 (Figure 3.28 B). However decreased, not statistically significant, protein level of cleaved Caspase 9 was noticed in both 2-month-old Galgt-/- and Neu1-/-Galgt-/- mice (Figure 3.28 B). Obvious decrease in the level of cleaved Caspase 3 was found in 2-month-old Neu1-/-Galgt-/- mice but meaningful changes were not detected in 4-month-old mice group (Figure 3.29 B). Although 4-month-old single knockout mice had elevated protein level of BiP, Neu1-/- Galgt-/- mice displayed decreased level of BiP (Figure 3.30 B).

In thalamus, 4-month-old single and double knockout mice had lower protein level of Fas-Ligand than control group even though it was not statistically significant (Figure 3.31 B). Increased protein level of cleaved Caspase 9 was noticed in 4-month-old Neu1-/- mice and slight increase of cleaved Caspase 9 in 4-month-old Neu1-/-Galgt-/- mice could be related with Neu1 deficiency (Figure 3.32 B). Significant changes were not seen in protein level of cleaved Caspase 3 but slight increase in both 2-and 4-month-old Galgt-/- mice was noted (Figure 3.33 B). According to protein level of BiP, 2-month-old Neu1-/-Galgt-/- mice had lower level compared to age-matched Galgt-/- mice while 4-month-old Neu1-/-Galgt-/- mice had lower level compared to age-matched Neu1-/- mice (Figure 3.34 B). Therefore effect of Neu1 and Galgt deficiencies on double knockout mice was observed in distinct apoptotic markers.

Even though Galgt-/- mice had elevated GD3 ganglioside, apoptotic ganglioside, and no GM1 ganglioside, anti-apoptotic ganglioside, in mouse brain, dramatic increase in apoptotic markers in Western Blot analysis could not be detected. Additionally, although GD3 and CD95/Fas-mediated apoptosis in lymphocytes was revealed, significant increase in Fas-Ligand expression in mouse brain was not detected in Western Blot study. This situation might be related abnormal accumulation of GD3 and GM3

(compensatory mechanism) in Galgt-/- and Neu1-/-Galgt mouse brain. Additionally, studying mouse brain as three different regions, cortex, cerebellum and thalamus could lead detection of apoptosis as locally. Distinct distribution of gangliosides in the mouse brain could affect the obtaining apoptotic results. Therefore total brain could be used for apoptotic markers or detailed ganglioside distribution in the different brain regions by LC/MS analysis might be indicated. On the other hand effect of Neu1 enyzme on apoptosis (accumulation of sialylated molecules/glycolipids) and combined effect of Galgt and Neu1 enzymes on apoptosis of mouse brain was observed in that study. In order to detect apoptosis in the specific location of mouse brain, histologic staining, anti-NeuN immunostaining (detect neurons) and TUNEL assay were performed.

Previously, pathologic abnormalities were observed in Neu1-/- mice hippocampus. APP accumulation was noted (oversialylated APP) and it was concluded that excessive lysosomal exocytosis triggers Aβ peptide relase (Annunziata et al, 2013). Moreover in GM1 deficient mouse model (Galgt-/-) α-synuclein accumulation was noted and importance of GM1 ganglioside in the intracellular event was emphasized. GM1 ganglioside roles in association with α-synuclein to prevent fibrillation and provide helical conformation of this structure, nuclear Na/Ca exchanger potentiation and Ca regulation in dopaminergic neurons which contributes neuron protection (Wu et al.2011) were remarked. In addition to that findings , to analyze contribution of Neu1 and Galgt gene to brain histology, histologic staining were performed in 2-and 4-month-old WT, Neu1-/-, Galgt-/- and Neu1-/-Galgt-/- mice. To detect morphologic changes H&E staining, to analyze neuron structure Cresyl Echt Violet staining, to obtain glycosphingolipid accumulation Periodic Acid-Schiff (PAS) staining, to show demyelinzation Luxol Fast Blue staining were done.

In Hemotoxylin-Eosin staining results, obvious edema, vein dilation were noted in cortex, thalamus and hippocampus region of 2-and 4-month-old Neu1-/- mice compared to age-matched WT (Figure 3.35 and Figure 3.36). This finding was consistent with previous study in which vacuolated neurons and abnormalities in neuron cells were noted both in PPCA-/- and Neu1-/- mice brain with H&E staining (de Geest et al.2002). Although similar symptoms were detected in 2-and 4-month-old Galgt-/- mice brain in cortex, thalamus and hippocampus regions, these symptoms were not as severe as Neu1-/- mice (Figure 3.35 and Figure 3.36). Both 2-and 4-month-old Neu1-/-Galgt-/-mice exhibited the most dramatic changes that were characterized as cellular death, high level edema, dilations in veins and vacuolization. Morphologic changes in cortex,

hippocampus and thalamus regions might be result in apoptosis which was detected by TUNEL assay. Additionally morphologic problems in cortex region could be associated with anxiety-like behavior of Neu1-/- and Neu1-/-Galgt-/- mice. Moreover defects in hippocampus region could lead problems in memory which was noted in Passive Avoidance Test (Figure 3.49)

In cerebellum region, especially in Purkinje cells, cellular edema and clearance symptoms were seen in both 2-and 4-month-old age Neu1-/- and Galgt-/- mice (Figure 3.35 and Figure 3.36). Although Purkinje cell death was clearly observed by H&E staining in 5-month-old PPCA-/- mice compared to Neu1-/- mice, abnormalities in the Purkinje cell were also noted in 2-and 4-month-old Neu1-/- mice in this study (de Geest 2002). Additionally, noticeable Purkinje cell death in 2-and 4-month-old Neu1-/-Galgt-/- mice compared to age-matched littermates was observed (Figue 3.35 and Figure 3.36). Owing to being control center for motor coordination,balance, Purkinje cell death in cerebellum could be the explanation of impaired motor coordination and locomotor activity of Neu1-/-Galgt-/- mice in the rotarod and open field behavioral analysis.

In Cresyl Echt Staining, although there was locally karyolysis in 2-and 4-month-old Neu1-/- and Galgt-/- mice (Figure 3.37 and Figure 3.38), increament karyolysis and degenerative cell number were noted in 2-and 4-month-old Neu1-/-Galgt-/- mice brain (Figure 3.37 and Figure 3.38). Increased degenerative cell number could be related with apoptosis in that mice group.

In order to characterized abnormal sialylglycoconjugates accumulation, fibroblast derived from type I sialidosis patient was stained and N-glycosylated proteins with highly sialylated oligosaccharides were noticed (Oheda et al.2006). Consistent with result of previous study, in the results of Periodic acid-Schiff staining, glycoconjugate accumulation in 2-and 4-month-old Neu1-/- mice was observed (Figure 3.39 and Figure 3.40). However accumulated glycoconjugate amount was less in Galgt-/- mice than Neu1-/- mice group (Figure 3.39 and Figure 3.40). Increased glycoconjugate accumulation and disrupted cell organization was noticed in Neu1-/-Galgt-/- mice (Figure 3.39 and Figure 3.40). It could be concluded that there was combined effect of Neu1 and Galgt enzymes on glycosphingolipid degradation pathway. Although single deficiency of Neu1 had clear effect on glycoconjugate accumulation, double deficiency of Neu1 and Galgt had more dramatic effect on glycoconjugate degradation. This could be the sign for involvement of Galgt in glycoconjugate degradation in brain. Observed apoptosis, nerve cell density

decrease, oligodendrocyte decrease, failure in behavioral analysis for Neu1-/- mice could be associated with abnormal sialyglycoconjugates accumulutaion in that mice brain.

Luxol Fast Blue staining indicated that Neu1-/- mice brain had partially demyelinization. The most dramatic demyelination pattern was detected in Galgt-/- mice brain by Luxol Fast Blue staining (Figure 3.41 and Figure 3.42). Demyelination of Neu1-/-Galgt-/- mice was between Neu1-/- and Galgt-/- mice, lower than Galgt-/- mice but greater than Neu1-/- mice (Figure 3.41 and Figure 3.42). According to these results, impact of Galgt and Neu1 enzymes on myelination process was seen in both single and double knockout mice. In previous study, importance of complex gangliosides presence on myelin volume and axon degeneration was shown by electron microscopy analysis using 12-month-old Galgt-/- mice optic and syatic nerves. Similar to our findings, dramatic decrase in myelin volume was seen in Galgt-/- mice (Yao et al.2014). To support Luxol Fast Blue staining results, oligodendrocyte staining was performed for 4-month-old group and consistent results were obtained (Figure 3.43)

According to these morphologic findings, importance of Neu1 and complex gangliosides on developing normal brain morphology has revealed. Therefore accumulation of oversialylated components in the brain or excessive lysosomal exocytosis due to Neu1 absence could cause abnormalities in the nerve cells. Additionally GM1 deficit in the Galgt-/- mice could result in morphologic abnormalities in those mice. Furthermore, combined role of Neu1 and Galgt enzymes on nerve structure was remarked in Neu1-/-Galgt-/- mice.

In lysosomal storage disorders, neuronal dysfuntion/death, axonal damage and demyelination are charecterized as nervous sytem phenotypes. Loss of myelin, primary demyelination, is related with defect of oligodendrocytes/myelin sheath due to different pathagonesis in lysosomal storage disorders (Parenti et al.2015). Abnormal accumulated component in lysosome can lead problematic lipid and protein transportation from lysosome to plasma membrane resulting in myelin sheaths instability, cellular toxicity and neuron death.

For detailed analysis of neuron number, oligodendrocyte presence and apoptosis, immunostaining were performed by anti-NeuN antibody, anti-CNPase antibody, TUNEL assay respectively in 4-month-old WT,Neu1-/-,Galgt-/- and Neu1-/-Galgt-/- mice.

Oligodendrocyte analyses with anti-CNPase immunostaining have showed that 4-month-old Galgt-/- mice had the least oligodendrocyte intensity in cortex (Figure 3.43 C)

which could be associated with developing Wallerian degeneration and myelination defect in that mice brain (Sheikh et al.1999). Compared to Neu1-/- mice, lower oligodendrocyte intensity was detected in Neu1-/-Galgt-/- mice which could explain the Galgt enzyme importance for myelination in nerve cells (Figure 3.43 C) . Also Neu1-/- mice had decreased oligodendrocyte intensity compared to WT which could be the sign for role of Neu1 enzyme at the formation of myelin structure in central nervous system. Oversialylated components aggregation or abnormal exocytosis in nerve cells could result in impairment in myelination process. Anti-CNPase immunostaining results were supported by Luxol Fast Blue staining because in that staining the most dramatic demyelination was noted in Galgt-/- mice. Similar to Luxol Fast Blue staining results, moderate demyelination was detected in Neu1-/-Galgt-/- mice brain in anti-CNPase immunostaining. Unlike cortex, Neu1 enzyme deficiency caused more dramatic decrease in oligodendrocyte intensity in cerebellum (Figure 3.43 D). Both Neu1-/- and Neu1-/-Galgt-/- mice had significant reduction in oligodendrocyte intensity (Figure 3.43 D). These results could be explained by the distinct role of Galgt and Neu1 enzymes in different brain regions for nerve cell myelination.

In neuron density analysis it have revealed that 4-month-old Neu1-/- and Galgt-/- mice had decreased neuron number in cortex, thalamus and hippocampus regions compared to WT (Figure 3.44). Neuronal loss in Neu1-/- and Galgt-/- mice could be related with observed degeneration in H&E staining in that mice brain (Figure 3.35 and Figure 3.36). However noticed dramatic changes by histologic stainings in Neu1-/-Galgt-/- mice brain, could not be supported by NeuN staining. Since in that mice group neuronal density was almost the same with WT (Figure 3.44). This result could be explained by the more dramatic loss of neuroglia cells in Neu1-/-Galgt-/- mice rather than neuron cells because anti-NeuN antibody recognizes only neuron cells. On the other hand, there could be a compensatory mechanism to protect neuron cell in the absence of both Neu1 and Galgt enzymes. Expression of other sialidases could raises in the absence of these two enzymes or increased expression of GM3 and GD3 could play protective role in the absence of both Neu1 and Galgt enzymes.

Apoptotic neuronal death was detected via TUNEL assay kit. In the result of this analysis, effect of single and double deficiency of Neu1 and Galgt enzymes on neuron death in different brain regions was observed clearly. Impact of Neu1 enzyme deficiency on apoptosis was obviously noted in cortex and thalamus region because in that regions both Neu1-/- and Neu1-/-Galgt-/- mice had elevated TUNEL positive neurons (Figure

3.45 C and Figure 3.46 D). In hippocampus Galgt enzyme deficiency exhibited significant effect on apoptosis in which Galgt-/- and Neu1-/-Galgt-/- mice had increased apoptotic neuronal death (Figure 3.46 C). Elevated apoptosis in Neu1-/- and Galgt-/- mice could be associated with decreased neuronal density in that mice group. Therefore it could be concluded that Neu1 and Galgt enzyme deficiencies lead apoptosis in Neu1-/- and Galgt-/- mice that results in neuronal loss. Moreover absence of complex gangliosides in Galgt-/- mice, increased lysosomal exocytosis and accumulation of sialylated glycoconjugates in Neu1-/-mice could cause apoptosis and neuronal death. Impact of these two enzymes on neuronal apoptosis was observed in Neu1-/-Galgt-/- mice because increased TUNEL positive neurons were seen in those mice. Apoptosis analysis by Western Blot and RT-PCR also supported cell death in those mice. However apoptosis that was found in Neu1-/-Galgt-/- mice could not be associated with neuronal loss because Neu1-/-Galgt-/- mice had the similar neuron density with WT group (Figure 3.44). Therefore another mechanism could compensate apoptosis in those mice to have normal neuronal density. To clarify this inconclusive result in Neu1-/-Galgt-/- mice (neuronal density vs. apoptosis), more detailed analysis (inflammation etc.) might be done.

Behavioral tests were carried on to understand the effect of single and double deficiencies of Neu1 and Galgt genes on motor coordination, balance, anxiety-like behavior, locomotor activity, nerve-muscle function, muscle strength and memory. For these purposes, six different mice were tested from 2-and 4-month-old WT, Neu1-/-,Galgt-/- and Neu1-/-Galgt-/- mice.

Motor coordination and balance of mice were measured by Rotarod Test. In previous studies, latency time fall from the rod of Galgt-/- mice was tested in both young (2-3 month-old-age) and older (>6-month-old-age) mice groups. Significant deteretion in locomotor activity of older Galgt-/- mice was noted not in younger group (Yao et al.2014). Similar to previous studies, insignificant changes were noted between 2-and 4-month-old WT and Galgt-/- mice (Figure 3.47). According to spent time on the acceleration rod, 2-month-old Neu1-/-Galgt-/- mice had the lowest score compared to age-matched littermates (Figure 3.47). Similar result was obtained from 4-month-old Neu1-/-Galgt-/- mice. Cerebellum is control center for motor coordination and balance so Purkinje cell death (Figure 3.35 P and Figure 3.36 P), neurodegeneration, oligodendrocyte decrease (Figure 3.43 D) in that region could be the reason for impairment in motor coordination and balance of double knockout mice. Additionally, 4-month-old Neu1-/- mice had the highest score on the accelerating rod compared to age-

matched littermates (Figure 3.47). However in histologic and immunohistochemical staining, it was shown that there were neuron death, neurodegeneration, glycosphingolipid accumulation, oligodendrocyte decrement in cerebellum of 4-month-old Neu1-/- mice. Therefore highest score of these mice on the rod could be result of obvious spinal curvature in Neu1-/- mice that helpt mice to stay on the rod longer time.

Muscle strength, nerve-muscle function of mice was tested by Limb Grip Strength analysis. Forelimb grip strength scores indicated that 2-and 4-month-old Neu1-/-Galgt-/- mice had decreased muscle strength compared to age-matched littermates (Figure 3.48). Defect in muscle strength and nerve-muscle coordination could be the explained by histologic staining findings about cortex;degeneration, cellular death, high level edema, dilations in veins, vacuolization (Figure 3.35and Figure 3.36), glycosphingolipid accumulation (Figure 3.39 and Figure 3.40) , and by immunohistochemical analysis findings, oligodendrocyte decrease (Figure 3.43 A), increased apoptosis detected by TUNEL assay (Figure 3.45 C).

Fear-aggravated learning and memory test was performed to mice by Passive avoidance test. Test lasted during three days in which first day was habituation, second day was training and third day was testing. Scores belongs to third day were analyzed to evaluate learning and memory capabilities of 2-and 4-month-old WT, Neu1-/-, Galgt-/- and Neu1-/-Galgt-/- mice. In the brain, hippocampus is responsible for learning and memory functions. Therefore neurodegeneration, neuron loss in hippocampus can lead learning and memory defect in the mice. 2-month-old Neu1-/- mice had the lowest latency time to re-enter the dark box compared to age-matched littermates (Figure 3.49). This result could be associated with edema, karyolysis (Figure 3.35 F and Figure 3.36 F), glycosphingolipid accumulation in the hippocampus (Figure 3.39 F and Figue 3.40 F) of 2-month-old Neu1-/- mice. Additionally, amyloid β accumulation was detected in hippocampus of Neu1-/- mice and this could also lead defect in memory (Annunziata et al. 2014).

In 4-month-old mice group, Neu1-/- (36 ± 4s) and Neu1-/-Galgt-/- (69 ± 4s) mice displayed significantly decreased latency time compared to age-matched WT (295 ± 5s) and Galgt-/- mice (234 ± 65s) (Figure 3.49). Owing to obtaining more dramatic results from 4-month-old Neu1-/- and Neu1-/-Galgt-/- mice by histologic stainings, progressive degeneration could be considered for hippocampus region. Therefore dramatic changes in hippocampus morphology could explain the learning and memory capability decrement in Neu1-/- and Neu1-/-Galgt-/- mice. Additionally, impact of Neu1 deficiency on

hippocampus and learning/memory function might be noticed. Previous studies about Galgt-/- mice have revealed cognitive function deficit but neurodegenerative changes get more obvious with age (Sha et al.2014). Therefore obtaining close results in 4-month-old Galgt-/- mice compared to 4-month-old WT mice might arise from testing young age group so more obvious results could be gained from older Galgt-/- mice.

Mice' anxiety-like behavior and locomotor activities were analyzed by Open Field Test. In that test two separate results were obtained: time in center (Figure 3.50 A) and total distance (Figure 3.50 B). Time in center scores were related with mice' anxiety-like behavior whereas total distance scores were related with mice' locomotor activity. When looked at the spending time in the center, 2-and 4-month-old Neu1-/-, Galgt-/- and Neu1-/-Galgt-/- mice exhibited anxiety-like behavior compared to age-matched control group (Figure 3.50 A). Anxiety behavior is control by amygdala in the limbic system (Panksepp et al.2000). However there are many different network and communications to supply transmission of signals to amygdala in the brain. Therefore observed anxiety-like behavior in Neu1-/-, Galgt-/- and Neu1-/-Galgt-/- mice could be the result of detected neurodegeneration (Figure 3.35 and Figure 3.36), oligodendrocyte loss(Figure 3.43), neuronal loss (Figure 3.44),apoptosis (Figure 3.45) in cortex and hippocampus of these mice group. Any interruption in signal transduction through amygdala might result in anxiety-like behavior in those mice. Additionally, 4-month-old Neu1-/-Galgt-/- mice almost spent no time in the center (Figure 3.50 A) and this situation might be the evidence for progressive degeneration in the nerve cells in that mice group. Total distance results have revealed that 2-and 4-month-old Neu1-/-, Galgt-/- and Neu1-/-Galgt-/- mice walked less than age-matched control group (Figure 3.50 B). When compared to Galgt-/- and Neu1-/- mice in both age group, Galgt-/- mice tend to walk longer distance than Neu1-/- mice (Figure 3.50 B). This result could arise from less motor dysfunctionality of Galgt-/- mice in that age group compared to Neu1-/-. More significant changes were detected in locomotor activity of Galgt-/- mice in older age group (Chiavegatto et al. 2000). In histologic staining more dramatic results were obtained from Neu1-/- mice compared to Galgt-/- mice for cortex and cerebellum regions. Therefore impairment in locomotor activity in Neu1-/- mice could be associated with these staining results. Moreover effect of Neu1 deficiency on Neu1-/-Galgt-/- mice was obviously seen rather than effect of Galgt deficiency in locomotor activity result of Open Field Test.

In lysosomal storage diseases, besides primary storage compound due to lysosomal enzyme, cofactors or transport proteins defects, secondary metabolites are also

accumulated. Glycoprotein or glycolipid degradation pathway can result secondary metabolite, oligosaccharides and glycoaminoacids, accumulation in the urine (Xia et al.2013). It was known that sialidosis patients excretes urinary oligosaccharide, especially sialyl oligosacchraides (Takahashi et al.1991). Studies carried out on Neu1-/- mice also have been revealed increased urinary excretion of high-molecular-weight oligosaccharides (de Geest 2002). In the light of these information, urines of 2-and 4-month-old WT, Neu1-/-,Galgt-/- and Neu1-/-Galgt-/- mice were analyzed by Thin Layer Chromotography to understand effect of Galgt enzyme on oligosaccharide degradation in the presence and absence of Neu1 enzyme.Although different urinary pattern was observed among genotypes, intensities of two bands were focused. Because these two bands are characterized for sialidosis or GM1-gangliosidosis diagnosis (Mütze et al.2016). These two bands, Band1 and Band2, were observed in both 2-and 4-month-old Neu1-/- and Neu1-Galgt-/- mice but not in WT and Galgt-/-mice (Figure 3.51). When looked at the Band1 intensity, noticeable change was not detected between 2-and 4-month-old Neu1-/- mice (Figure 3.52 A). Even though it was insignificant, Band1 intensity was higher in 2-month-old Neu1-/- mice than 4-month-old Neu1-/-. This situation could be explained by the severity of 2-month-old Neu1-/- mice or absence of progressive accumulation of oligosaccharides in urine. Significant decrement was determined in Band1 intensity of both 2-and 4-month-old Neu1-/-Galgt-/- mice compared to age matched Neu1-/- mice. In Band2 intensity no significant change was noted between 2-and 4-month-old Neu1-/- mice (Figure 3.52 B). Although Band 2 intensity of 2-month-old Neu1-/-Galgt-/- mice very low, this band intensity significantly increased in 4-month-old Neu1-/-Galgt-/- mice (Figure 3.52 B). According to these results it could be said that Galgt enzyme does not involve oligosaccharide degradation in urine. However decreased Band 1 and Band 2 intensity,especially in the 2-month-old Neu1-/-Galgt-/- mice could be explained by the involvement of other enzymes in the absence of Galgt in oligosaccharide metabolism. In order to clarify this result, expression of other enzymes which could be related with oligosaccharide metabolism should be analyzed. Moreover an intense band around glucose was seen in 2-month-old double knockout mice while 4-month-old double knockout mice had intense band around galactose (Figure 3.51). These bands were exhibited neither Neu1-/- nor Galgt-/- mice so making an interpretation about these bands was hard. Therefore conclusive results can be obtained for these bands by using more precise methods such as MALDI-TOF mass spectrometry.

CHAPTER 5

CONCLUSION

In this study, combined biological role of Neu1 and Galgt enzymes on glycolipid metabolism was investigated by generating Neu1-/-Galgt-/- double deficient mice. Additionally, separate and combined role of Neu1 and Galgt enzymes on ganglioside metabolism, cellular events such as apoptosis, ER stress, oxidative stress, neuron structure, nerve-muscle relation ,locomotor activity, fear aggrevated learning and memory and oligosaccharide metabolism were realized.

Studying with four different genotype and two different age groups provided comparative results for involvement of Neu1 and Galgt enzymes on cellular events as age dependent manner, *in vivo*. Based on the ganglioside TLC results, it can be said that Neu1 enzyme does not show its activity on the brain gangliosides,*in vivo*. Apoptosis,ER Stress, and oxidative stress results indicate that each enzyme has distinct role in three different brain regions. Oligosaccharide analysis revealed that Galgt enzyme does not cause oligosaccharide accumulation. According to observed morphological changes in neuron structure for single and double knockout mice brain by histologic and immunohistochemical analysis, it is speculated that abnormal exocytosis, oversialylated component presence and complex ganglioside deficient cause impairment in neuron structure. Moreover Neu1-/-Galgt-/- mice exhibited severe phenotype in terms of neuron structure and behavioral analysis compared to Neu1-/- and Galgt-/- mice, and severity of phenotype of Neu1-/-Galgt-/- mice got worst with age.

This study showed distinct function of sialidase Neu1 and Galgt enzymes on the brain *in vivo*. Although GM3 is a one of the substrate of sialidase Neu1, direct effect of Neu1 enzyme on ganglioside metabolism was not observed in this study. However importance of both Neu1 and Galgt enzymes on normal brain development was noticed. Understanding of relation between gangliosides and Neu1 enzyme and abnormalities due to Neu1 and complex ganglioside deficiencies on the brain seems important for the enlighten and therapy of Sialidosis. Recently, Galgt-/- mice is used as model for Parkinson's disease and HSP. Enlighted relation between gangliosides and Neu1 I n the brain can supply new point of view for these diseases and treatments.

Detailed ganglioside distiribuiton in the brain can be performed by LC/MS analysis because all gangliosides could not be investigated by brain TLC method. With the help of detailed ganglioside analysis, level of different gangliosides, lipids and secondary metabolites could be revealed. Therefore effect of Neu1 on these components could be noticed. Additionally similar detailed analysis could be performed with oligosaccharide samples because only six known sugar and their levels could be detected by TLC analysis. In that analysis, impact of Galgt enzyme on oligosaccharide metabolism could not be observed. As known, Sialidosis is a systematic disease so multiple organs are affected at the same time (d'Azzo et al. 2015). Other tissues such as liver,kidney,spleen of single and double knockout mice can be analyzed in order to realize relation between sialidase Neu1 and gangliosides. Double knockout mice have shorter lifetime compared to Neu1-/- and Galgt-/- mice so this situation can be related with the systematic problem in Neu1-/-Galgt-/- mice.

In previous studies, amyloid beta accumulation in Neu1-/- mice brain and alpha synuclein accumulation in Galgt-/- mice brain was noted. However certain reason of these accumulation in these mice was not clear. In this study, possible cellular events (apoptosis, ER stress, oxidative stress) that cause these accumulation were investigated. However amyloid beta and alpha synuclein accumulation in double knockout mice was not examined. Therefore these accumulated protein could be analyzed and importance of Neu1 or Galgt enzymes could be revealed for these accumulations ,if there might any.

In histologic and immunohistochemical analysis, Neu1-/-Galgt-/- mice brain was observed as the most dramatically effected compared to Neu1-/- and Galgt-/- mice brain. However neuron density analysis and TUNEL analysis had conflicting results. Although, Neu1-/-Galgt-/- mice brain exhibited neurodegeneration, neuron and Purkinje cell loss, similar neuron density was observed in Neu1-/-Galgt-/- mice with the control group. These inconclusive result, could be enlighten with the analysis of glial cell in these mice groups and any compensatory mechanism in the Neu1-/-Galgt-/- mice could be detected,if there might any.

REFERENCES

Aerts, Johannes M.F.G., Chi-Lin Kuo, Lindsey T. Lelieveld, Daphne E.C. Boer, Martijn J.C. van der Lienden, Herman S. Overkleeft, and Marta Artola. (2019). "Glycosphingolipids and Lysosomal Storage Disorders as Illustrated by Gaucher Disease." Current Opinion in Chemical Biology 53: 204–15.

Ando, Susumu, Nan-Chen Chang, and Robert K. Yu. (1978). "High-Performance Thin-Layer Chromatography and Densitometric Determination of Brain Ganglioside Compositions of Several Species." Analytical Biochemistry 89 (2): 437–50.

Annunziata, Ida, Annette Patterson, Danielle Helton, Huimin Hu, Simon Moshiach, Elida Gomero, Ralph Nixon, and Alessandra d'Azzo. (2013). "Lysosomal NEU1 Deficiency Affects Amyloid Precursor Protein Levels and Amyloid-β Secretion via Deregulated Lysosomal Exocytosis." Nature Communications 4 (1).

Aoki, Kazuhiro, Adam D. Heaps, Kevin A. Strauss, and Michael Tiemeyer. (2019). "Mass Spectrometric Quantification of Plasma Glycosphingolipids in Human GM3 Ganglioside Deficiency." Clinical Mass Spectrometry 14 (November): 106–14.

Boccuto, L., Aoki, K., Flanagan-Steet, H., Chen, C. F., Fan, X., Bartel, F., ... & Alexov, E. 2014. A mutation in a ganglioside biosynthetic enzyme, ST3GAL5, results in salt & pepper syndrome, a neurocutaneous disorder with altered glycolipid and glycoprotein glycosylation. Human molecular genetics, 23(2), 418-433.

Bonten, E, A van der Spoel, M Fornerod, G Grosveld, and A d'Azzo. (1996). "Characterization of Human Lysosomal Neuraminidase Defines the Molecular Basis of the Metabolic Storage Disorder Sialidosis." Genes & Development 10 (24): 3156–69.

Borodzicz, Sonia, Katarzyna Czarzasta, Marek Kuch, and Agnieszka Cudnoch-Jedrzejewska. (2015). "Sphingolipids in Cardiovascular Diseases and Metabolic Disorders." Lipids in Health and Disease 14 (1).

Bostwick, David G., Erik E. Alexander, Rohini Singh, Ailin Shan, Junqi Qian, Regina M. Santella, Larry W. Oberley, et al. (2000). "Antioxidant Enzyme Expression and

Reactive Oxygen Species Damage in Prostatic Intraepithelial Neoplasia and Cancer." Cancer 89 (1): 123–34.

Boustany, Rose-Mary Naaman. (2013). "Lysosomal Storage Diseases—the Horizon Expands." Nature Reviews Neurology 9 (10): 583–98.

Brandenburg, K., & Holst, O. (2015). "Glycolipids: Distribution and Biological Function." In eLS (pp. 1–10).

Breiden, Bernadette, and Konrad Sandhoff. (2020). "Mechanism of Secondary Ganglioside and Lipid Accumulation in Lysosomal Disease." International Journal of Molecular Sciences 21 (7): 2566.

Carter, H. E., Haines, W. J., Ledyard, W. E., & Norris, W. P. 1947. Biochemistry of the sphingolipides I. Preparation of sphingolipides from beef brain and spinal cord. Journal of Biological Chemistry, 169(1), 77-82.

Chen, X. P., Enioutina, E. Y., & Daynes, R. A. (1997). "The Control of IL-4 Gene Expression in Activated Murine T Lymphocytes: A Novel Role for Neu-1 Sialidase. " The Journal of Immunology, 158(7), 3070-3080.

Chen, Guo-Yun, Nicholas K Brown, Wei Wu, Zahra Khedri, Hai Yu, Xi Chen, Diantha van de Vlekkert, Alessandra D'Azzo, Pan Zheng, and Yang Liu. (2014). "Broad and Direct Interaction between TLR and Siglec Families of Pattern Recognition Receptors and Its Regulation by Neu1." ELife 3 (September).

Coet, Timothy, Kunihiko Suzuki, Brian Popko, Kunihiko Suzuki, Brian Popko, Kunihiko Suzuki, and Brian Popko. (1998). "New Perspectives on the Function of Myelin Galactolipids." Trends in Neurosciences 21 (3): 126–30.

Conzelmann, E., and K. Sandhoff. (1983). "Partial Enzyme Deficiencies: Residual Activities and the Development of Neurological Disorders." Developmental Neuroscience 6 (1): 58–71. https://doi.org/10.1159/000112332.

D’Azzo, Alessandra, Eda Machado, and Ida Annunziata. (2015). “Pathogenesis, Emerging Therapeutic Targets and Treatment in Sialidosis.” Expert Opinion on Orphan Drugs 3 (5): 491–504.

D’Azzo, A., A. Hoogeveen, A. J. Reuser, D. Robinson, and H. Galjaard. (1982). “Molecular Defect in Combined Beta-Galactosidase and Neuraminidase Deficiency in Man.” Proceedings of the National Academy of Sciences 79 (15): 4535–39.

Geest, N. de. (2002). “Systemic and Neurologic Abnormalities Distinguish the Lysosomal Disorders Sialidosis and Galactosialidosis in Mice.” Human Molecular Genetics 11 (12): 1455–64.

Donida, B., Marchetti, D. P., Biancini, G. B., Deon, M., Manini, P. R., da Rosa, H. T., ... & Coitinho, A. S. (2015). Oxidative stress and inflammation in mucopolysaccharidosis type IVA patients treated with enzyme replacement therapy. Biochimica et Biophysica Acta (BBA)-Molecular Basis of Disease, 1852(5), 1012-1019

Dridi, L., V. Seyrantepe, A. Fougerat, X. Pan, E. Bonneil, P. Thibault, A. Moreau, et al. (2013). “Positive Regulation of Insulin Signaling by Neuraminidase 1.” Diabetes 62 (7): 2338–46.

Elmore, Susan. (2007). “Apoptosis: A Review of Programmed Cell Death.” Toxicologic Pathology 35 (4): 495–516.

Ferreira, Carlos R., and William A. Gahl. (2017). “Lysosomal Storage Diseases.” Translational Science of Rare Diseases 2 (1–2): 1–71.

Fingerhut, Ralph, Gijsbertus T. J. Horst, Frans W. Verheuen, and Ernst Conzelmann. (1992). “Degradation of Gangliosides by the Lysosomal Sialidase Requires an Activator Protein.” European Journal of Biochemistry 208 (3): 623–29.

Fletcher, Jessica L., Gauthami S. Kondagari, Charles H. Vite, Peter Williamson, and Rosanne M. Taylor. (2014). “Oligodendrocyte Loss During the Disease Course in a Canine Model of the Lysosomal Storage Disease Fucosidosis.” Journal of Neuropathology & Experimental Neurology 73 (6): 536–47.

Folkerth, Rebecca D., Joseph Alroy, Ina Bhan, and Edward M. Kaye. (2000). “Infantile G M1 Gangliosidosis: Complete Morphology and Histochemistry of Two Autopsy Cases, with Particular Reference to Delayed Central Nervous System Myelination.” Pediatric and Developmental Pathology 3 (1): 73–86.

Fragaki, Konstantina, Samira Ait-El-Mkadem, Annabelle Chaussenot, Catherine Gire, Raymond Mengual, Laurent Bonesso, Marie Bénéteau, et al. (2012). “Refractory Epilepsy and Mitochondrial Dysfunction Due to GM3 Synthase Deficiency.” European Journal of Human Genetics 21 (5): 528–34.

Frisch, Amos, and Elizabeth F. Neufeld. (1979). “A Rapid and Sensitive Assay for Neuraminidase: Application to Cultured Flbroblasts.” Analytical Biochemistry 95 (1): 222–27.

Furukawa K., Ohmi, Y., Ohkawa, Y., Tajima, O., & Furukawa, K.. (2014). “Glycosphingolipids in the Regulation of the Nervous System. “ Advances in Neurobiology 9, 307–20.

Futerman, A. H., & Van Meer, G. (2004). “The Cell Biology of Lysosomal Storage Disorders. “ Nature Reviews Molecular Cell Biology, 5(7), 554-565.

Geboes, Lies, Laure Dumoutier, Hilde Kelchtermans, Evelien Schurgers, Tania Mitera, Jean-Christophe Renauld, and Patrick Matthys. (2009). “Proinflammatory Role of the Th17 Cytokine Interleukin-22 in Collagen-Induced Arthritis in C57BL/6 Mice.” Arthritis & Rheumatism 60 (2): 390–95.

Giussani, Paola, Cristina Tringali, Laura Riboni, Paola Viani, and Bruno Venerando. (2014). “Sphingolipids: Key Regulators of Apoptosis and Pivotal Players in Cancer Drug Resistance.” International Journal of Molecular Sciences 15 (3): 4356–92.

Gordon-Lipkin, Eliza, Julie S. Cohen, Siddharth Srivastava, Bruno P. Soares, Eric Levey, and Ali Fatemi. (2018). "ST3GAL5-Related Disorders: A Deficiency in Ganglioside Metabolism and a Genetic Cause of Intellectual Disability and Choreoathetosis." Journal of Child Neurology 33 (13): 825–31.

Gusel'nikova, V. V., and D. E. Korzhevskiy. (2015). "NeuN As a Neuronal Nuclear Antigen and Neuron Differentiation Marker." Acta Naturae 7 (2): 42–47.

Hill, A. S., Sahay, A., & Hen, R. 2015. Increasing adult hippocampal neurogenesis is sufficient to reduce anxiety and depression-like behaviors. Neuropsychopharmacology, 40(10), 2368-2378.

Hinek, Aleksander, Alexey V. Pshezhetsky, Mark von Itzstein, and Barry Starcher. (2005). "Lysosomal Sialidase (Neuraminidase-1) Is Targeted to the Cell Surface in a Multiprotein Complex That Facilitates Elastic Fiber Assembly." Journal of Biological Chemistry 281 (6): 3698–3710.

Hiraoka, Miki, Ei Ohkawa, Akira Abe, Masaki Murata, Shinji Go, Jin-ichi Inokuchi, and Hiroshi Ohguro. (2019). "Visual Function in Mice Lacking GM3 Synthase." Current Eye Research 44 (6): 664–70.

Ho, Nurulain, Chengchao Xu, and Guillaume Thibault. (2018). "From the Unfolded Protein Response to Metabolic Diseases – Lipids under the Spotlight." Journal of Cell Science 131 (3): jcs199307.

Huang, J. Q., J. M. Trasler, S. Igdoura, J. Michaud, N. Hanal, and R. A. Gravel. (1997). "Apoptotic Cell Death in Mouse Models of GM2 Gangliosidosis and Observations on Human Tay-Sachs and Sandhoff Diseases." Human Molecular Genetics 6 (11): 1879–1885.

Igdoura, S. A., C. Gafuik, C. Mertineit, F. Saberi, A. V. Pshezhetsky, M. Potier, J. M. Trasler, and R. A. Gravel. (1998). "Cloning of the CDNA and Gene Encoding Mouse Lysosomal Sialidase and Correction of Sialidase Deficiency in Human Sialidosis and Mouse SM/J Fibroblasts." Human Molecular Genetics 7 (1): 115–20.

Iqbal, Jahangir, Meghan T. Walsh, Samar M. Hammad, and M. Mahmood Hussain. (2017). “Sphingolipids and Lipoproteins in Health and Metabolic Disorders.” Trends in Endocrinology & Metabolism 28 (7): 506–18.

Kakugawa, Y., T. Wada, K. Yamaguchi, H. Yamanami, K. Ouchi, I. Sato, and T. Miyagi. (2002). “Up-Regulation of Plasma Membrane-Associated Ganglioside Sialidase (Neu3) in Human Colon Cancer and Its Involvement in Apoptosis Suppression.” Proceedings of the National Academy of Sciences 99 (16): 10718–23.

Kamphoven, Joep H.J, Martijn M de Ruiter, Leon P.F Winkel, Hannerieke M.P Van den Hout, Jan Bijman, Chris I De Zeeuw, Hans L Hoeve, Bert A Van Zanten, Ans T Van der Ploeg, and Arnold J.J Reuser. (2004). “Hearing Loss in Infantile Pompe’s Disease and Determination of Underlying Pathology in the Knockout Mouse.” Neurobiology of Disease 16 (1): 14–20.

Kaye, Edward M., Joseph Alroy, Srinivasa S. Raghavan, Gerald A. Schwarting, Lester S. Adelman, Val Runge, Dafna Gelblum, Johann G. Thalhammer, and Gonzalo Zuniga. (1992). “Dysmyelinogenesis in Animal Model of GM1 Gangliosidosis.” Pediatric Neurology 8 (4): 255–61.

Kiguchi, Kaoru, Cynthia B. Henning-Chubb, and Eliezer Huberman. (1990). “Glycosphingolipid Patterns of Peripheral Blood Lymphocytes, Monocytes, and Granulocytes Are Cell Specific1.” The Journal of Biochemistry 107 (1): 8–14.

Kleizen, Bertrand, and Ineke Braakman. (2004). “Protein Folding and Quality Control in the Endoplasmic Reticulum.” Current Opinion in Cell Biology 16 (5): 597.

Kolter, Thomas. (2012). “Ganglioside Biochemistry.” ISRN Biochemistry 2012: 1–36.

Kolter, Thomas, and Konrad Sandhoff. (2009). “Lysosomal Degradation of Membrane Lipids.” FEBS Letters 584 (9): 1700–1712.

Lee, Jae-Min, Chang-Ju Kim, Jong-Min Park, Min Song, and Youn-Jung Kim. (2018). "Effect of Treadmill Exercise on Spatial Navigation Impairment Associated with Cerebellar Purkinje Cell Loss Following Chronic Cerebral Hypoperfusion." Molecular Medicine Reports, April.

Liu, Yujing, Ryuichi Wada, Hiromichi Kawai, Kazunori Sango, Chuxia Deng, Tadashi Tai, Michael P. McDonald, et al. (1999). "A Genetic Model of Substrate Deprivation Therapy for a Glycosphingolipid Storage Disorder." Journal of Clinical Investigation 103 (4): 497–505.

Liu, Y., A. Hoffmann, A. Grinberg, H. Westphal, M. P. McDonald, K. M. Miller, J. N. Crawley, K. Sandhoff, K. Suzuki, and R. L. Proia. (1997). "Mouse Model of GM2 Activator Deficiency Manifests Cerebellar Pathology and Motor Impairment." Proceedings of the National Academy of Sciences 94 (15): 8138–43.

Mah, Linda, Claudia Szabuniewicz, and Alexandra J. Fiocco. (2016). "Can Anxiety Damage the Brain?" Current Opinion in Psychiatry 29 (1): 56–63.

Malhotra, Renuka. (2012). "Membrane Glycolipids: Functional Heterogeneity: A Review." Biochemistry & Analytical Biochemistry 1 (2).

Miyagi, Taeko, Junji Sagawa, Kimio Konno, and Shigeru Tsuiki. (1990). "Immunological Discrimination of Intralysosomal, Cytosolic, and Two Membrane Sialidases Present in Rat Tissues1." The Journal of Biochemistry 107 (5): 794–98.

Miyagi T, Yamaguchi K. 2007. Sialic Acids. In: Kamerling JP, Ed. Comprehensive Glycoscience: From Chemistry to Systems Biology: Elsevier Ltd. pp. 297-323.

Miyagi, Taeko. (1990). "Multiple Forms of Mammalian Sialidase. Altered Expression in Carcinogenesis." The Tohoku Journal of Experimental Medicine 168 (2): 223–29.

Miyagi, Taeko, and Shigeru Tsuiki. (1985). "Rat-Liver Lysosomal Sialidase. Solubilization, Substrate Specificity and Comparison with the Cytosolic Sialidase." European Journal of Biochemistry 141 (1): 75–81.

Miyagi, Taeko., and K. Yamaguchi. (2012). “Mammalian Sialidases: Physiological and Pathological Roles in Cellular Functions.” Glycobiology 22 (7): 880–96.

Monti, E., Preti, A., Venerando, B., & Borsani, G. 2002. Recent development in mammalian sialidase molecular biology. Neurochemical research, 27(7-8), 649-663.

Mütze, Ulrike, Friederike Bürger, Jessica Hoffmann, Helmut Tegetmeyer, Jens Heichel, Petra Nickel, Johannes R Lemke, Steffen Syrbe, and Skadi Beblo. (2017). “Multigene Panel next Generation Sequencing in a Patient with Cherry Red Macular Spot: Identification of Two Novel Mutations in NEU1 Gene Causing Sialidosis Type I Associated with Mild to Unspecific Biochemical and Enzymatic Findings.” Molecular Genetics and Metabolism Reports 10 (March): 1–4.

Nakamura, K., Koike, M., Shitara, K., Kuwana, Y., Kiuragi, K., Igarashi, S., ... & Hanai, N. 1994. Chimeric anti-ganglioside GM2 antibody with antitumor activity. Cancer research, 54(6), 1511-1516.

Nakamura, Hideo, Takahiro Maeda, Tomoko Kohno, Naoki Sadamori, and Michito Ichimaru. (1991). “Hypoplastic Acute Leukemia Associated with Inv(16)(P13q22).” Cancer Genetics and Cytogenetics 51 (1): 63–66.

Nampoothiri, Sreekala, and Rajanikant G. K. (2017). “Evaluating Rodent Aerobics For Preclinical Ischemic Stroke Intervention Assessments.” Science Trends, February.

Nan, Xinli, Ivan Carubelli, and Nicholas M. Stamatos. (2006). “Sialidase Expression in Activated Human T Lymphocytes Influences Production of IFN-γ.” Journal of Leukocyte Biology 81 (1): 284–96.

Nath, Shalini, Chhabinath Mandal, Uttara Chatterjee, and Chitra Mandal. (2018). “Association of Cytosolic Sialidase Neu2 with Plasma Membrane Enhances Fas-Mediated Apoptosis by Impairing PI3K-Akt/MTOR-Mediated Pathway in Pancreatic Cancer Cells.” Cell Death & Disease 9 (2).

Neufeld, Elizabeth F. (1991). “Lysosomal Storage Diseases.” Annual Review of Biochemistry 60 (1): 257–80.

Niimi, Kimie, Chieko Nishioka, Tomomi Miyamoto, Eiki Takahashi, Ichiro Miyoshi, Chitoshi Itakura, and Tadashi Yamashita. (2011). “Impairment of Neuropsychological Behaviors in Ganglioside GM3-Knockout Mice.” Biochemical and Biophysical Research Communications 406 (4): 524–28.

Onyenwoke, Rob U., and Jay E. Brenman. (2015). “Lysosomal Storage Diseases-Regulating Neurodegeneration.” Journal of Experimental Neuroscience 9s2 (January): JEN.S25475.

Olsen, Anne S. B., and Nils J. Færgeman. (2017). “Sphingolipids: Membrane Microdomains in Brain Development, Function and Neurological Diseases.” Open Biology 7 (5): 170069.

Palmano, Kate, Angela Rowan, Rozey Guillermo, Jian Guan, and Paul McJarrow. (2015). “The Role of Gangliosides in Neurodevelopment.” Nutrients 7 (5): 3891–3913.

Pan, Xuefang, Camila De Britto Pará De Aragão, Juan P. Velasco-Martin, David A. Priestman, Harry Y. Wu, Kohta Takahashi, Kazunori Yamaguchi, et al. (2017). “Neuraminidases 3 and 4 Regulate Neuronal Function by Catabolizing Brain Gangliosides.” The FASEB Journal 31 (8): 3467–83.

Pasquel-Davila Daniela, S., Yanez-Vaca Sabrina, A., Espinosa-Hidalgo Nicole, D., & Cuadros-Buenaventura Evelin, G. CS 2019.02. 01.28 Bionature Conference Series Vol.2 No.1. cancer, 7, 9.

Peferoen, Laura, Markus Kipp, Paul van der Valk, Johannes M. van Noort, and Sandra Amor. (2014). “Oligodendrocyte-Microglia Cross-Talk in the Central Nervous System.” Immunology 141 (3): 302–13.

Platt, Frances M., Barry Boland, and Aarnoud C. van der Spoel. (2012). “Lysosomal Storage Disorders: The Cellular Impact of Lysosomal Dysfunction.” The Journal of Cell Biology 199 (5): 723–34.

Plomp, Jaap J., and Hugh J. Willison. (2009). “Pathophysiological Actions of Neuropathy-Related Anti-Ganglioside Antibodies at the Neuromuscular Junction.” The Journal of Physiology 587 (16): 3979–99.

Plotegher, Nicoletta, and Michael R. Duchen. (2017). “Mitochondrial Dysfunction and Neurodegeneration in Lysosomal Storage Disorders.” Trends in Molecular Medicine 23 (2): 116–34.

Prokazova, N. V., N. N. Samovilova, E. V. Gracheva, and N. K. Golovanova. (2009). “Ganglioside GM3 and Its Biological Functions.” Biochemistry (Moscow) 74 (3): 235–49.

Pshezhetsky, Alexey V., Catherine Richard, Lorraine Michaud, Suleiman Igdoura, Shupei Wang, Marc-André Elsliger, Jingyi Qu, et al. (1997). “Cloning, Expression and Chromosomal Mapping of Human Lysosomal Sialidase and Characterization of Mutations in Sialidosis.” Nature Genetics 15 (3): 316–20.

Rama Rao, K.V., and T. Kielian. (2016). “Astrocytes and Lysosomal Storage Diseases.” Neuroscience 323 (May): 195–206.

Ren, Li-rong, Li-ping Zhang, Shu-ying Huang, Yuan-fang Zhu, Wen-juan Li, Shan-yu Fang, Li Shen, and Yan-ling Gao. (2015). “Effects of Sialidase NEU1 SiRNA on Proliferation, Apoptosis, and Invasion in Human Ovarian Cancer.” Molecular and Cellular Biochemistry 411 (1–2): 213–19.

Richardson, Katie, Achilleas Livieratos, Richard Dumbill, Steven Hughes, Gauri Ang, David A. Smith, Lauren Morris, et al. (2016). “Circadian Profiling in Two Mouse Models of Lysosomal Storage Disorders; Niemann Pick Type-C and Sandhoff Disease.” Behavioural Brain Research 297 (January): 213–23.

Risher, W. C., Patel, S., Kim, I. H., Uezu, A., Bhagat, S., Wilton, D. K., ... & Stevens, B. 2014. Astrocytes refine cortical connectivity at dendritic spines. Elife, 3, e04047.

Saher, Gesine, and Sina Kristin Stumpf. (2015). “Cholesterol in Myelin Biogenesis and Hypomyelinating Disorders.” Biochimica et Biophysica Acta (BBA) - Molecular and Cell Biology of Lipids 1851 (8): 1083–94.

Saito, Megumi, and Kiyoshi Sugiyama. (2002). “Characterization of Nuclear Gangliosides in Rat Brain: Concentration, Composition, and Developmental Changes.” Archives of Biochemistry and Biophysics 398 (2): 153–59.

Sandhoff, Roger, Stefan T. Hepbildikler, Richard Jennemann, Rudolf Geyer, Volkmar Gieselmann, Richard L. Proia, Herbert Wiegandt, and Hermann-Josef Gröne. (2002). “Kidney Sulfatides in Mouse Models of Inherited Glycosphingolipid Disorders.” Journal of Biological Chemistry 277 (23): 20386–98.

Sasazawa, F., T. Onodera, T. Yamashita, N. Seito, Y. Tsukuda, N. Fujitani, Y. Shinohara, and N. Iwasaki. (2014). “Depletion of Gangliosides Enhances Cartilage Degradation in Mice.” Osteoarthritis and Cartilage 22 (2): 313–22.

Schengrund, Cara-Lynne. (2015). “Gangliosides: Glycosphingolipids Essential for Normal Neural Development and Function.” Trends in Biochemical Sciences 40 (7): 397–406.

Schnaar, Ronald L. (2009). “Brain Gangliosides in Axon-Myelin Stability and Axon Regeneration.” FEBS Letters 584 (9): 1741–47.

Schneider Gasser, Edith M, Carolin J Straub, Patrizia Panzanelli, Oliver Weinmann, Marco Sassoè-Pognetto, and Jean-Marc Fritschy. (2006). “Immunofluorescence in Brain Sections: Simultaneous Detection of Presynaptic and Postsynaptic Proteins in Identified Neurons.” Nature Protocols 1 (4): 1887–97.

Schneider-Jakob, Helge Renate, and Michael CANTZ. (1991). “Lysosomal and Plasma Membrane Ganglioside GM3 Sialidases of Cultured Human Fibroblasts.

Differentiation by Detergents and Inhibitors." Biological Chemistry Hoppe-Seyler 372 (1): 443–50.

Seibenhener, Michael L., and Michael C. Wooten. (2015). "Use of the Open Field Maze to Measure Locomotor and Anxiety-like Behavior in Mice." Journal of Visualized Experiments, no. 96 (February).

Sekijima, Yoshiki, Katsuya Nakamura, Dai Kishida, Aya Narita, Kaori Adachi, Kosaku Ohno, Eiji Nanba, and Shu-ichi Ikeda. (2013). "Clinical and Serial MRI Findings of a Sialidosis Type I Patient with a Novel Missense Mutation in the NEU1 Gene." Internal Medicine 52 (1): 119–24

Seyrantepe, Volkan, Alexandre Iannello, Feng Liang, Evgeny Kanshin, Preethi Jayanth, Suzanne Samarani, Myron R. Szewczuk, Ali Ahmad, and Alexey V. Pshezhetsky. (2010). "Regulation of Phagocytosis in Macrophages by Neuraminidase 1." Journal of Biological Chemistry 285 (1): 206–15.

Seyrantepe, Volkan, Helena Poupetova, Roseline Froissart, Marie-Thrse Zabot, Irane Maire, and Alexey V. Pshezhetsky. (2003). "Molecular Pathology of NEU1 Gene in Sialidosis." Human Mutation 22 (5): 343–52.

Seyrantepe, Volkan, Maryssa Canuel, Stéphane Carpentier, Karine Landry, Stéphanie Durand, Feng Liang, Jibin Zeng, et al. (2008). "Mice Deficient in Neu4 Sialidase Exhibit Abnormal Ganglioside Catabolism and Lysosomal Storage." Human Molecular Genetics 17 (11): 1556–68.

Seyrantepe, Volkan, Secil Akyildiz Demir, Zehra Kevser Timur, Johanna Von Gerichten, Christian Marsching, Esra Erdemli, Emin Oztas, et al. (2018). "Murine Sialidase Neu3 Facilitates GM2 Degradation and Bypass in Mouse Model of Tay-Sachs Disease." Experimental Neurology 299 (Pt A): 26–41.

Seyrantepe, Volkan, Karine Landry, Stéphanie Trudel, Jacob A. Hassan, Carlos R. Morales, and Alexey V. Pshezhetsky. (2004). "Neu4, a Novel Human Lysosomal Lumen Sialidase, Confers Normal Phenotype to Sialidosis and Galactosialidosis Cells." Journal of Biological Chemistry 279 (35): 37021–29.

Simpson, Michael A, Harold Cross, Christos Proukakis, David A Priestman, David C A Neville, Gabriele Reinkensmeier, Heng Wang, et al. (2004). “Infantile-Onset Symptomatic Epilepsy Syndrome Caused by a Homozygous Loss-of-Function Mutation of GM3 Synthase.” Nature Genetics 36 (11): 1225–29.

Stewart, B. W. (1994). “Mechanisms of Apoptosis: Integration of Genetic, Biochemical, and Cellular Indicators.” JNCI Journal of the National Cancer Institute 86 (17): 1286–96.

Tardy, Claudine, Nathalie Andrieu-Abadie, Robert Salvayre, and Thierry Levade. (2004). “Lysosomal Storage Diseases: Is Impaired Apoptosis a Pathogenic Mechanism?” Neurochemical Research 29 (5): 871–80.

Tourtellotte, W. W. (1965). “Tay-Sachs’ Disease.” Archives of Neurology 13 (4): 452–53.

Tessitore, Alessandra, Maria del P. Martin, Renata Sano, Yanjun Ma, Linda Mann, Angela Ingrassia, Eric D. Laywell, Dennis A. Steindler, Linda M. Hendershot, and Alessandra d’Azzo. (2004). “GM1-Ganglioside-Mediated Activation of the Unfolded Protein Response Causes Neuronal Death in a Neurodegenerative Gangliosidosis.” Molecular Cell 15 (5): 753–66.

Thulasiraman, Padmamalini, Kelbie Kerr, Kathleen McAlister, Samantha Hardisty, Albany Wistner, and Ian McCullough. (2019). “Neuraminidase 1 Regulates Proliferation, Apoptosis and the Expression of Cadherins in Mammary Carcinoma Cells.” Molecular and Cellular Biochemistry 462 (1–2): 207–15.

Tsay, Grace Chen, and Glyn Dawson. (1976). “Oligosaccharide storage in brains from patients wıth fucosidosis, GM1-gangliosidosis and GM2-gangliosidosis (sandhoff’s dısease).” Journal of Neurochemistry 27 (3): 733–40.

Uemura, T, K Shiozaki, K Yamaguchi, S Miyazaki, S Satomi, K Kato, H Sakuraba, and T Miyagi. (2009). “Contribution of Sialidase NEU1 to Suppression of Metastasis

of Human Colon Cancer Cells through Desialylation of Integrin B4." Oncogene 28 (9): 1218–29.

Van der Horst, G. T., Galjart, N. J., d'Azzo, A., Galjaard, H., & Verheijen, F. W. 1989. Identification and in vitro reconstitution of lysosomal neuraminidase from human placenta. Journal of Biological Chemistry, 264(2), 1317-1322.

Pelt, Johannes, Danielle G. J. L. BILSEN, Johannis P. KamerlİNg, and Johannes F. G. Vlıegenthart. (1988). "Structural Analysis of O-Glycosidic Type of Sialyloligosaccharide-Alditols Derived from Urinary Glycopeptides of a Sialidosis Patient." European Journal of Biochemistry 174 (1): 183–87.

Vidal-Donet, José Manuel, Jaime Cárcel-Trullols, Bonaventura Casanova, Carmen Aguado, and Erwin Knecht. (2013). "Alterations in ROS Activity and Lysosomal PH Account for Distinct Patterns of Macroautophagy in LINCL and JNCL Fibroblasts." Edited by Anthony Robert White. PLoS ONE 8 (2): e55526.

Vilaça, Rita, Elísio Silva, André Nadais, Vítor Teixeira, Nabil Matmati, Joana Gaifem, Yusuf A. Hannun, Maria Clara Sá Miranda, and Vítor Costa. (2014). "Sphingolipid Signalling Mediates Mitochondrial Dysfunctions and Reduced Chronological Lifespan in the Yeast Model of Niemann-Pick Type C1." Molecular Microbiology 91 (3): 438–51.

Walter, P., and D. Ron. (2011). "The Unfolded Protein Response: From Stress Pathway to Homeostatic Regulation." Science 334 (6059): 1081–86.

Wei, Hui, Sung-Jo Kim, Zhongjian Zhang, Pei-Chih Tsai, Krystyna E. Wisniewski, and Anil B. Mukherjee. (2007). "ER and Oxidative Stresses Are Common Mediators of Apoptosis in Both Neurodegenerative and Non-Neurodegenerative Lysosomal Storage Disorders and Are Alleviated by Chemical Chaperones." Human Molecular Genetics 17 (4): 469–77.

Woods, Amina S., Benoit Colsch, Shelley N. Jackson, Jeremy Post, Kathrine Baldwin, Aurelie Roux, Barry Hoffer, et al. (2013). "Gangliosides and Ceramides Change in

a Mouse Model of Blast Induced Traumatic Brain Injury." ACS Chemical Neuroscience 4 (4): 594–600.

Woś, Marcin, Joanna Szczepanowska, Sławomir Pikuła, Anna Tylki-Szymańska, Krzysztof Zabłocki, and Joanna Bandorowicz-Pikuła. (2016). "Mitochondrial Dysfunction in Fibroblasts Derived from Patients with Niemann-Pick Type C Disease." Archives of Biochemistry and Biophysics 593 (March): 50–59.

Wraith, Ed. (2009). "New Therapies in the Management of Niemann-Pick Type C Disease: Clinical Utility of Miglustat." Therapeutics and Clinical Risk Management, November, 877.

Wu, Xudong, Katherine A. Steigelman, Erik Bonten, Huimin Hu, Wenxuan He, Tianying Ren, Jian Zuo, and Alessandra d'Azzo. (2010). "Vacuolization and Alterations of Lysosomal Membrane Proteins in Cochlear Marginal Cells Contribute to Hearing Loss in Neuraminidase 1-Deficient Mice." Biochimica et Biophysica Acta (BBA) - Molecular Basis of Disease 1802 (2): 259–68.

Xia, Baoyun, Ghazia Asif, Leonard Arthur, Muhammad A Pervaiz, Xueli Li, Renpeng Liu, Richard D Cummings, and Miao He. (2013). "Oligosaccharide Analysis in Urine by MALDI-TOF Mass Spectrometry for the Diagnosis of Lysosomal Storage Diseases." Clinical Chemistry 59 (9): 1357–68.

Yamaguchi, Kazunori, Keiko Hata, Koichi Koseki, Kazuhiro Shiozaki, Hirotoshi Akita, Tadashi Wada, Setsuko Moriya, and Taeko Miyagi. (2005). "Evidence for Mitochondrial Localization of a Novel Human Sialidase (NEU4)." Biochemical Journal 390 (1): 85–93.

Yamanaka, S., M. D. Johnson, A. Grinberg, H. Westphal, J. N. Crawley, M. Taniike, K. Suzuki, and R. L. Proia. (1994). "Targeted Disruption of the Hexa Gene Results in Mice with Biochemical and Pathologic Features of Tay-Sachs Disease." Proceedings of the National Academy of Sciences 91 (21): 9975–79.

Yamashita, T., A. Hashiramoto, M. Haluzik, H. Mizukami, S. Beck, A. Norton, M. Kono, et al. (2003). "Enhanced Insulin Sensitivity in Mice Lacking Ganglioside GM3." Proceedings of the National Academy of Sciences 100 (6): 3445–49.

Yao, Denggao, Rhona McGonigal, Jennifer A. Barrie, Joanna Cappell, Madeleine E. Cunningham, Gavin R. Meehan, Simon N. Fewou, et al. (2014). “Neuronal Expression of GalNAc Transferase Is Sufficient to Prevent the Age-Related Neurodegenerative Phenotype of Complex Ganglioside-Deficient Mice.” The Journal of Neuroscience 34 (3): 880–91.

Yogalingam, Gouri, Erik J. Bonten, Diantha van de Vlekkert, Huimin Hu, Simon Moshiach, Samuel A. Connell, and Alessandra d’Azzo. (2008). “Neuraminidase 1 Is a Negative Regulator of Lysosomal Exocytosis.” Developmental Cell 15 (1): 74–86. Yoo, Soojin, and June-Bum Kim. (2015). “Anti-Apoptotic and Beneficial Metabolic Activities of Resveratrol in Type II Gaucher Disease.” Biological & Pharmaceutical Bulletin 38 (6): 913–18.

Yoshikawa, M., S. Go, S.-i. Suzuki, A. Suzuki, Y. Katori, T. Morlet, S. M. Gottlieb, et al. (2015). “Ganglioside GM3 Is Essential for the Structural Integrity and Function of Cochlear Hair Cells.” Human Molecular Genetics 24 (10): 2796–2807.

Yoshikawa, M., S. Go, K. Takasaki, Y. Kakazu, M. Ohashi, M. Nagafuku, K. Kabayama, et al. (2009). “Mice Lacking Ganglioside GM3 Synthase Exhibit Complete Hearing Loss Due to Selective Degeneration of the Organ of Corti.” Proceedings of the National Academy of Sciences 106 (23): 9483–88.

Yu, Robert K, Yi-Tzang Tsai, Toshio Ariga, and Makoto Yanagisawa. (2011). “Structures, Biosynthesis, and Functions of Gangliosides--an Overview.” Journal of Oleo Science 60 (10): 537–44.

Zammarchi, Enrico, Maria Alice Donati, Amelia Morrone, Gian Paolo Donzelli, Xiao Yan Zhou, and Alessandra D’Azzo. (1996). “Early-Infantile Galactosialidosis: Clinical, Biochemical, and Molecular Observations in a New Patient.” American Journal of Medical Genetics 64 (3): 453–58.

Zanoteli, Edmar, Diantha van de Vlekkert, Erik J. Bonten, Huimin Hu, Linda Mann, Elida M. Gomero, A. John Harris, Giulio Ghersi, and Alessandra d'Azzo. (2010). "Muscle Degeneration in Neuraminidase 1-Deficient Mice Results from Infiltration of the Muscle Fibers by Expanded Connective Tissue." Biochimica et Biophysica Acta (BBA) - Molecular Basis of Disease 1802 (7–8): 659–72.

Zhang, Zhongjian, Yi-Ching Lee, Sung-Jo Kim, Moonsuk S. Choi, Pei-Chih Tsai, Yan Xu, Yi-Jin Xiao, Peng Zhang, Alison Heffer, and Anil B. Mukherjee. (2005). "Palmitoyl-Protein Thioesterase-1 Deficiency Mediates the Activation of the Unfolded Protein Response and Neuronal Apoptosis in INCL." Human Molecular Genetics 15 (2): 337–46.